BANDPASS FILTERS FOR GIGAHERTZ FREQUENCIES USING INTERDIGITAL PARALLEL COUPLED RESONATORS

A

Thesis

Submitted to the Department of Electrical and Electronic Engineering B.U.E.T. Dhaka, in partial fulfilment of the requirements for the degree of Master of Science in Engineering (Electrical and Electronic).

PROVASH CHANDRA ROY

November 1990

Declaration

I hereby declare that this work has not been submitted elsewhere for the award of any degree or diploma or for publication.

Provash Chandra Roy

(Provash Chandra Roy)

The thesis "**BANDPASS FILTERS FOR GIGAHERTZ FREQUENCIES USING INTERDIGITAL PARALLEL COUPLED RESONATORS**" submitted by Provash Chandra Roy, Roll No. 871343F, Session '85-86 to the Department of Electrical and Electronic Engineering B.U.E.T. has been accepted as satisfactory for partial fulfilment of the requirements for the degree of Master of Science and Engineering (Electrical and Electronic Engineering).

<u>Board of Examiners:</u>

1. Dr. Saiful Islam
   Professor,
   EEE Department
   Bangladesh University of
   Engineering and Technology,
   Dhaka 1000

   Saiful Islam 6.11.90 — Chairman

2. Dr. Md. Abdul Matin
   Professor and Head,
   EEE Department
   Bangladesh University of
   Engineering and Technology,
   Dhaka 1000

   M. A. Matin 6.11.90 — Member (Ex-officio)

3. Dr. A. B. M. Siddique Hossain
   Professor,
   EEE Department
   Bangladesh University of
   Engineering and Technology,
   Dhaka 1000

   ABM Hossain 6.11.90 — Member

4. Dr. K. Mohiuddin Ahmed
   Associate Professor,
   EEE Department
   Bangladesh University of
   Engineering and Technology,
   Dhaka 1000

   6/11/90 — Member

5. Dr. Shamsuddin Ahmed
   Professor and Head,
   EEE Department
   ICTVTR, Gazipur.

   Ahmed 6/11/90 — Member (External)

Acknowledgement

With deep sincerity, the author wishes to acknowledge his profound gratitude to Professor Dr. Saiful Islam of Electrical and Electronic Engineering Department BUET for his incessant and meticulous guidance in completing this work. The author thanks him for his outstanding suggestions in fabricating the experimental interdigital filters. The author also feels proud to acknowledge him for his expert opinion in improving the performances of the experimental filters.

The author wishes to acknowledge his indebtedness Professor Dr. M. A. Matin, Head of Electrical and Electronic Engineering Department BUET for his all-out inspiration and encouragement at all stages of this work.

Thanks are given to Mr. Molla Ahmed Ali, Foreman Instructor and Mr. Hossain Ali of Machine shop for their active help and assistance in fabricating the experimental filters.

Finally, the author wishes to thank the teachers of EEE department and CSE department who helped him in overcoming the difficulties with micro-computers and softwares while using the PCs of the EEE Department and the CSE department.

Contents

Abstract

A method for designing bandpass filters with Chebyshev characteristics has been developed using a combination of image parameter theory and insertion- loss technique. For developing this method, at first, a lumped element lowpass prototype filter is converted to another lumped lowpass filter circuit containing J-inverters and shunt capacitances using image parameter theory. A technique of transforming the modified lumped lowpass filter into distributed network filter has been used which is established on the basis of correspondences of image impedances and image phases of the modified lowpass prototype and the bandpass filter network at various frequency points. By using this lowpass to bandpass transformation technique, each J-parameter section of the converted lowpass lumped filter circuit is transformed into a distributed network containing one piece of quarter wave link transmission- line having shunt connected quarter wave long short circuited stubs on its two sides. Following this technique the complete distributed bandpass filter network is obtained. The input and output sections are modified into transformer elements in order to achieve matched condition at the input and output sides. In the last step, equivalent circuit of each of the distributed line sections containing two shunt quarter wave shorted stubs and one quarter wave link line sections are obtained in the form of a pair of coupled interdigital TEM lines between ground planes. The complete filter structure may be seen as formed by two interleaved combline structures so that the parallel coupled lines are alternately grounded and open circuited on the opposite sides.

A computer programme for IBM 370 in fortran has been developed for the design of this type of filters. Using this programme, an experimental filter with 12% BW and 1.5 GHz center frequency for six resonators has been designed. Using the obtained line parameters, the physical dimensions of the filter are then determined by using the graphs and analytical expressions for parallel coupled rectangular bars between ground planes. With the help of these dimensions, an experimental filter has been fabricated using brass plates and tested in the microwave laboratory of the department.

List of principal symbols

ω' = random frequency variable for lowpass prototype filter
ω = random frequency variable for bandpass filter
ω_0 = mid band frequency
w = fractional bandwith
ω_1 = lower cutoff frequency
ω_2 = higher cutoff frequency
Ω = normalized frequency
g_k = lowpass prototype filter element values
β = image phase factor
ρ = reflection co-efficient
λ_0 = wave-length at centre frequency
η_0 = intrinsic-impedance for free space
ϵ = absolute dielectric constant
ϵ_r = relative dielectric constant
v = velocity of light in the medium of propagation
w_k = widths of rectangular bars
t = thickness of rectanguar bars
b = distance between two parallel ground planes
s_{kk+1} = separation between two adjacent bars
J_{kk+1} = admittance inverter
Y_k = characteristic admittances of shunt-stub
Y_{kk+1} = characteristic admittances of connecting lines
C_k = self capacitances
C_{kk+1} = mutual capacitances
n = number of resonators
h = admittance scaling factor
C_{fe}' = even-mode fringing capacitance
C_{fo}' = odd-mode fringing capacitance

CHAPTER 1

INTRODUCTION

1.1 Historical Review

In communication networks usually four types of filters are used. These are: (i) lowpass, (ii) highpass, (iii) bandpass and (iv) bandstop filters. The first three of these are used to separate signals of a particular group of frequencies and the fourth one is used to stop a particular band of frequencies. Bandpass filters are used to separate signals of a desired band of frequencies from a source containing network in order to pass the selected band of signals to another network. The demand for different types of characteristics of these filters vary depending upon applications. For example, some operations may demand sharp cutoff narrow band bandpass filter, some operations may require very small insertion-loss in the passband, some may demand strong stopband rejection and some may require an octave bandwidth. Some of the applications may demand certain limitations on physical parameters. For example, if the application is in satellites, aircrafts or missiles, compactness in weight and volume is very much required. Needless to say that almost all applications in communication networks especially applications in satellites and aircrafts strongly demand reliability in operation. Therefore, it is necessary to develop design methods to fullfil these requirents.

In order to meet these varieties of requirements a lot of researches in the field of microwave bandpass filter have been done in the past and a significant amount of work is still going on at different places in the world. It is well known that at microwave frequencies lumped-element bandpass filters do not work since at these frequencies the circuit behaviour is distributed in nature. Therefore, theories related to distributed networks must be applied in order to analyze and synthesize a network at microwave frequencies. Parallel coupled lines between ground planes is a well known distributed type of line which can support TEM waves. A number of configurations of coupled rectangular lines between parallel ground planes may be used for realizing bandpass filters.

Of these, the configurations of shorted stub (herringbone) and comblines as shown in figures 1.1(a) and 1.1(b) are well known for bandpass filters. It will be shown later that another configuration known as interdigital structure (figure 1.1(c)) may also be used for bandpass filters.

In 1952, R.C. Flectcher [15] presented an analytical treatment of broad-band interdigital circuits for use in traveling wave type amplifiers. It was shown in this paper [15] that an interdigital structure with its capability for dissipating large power can be arranged to give broad-band performance. Butcher [14] in 1957 presented an analytical treatment of coupling impedances of interdigital lines having negligible thickness. Both Fletcher[15] and Butcher [14] found that the interdigital coupled lines are slow-wave structures.

Cohn [7] in 1958 showed that bandpass filters can be realized with half-wave parallel coupled striplines having zero thickness. Cohn [7] presented design formulas for bandpass filters using this type of parallel coupled transmission lines. The design formulas derived for this type of filters permit accurate design for Chebyshev, Butterworth and other physically realizible characteristics. According to Cohn [7], the formulas are theoretically exact for very narrow bandwidth, but frequency response calculations showed good results for bandwidth upto about 30 per cent. Cohn [7] designed and constructed a six resonator experimental filter having 10 per cent bandwidth with a center frequency of 1.2 GHz. The experimental results of Cohn [7] showed good agreement with the expected values. In this work [7] nomograms were used for determining the physical dimensions.

Matthaei [1] in 1960 presented an improved design method for Parallel-coupled strip line resonator bandpass filters which was based on insertion loss basis. This design method was for wide-band as well as narrow-band bandpass filters. By using thick-strips and having air instead of heavy dielectric in between the lines and the ground planes improvement on insertion losses in the passband were obtained by Matthaei [1]. Also, the thick-strips gave better mechanical strength. A Chebyshev bandpass filter having 2.2 to 1 bandwidth was designed using this method. The results of the experimental filter was in close agreement with the prescribed characteristics. The method was tested for a number of bandpass filters and satisfactory results were obtained.

Bolljahn and Matthaei [2] in 1962 analyzed a number of structures consisting of arrays of parallel conductors between ground planes. These include interdigital lines, meander line, one form of helical line and reactively loaded comblines. These authors [2] showed that interdigital lines and reactively loaded comb-lines have very interesting bandpass properties. In 1963 Matthaei [27] designed and constructed a bandpass filter using TEM parallel-coupled lines in comb geometry of figure 1.2. In this structure, lines 1 to n and their associated lumped capacitances C_1^s to C_n^s, constitute resonators. In this type of filters lines 0 and n+1 (i.e., the input and output lines) are not resonators, they are part of impedance transforming sections on the input and output sides of the filter. The presence of the capacitance C_k^s at the end of each resonator reduce the line-length of the resonator to less than $\lambda_0/4$ long at midband frequency. The tested result of the construrcted filter gave very good results. According to Matthaei [27] such parallel coupled bandpass filters are i) compact, ii) have strong stop-bands and the stop-band above the primary pass-band can be made to be very broad. Matthaei [27] claimed that if desired this type of filter can be designed to have steep rate of cutoff on the high-side of the pass-band and also adequate coupling can be maintained between resonator elements with sizeable spacings between resonator lines. Another advantage is that filters of this type can usually be fabricated without the use of dielectric support materials so that if desired, dielectric losses can be eliminated.

In early 1969 Rhodes[28] presented a new design technique for elliptic function bandpass filters fabricated using parallel-coupled stepped digital TEM-lines. This design method is for narrow-band bandpass TEM line elliptic function filters. In this design the filter synthesis results in two networks of parallel coupled resonators connected in shunt. When the two networks are connected together then the two resonators of i^{th} line appear as a single resonator with an impedance stepped at the center and open circuited at one end. Later, in 1969, Rhodes[29] presented another design technique for elliptic function bandpass filters which in

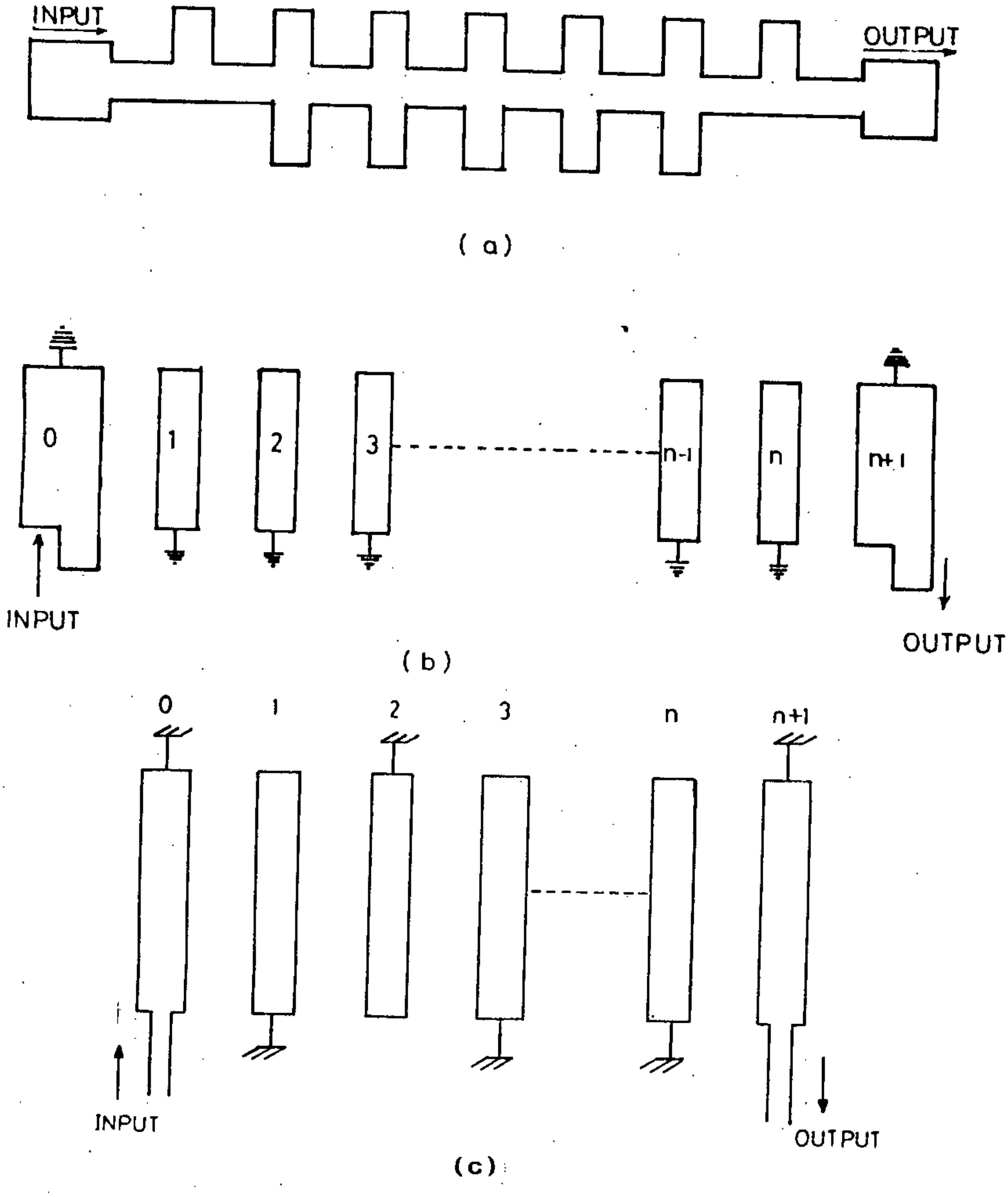

Figure 1.1. Different configurations of parallel coupled lines for realizing bandpass filters. (a) Short circuited stubs connected to a mainline, (b) comblines, (c) interdigital lines.

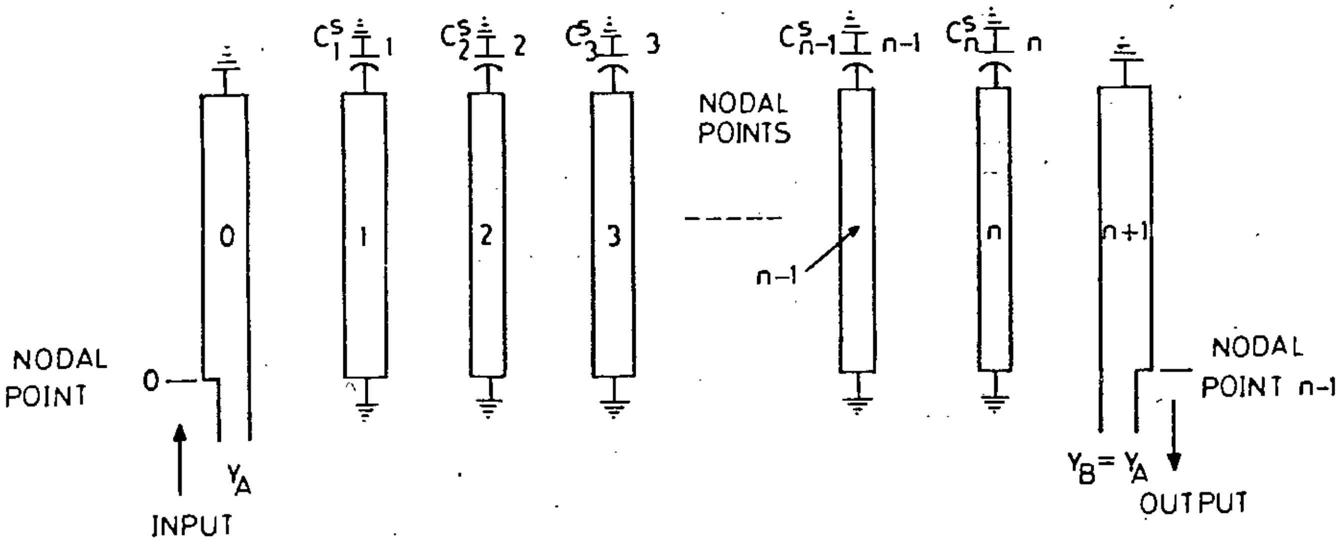

Figure 1.2. A Combline bandpass filter

appearance similarity with the above mentioned filter except that both the ends of the resonators are short circuited to ground and that the combined length of a single resonator is half wavelength long at centre frequency. The design method of Rhodes [29] requires obtaining two characteristic admittance matrices for two digital n number of coupled lines from the low-pass prototype element values. In this method the normalized impedance values of the elements in the filter are all of order of unity and independent of the actual band-width of the filter except for input and output transformer elements. A numerical example and experimental results of a seventh-degree 1-per cent bandwidth filter with center frequency at 3.7 GHz was presented in this [29] paper. These filters demonstrated significant improvements over-most of the other forms of microwave TEM-line narrow-band bandpass filter. An import feature of these filters [28][29] is compactness and inherent physical rigidity which makes these attractive for applications where size, weight and stabilty under mechanical vibrations are important. The unfavourable factor of the structure is its difficulty in fabricating without appropriate and precision tools.

1.2 Objective of this research

The first objective of this work is to develop a design technique for microwave bandpass filters using coupled rectangular TEM lines in the interdigital configuration. The design method will be developed for Chabyshev response. The developed design method should be easy to use so that one can design a filter within short time by using a personal computer. The second objective is to prepare a computer program with the help of which one can obtain the line parameters of a filter by simply providing the lowpass prototype element values as input. The final objective is to verify the validity of the design method by designing and fabricating an experimental filter and measuring its performances.

1.3 Brief introduction to this work

In chapter 2, discussions on impedance and admittance inverters are presented. By applying the concept of admittance inverters the technique of obtaining a Chebyshev lumped lowpass prototype is modified to another lowpass network containing J-inverters and shunt capacitances.

In chapter 3, analyses of a pair of interdigital lines and an array of interdigital lines are presented. Using these circuits, the equivalent circuit of one type of interdigital bandpass filter is presented.

In chapter 4, the analytical expression for power loss ratio and insertion loss of a filter are presented. The insertion loss function for Chebyshev response of a filter is presented. A transformation which transforms the lowpass insertion loss characteristic to bandpass insertion loss characteristic is also presented. A criteria for selecting filter complexity number n is also presented.

In the first part of chapter 5, relationships between the modified lowpass circuit containing the J-inverter of chapter 2 and the two wire equivalent circuit of the distributed interdigital bandpass filter of chapter 3 are established. The second part of the chapter deals with developing the design equations of the interdigital bandpass filter.

Chapter 6 deals with the procedure of obtaining physical dimensions of parallel coupled lines in the form of rectangular lines between ground planes from self and mutual capacitances.

Chapter 7 deals with the procedure of designing interdigital bandpass filters using the equations derived and presented in chapter 5. A design example and results of design computation for the same lowpass prototype filter for various bandwidth values are also presented.

In chapter 8, the process of fabricating an experimental interdigital filter is briefly presented.

Chapter 9 deals with the procedure of measuring insertion loss of the experimental filter at discrete frequency points and obtaining plots of insertion loss characteristic of the experimental filter.

Discussions on the measured results of the experimental filter are presented in chapter 10. Suggestions for future work are also presented in this chapter.
conversion of the prototype filter circuit using admittance inverters has been taken into account.

Chapter 2

Equivalent circuits of a lowpass prototype using impedance and admittance inverters

2.1 Introduction

This work deals with microwave bandpass filters using coupled TEM lines in interdigital configuration. The technique which will be used for developing the design equations for this type of filter will require converting lumped lowpass prototypes containing both capacitances and inductances into equivalent networks containing admittance inverters and capacitances or impedance inverters and inductances. In this chapter the concepts of impedance and admittance inverters and their properties are discussed. By applying these concepts the equivalent circuits of lumped lowpass prototypes are presented. The analytical relationship between the inverter parameters and the lowpass prototype element values are also presented. The equivalent circuits and the relationships will be used later to develop the design equations.

2.2 Definitions of impedance and admittance inverters

Impedance inverters and admittance inverters are the well known [18] types of inverter networks. The impedance inverters are known as K-inverters and the admittance inverters are known as J-inverters. An idealized impedance inverter operates like a quarter-wavelength line of characteristic impedance K at all frequencies [18]. Therefore, if it is terminated in an impedance Z_1 on one end, the impedance Z_i seen looking in at the other end is

$$Z_i = K^2 / Z_1 \qquad (2.1)$$

An idealized admittance inverter is defined as the admittance representation of the above case, i.e., it operates like a quarter-wavelength line of characteristic admittance J at all frequencies [18]. This means, if an admittance Y_1 is connected at one end, the admittance Y_i seen looking in the other end is

$$Y_i = J^2 / Y_1 \qquad (2.2)$$

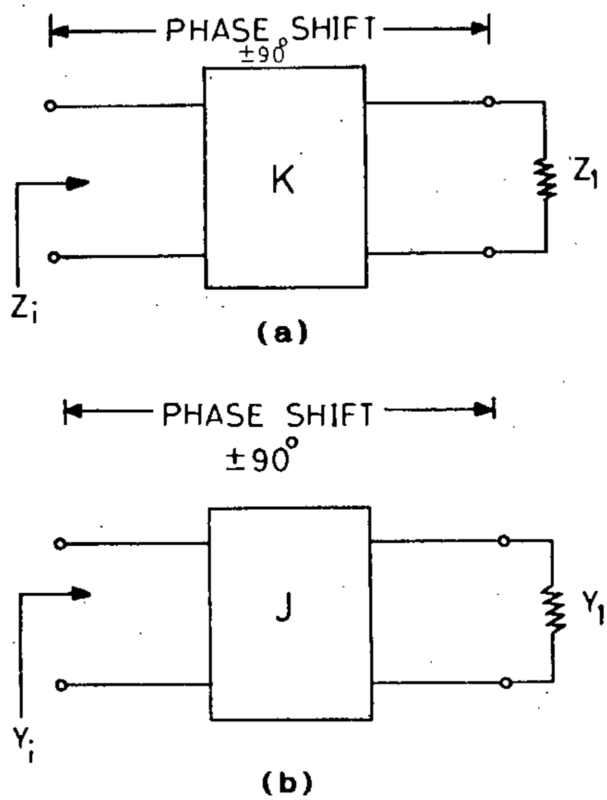

Figure 2.1. Impedance and admittance inverters. (a) A K-inverter with a terminating impedance Z_1. (b) A J- inverter with a terminating admittance Y_1.

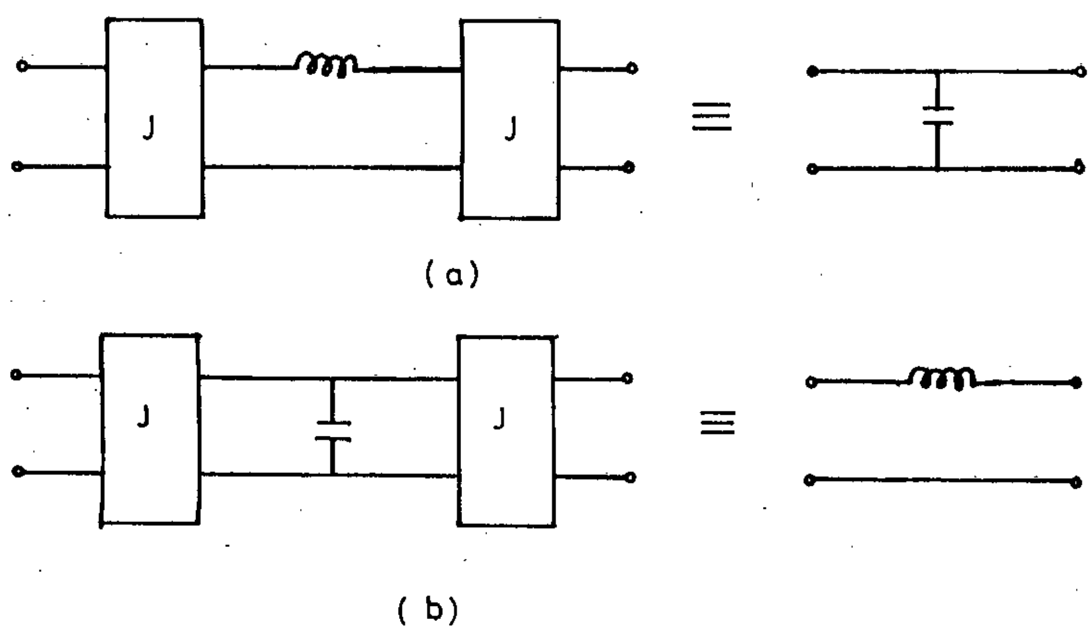

Figure 2.2. Equivalent circuits of series inductor with J-inverters and shunt capacitor with J inverters. (a) A series inductance between two admittance inverters and the equivalent circuit. (b) A shunt capacitance between two admittance inverters and the equivalent circuit.

2.3 Properties of inverters

The properties of inverters may be listed as follows.

Firstly, an ideal inverter may have an image phase shift of either ±90 degrees or even multiple thereof.

Secondly, because of inverting action, a series inductance with an inverter on each side looks like a shunt capacitance from its external terminals. Likewise, a shunt capacitance with an inverter on both sides looks like a series inductance from its external terminals. These equivalences are shown in figure 2.2.

Thirdly, the inverters have the ability to shift the impedance or admittance level depending on the choice of K or J parameters.

Making use of the above properties, a lowpass prototype circuit shown in figure 2.3(a) can be converted into either of the equivalent forms shown in figure 2.3(b) or (c). The prototype as well as these equivalent forms have identical characteristics provided the inverter parameters are defined appropriately.

2.4 Derivation of inverter parameters for a lowpass prototype filter

It is necessary to establish analytical relationships between the circuit parameters of the lowpass prototype of figure 2.3(a) and the same of the equivalent circuits of figure 2.3(b) and 2.3(c). A fundamental way of deriving these equations is to extract relation between the prototype circuit and the corresponding circuits using inverters by applying the concept of duality. A given circuit as seen through an admittance inverter looks like the dual of that given circuit. Thus, the admittances seen from the capacitor C_{a1} in figure 2.3(b) are the same as those seen from the capacitor C_1 in figure 2.3(a), except for an admittance scale factor. Similarly, the admittances seen from capacitor C_{a2} in figure 2.3(b) are identical to those seen from capacitor C_2 in figure 2.3(a), except for a possible admittance scale change. In this manner, the admittances in any point of the modified circuit in figure 2.3(b) may be quantitatively related to the corresponding admittances of the circuit shown in figure 2.3(a). In the present work of interdigital filter design method the J-inverters will be used in the equivalent circuit of the

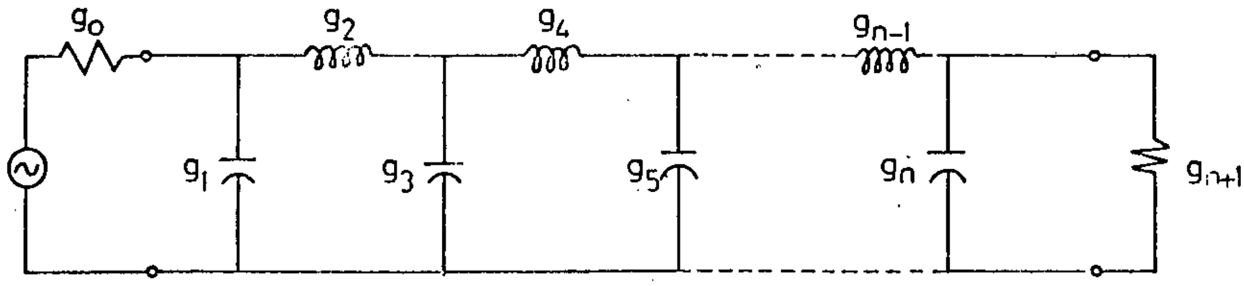

(a)

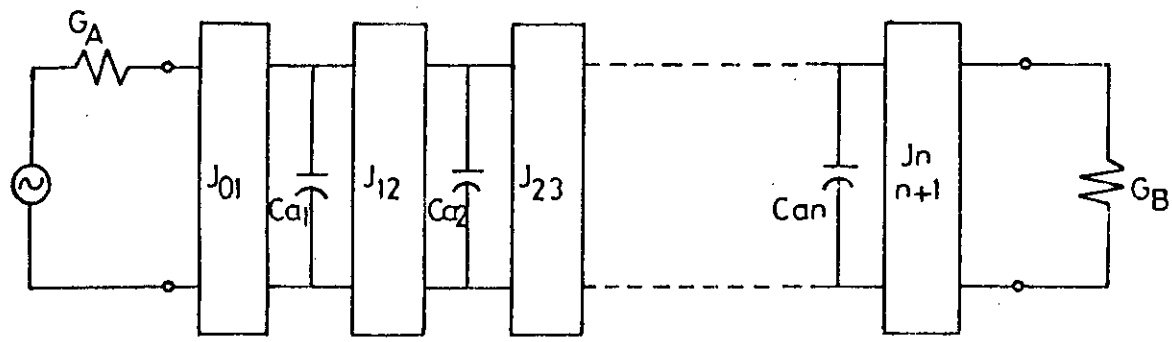

$J_{01}=\sqrt{\{G_A C_{a1}/(g_0 g_1)\}}$, $J_{k\;k+1}|_{k=1 \text{ to } n-1}=\sqrt{\{C_{ak+1} C_{ak}/(g_{k+1} g_k)\}}$,

$J_{n\;n+1}=\sqrt{\{(G_B C_{an})/(g_n g_{n+1})\}}$

(b)

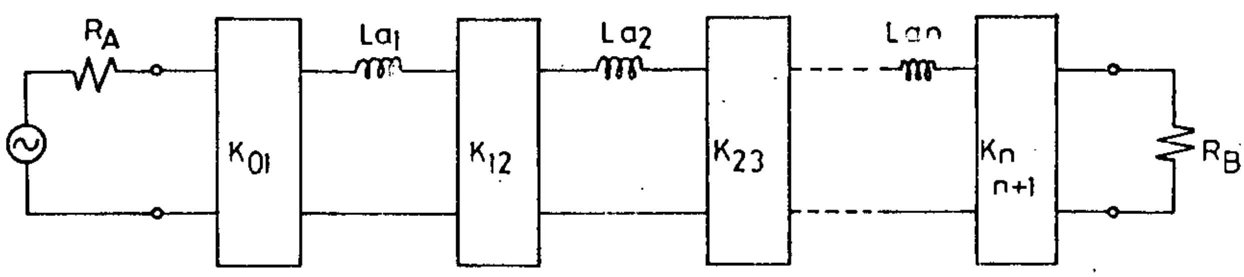

$K_{01}=\sqrt{\{R_A L_{a1}/(g_0 g_1)\}}$, $K_{k\;k+1}|_{k=1 \text{ to } n-1}=\sqrt{\{L_{ak+1} L_{ak}/(g_{k+1} g_k)\}}$,

$K_{n\;n+1}=\sqrt{\{(R_B L_{an})/(g_n g_{n+1})\}}$

(c)

__Figure 2.3.__ A generalized lowpass prototype circuit for Chebyshev response and its Equivalent forms using inverters. (a) A generalized lowpass prototype circuit for Chebyshev response. (b) The lowpass prototype of (a) converted into a network containing admittance inverters and shunt capacitances. (c) The lowpass prototype of (a) converted into a network containing impedance inverters and series inductances.

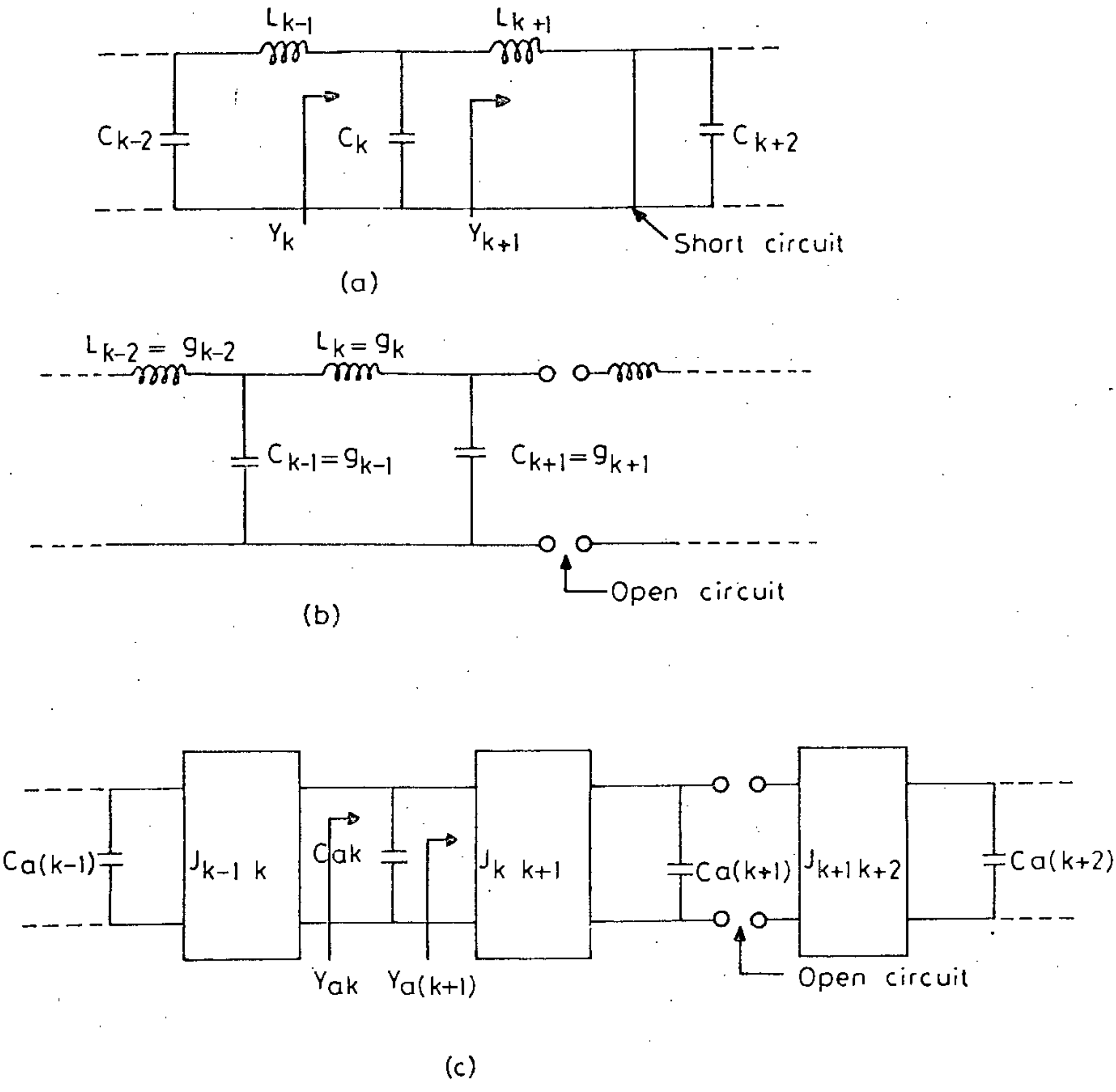

<u>Figure 2.4.</u> Converting a lowpass prototype with an applied short circuit into equivalent forms for deriving equations. (a) A portion of the prototype filter circuit with a short circuit applied after L_{k+1}. (b) Dual circuit of (a). (c) Analogue form of (a) with J-inverter.

lowpass prototype. Therefore, the equations in terms of J-inverter parameters will only be presented here. However, the equation for the K-inverter parameters can also be derived in a similar manner considering impedances instead of admittances.

Figure 2.4(a) shows part of a lowpass prototype circuit with a short circuit applied at just after the inductor L_{k+1}. The dual circuit of figure 2.4(a) is shown in figure 2.4(b) where it may be seen that the short circuit of figure 2.4(a) becomes an open circuit in dual case. The corresponding circuit using J-inverters is shown in figure 2.4(c). The circuits in figure 2.4 will be convenient for deriving the formulas for J_{kk+1} interms of C_{ak}, C_{ak+1} and the prototype element values gk and g_{k+1}. Short and open circuits will be introduced as per necessity to derive these equations.

From figure 2.4(a) we see that

$$Y_k = j\omega C_k + 1/(j\omega L_{k+1}) \tag{2.3}$$

and from figure 2.4(c)

$$Y_{ak} = j\omega C_{ak} + (J^2_{kk+1})/(j\omega C_{ak+1}) \tag{2.4}$$

For equivalence Y_{ak} must be indentical to Y_k except for an admittance scale factor of C_{ak}/C_k. This means

$$Y_{ak} = (C_{ak}/C_k)Y_k \tag{2.5}$$

Now, replacing Y_k in equation (2.3), we get

$$Y_{ak} = j\omega C_{ak} + C_{ak}/(C_k\ j\omega L_{k+1}) \tag{2.6}$$

Equating the right hand sides of equations (2.4) and (2.6) and after rearranging we get

$$J_{kk+1} = \sqrt{(C_{ak+1}C_{ak})/(C_k L_{k+1})} \tag{2.7}$$

Since $L_{k+1} = g_{k+1}$ and $C_k = g_k$, equation (2.7) becomes

$$J_{kk+1} = \sqrt{(C_{ak+1}C_{ak})/(g_k g_{k+1})} \tag{2.8}$$

The calculation of the J's for all the inverters except those at either ends, would be done in a similar manner by moving the short and open circuit points accordingly. Equation (2.8) applies for k = 1,2,3,.....,n-1.

For the end sections, considering figure 2.5(a) and 2.5(b) we may write

$$Y_n = j\omega C_n + 1/\ R_{n+1} \tag{2.9}$$

and, $$Y_{an} = j\omega C_{an} + J^2_{nn+1}/G_B \tag{2.10}$$

Since, Y_{an} must equal Y_n within a scale factor of C_{an}/C_n, it implies that,

$$Y_{an} = (C_{an}/C_n)Y_n \tag{2.11}$$

Therefore,

$$Y_{an} = j\omega C_{an} + C_{an}/(C_n\ R_{n+1}) \tag{2.12}$$

Comparing equations (2.10) and (2.12), we get after simplification

$$J_{nn+1} = \surd\ (C_{an}\ G_B)/(C_n\ R_{n+1}) \tag{2.13}$$

Replacing C_n and R_{n+1} in equation (2.13) by g_n and g_{n+1} it becomes,

$$J_{nn+1} = \surd\ (C_{an}\ G_B)/(g_n\ g_{n+1}) \tag{2.14}$$

The inverter parameter J_{01} at the other terminal can also be determined in a like manner considering the input end portion of the prototype circuit along with the J-inverter. Therefore, the parameter can be written as,

$$J_{01} = \surd\ (C_{a1}\ G_A)/(g_0\ g_1) \tag{2.15}$$

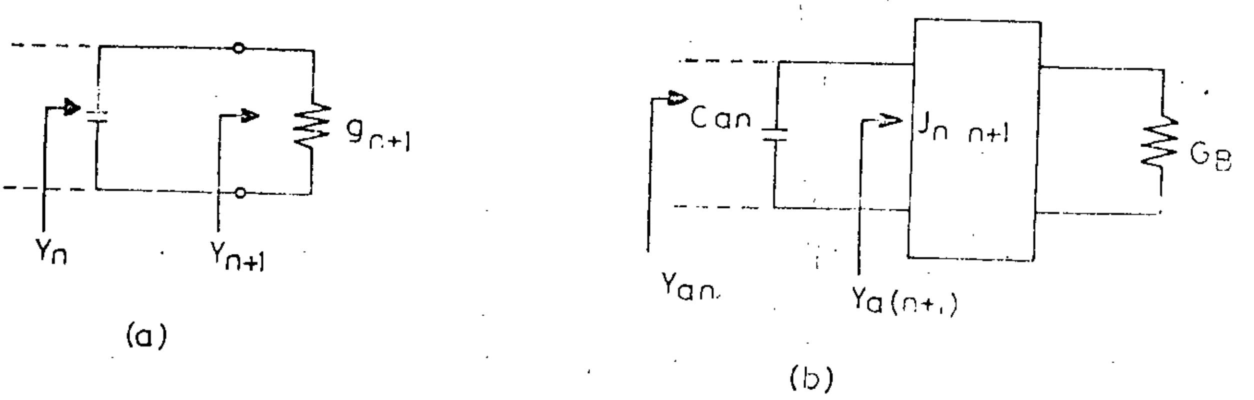

Figure 2.5. Converting the terminated section of the prototype into equivalent circuit containing inverters. (a) Terminated section of the prototype. (b) Equivalent circuit with J-inverter.

2.5 Practical realization of K and J inverters

A quarter- wavelength line of transmission line is one of the simplest forms of inverters. It obeys the basic impedance or admittance definitions presented in section 2.2. It will have either an impedance inverter parameter of $K = Z_0$ ohms where Z_0 is the characteristic impedance of the quarter- wavelength line or an admittance inverter parameter $J = Y_0$ where Y_0 is the characteristic admittance of the line. For this type of inverters the inverter properties are relatively narrowband in nature. As a result quarter- wavelength line can be used satisfactorily as an impedance or admittance inverter in narrow-band filters. Thus, if we have six identical cavity resonators, and if we connect them by lines which are a quarter- wavelength long at frequency ω_0, then by properly adjusting the coupling at each cavity it is possible to achieve a six resonator Chebyshev response.

Besides this, there are numerous other circuits which operate as inverters. All necessarily give an image phase of some odd-multiple of ±90 degrees, and may have good inverting properties over a much wider bandwidth than that of a quarter wavelength line. Figure 2.6 shows four inverting circuits which are used specially as K-inverters i,e., the inverters to be used with series type resonators. Inverters in figure 2.6(a) and (b) are used particularly in the circuits where the negative L or C can be absorbed into adjacent positive series elements of the same type so as to give the resulting circuit having all positive elements. The inverters shown in figure 2.6(c) and (d) are also particularly useful in circuits where the line of positive or negative electrical length θ shown in figures can be added to or subtracted from adjacent lines of the same impedance. The overall image phase-shift of the circuit in figures 2.6(a) and (c) is -90 degrees while that of circuit in figures 2.6(b) and (d) is +90 degress The impedance inverter parameter K indicated in the figure is equal to the image impedance of the inverter network and is analogous to the characteristic impedance of a tansmission line.

Figure 2.7 shows four inverter circuits which can be used as J-inverters. It is obvious that these circuits are simply the dual

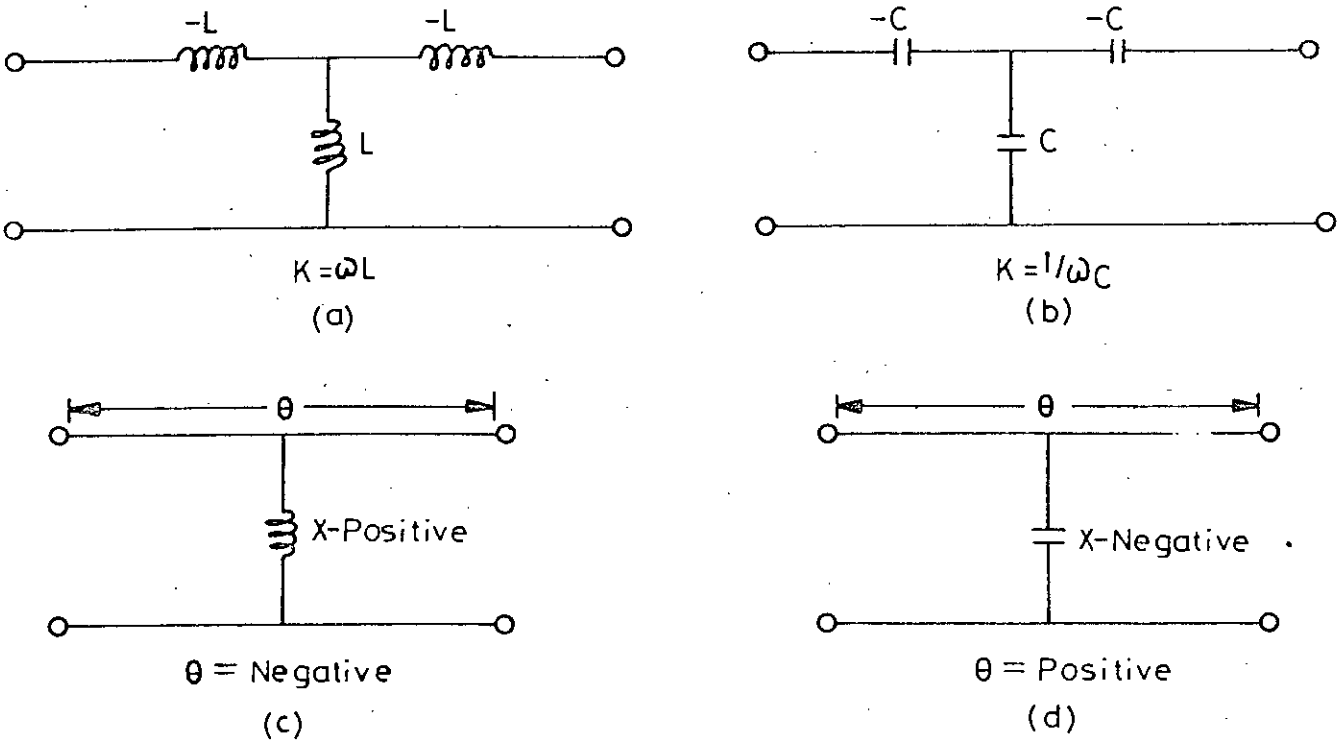

<u>Figure 2.6.</u> Four lumped element K- inverter circuits.

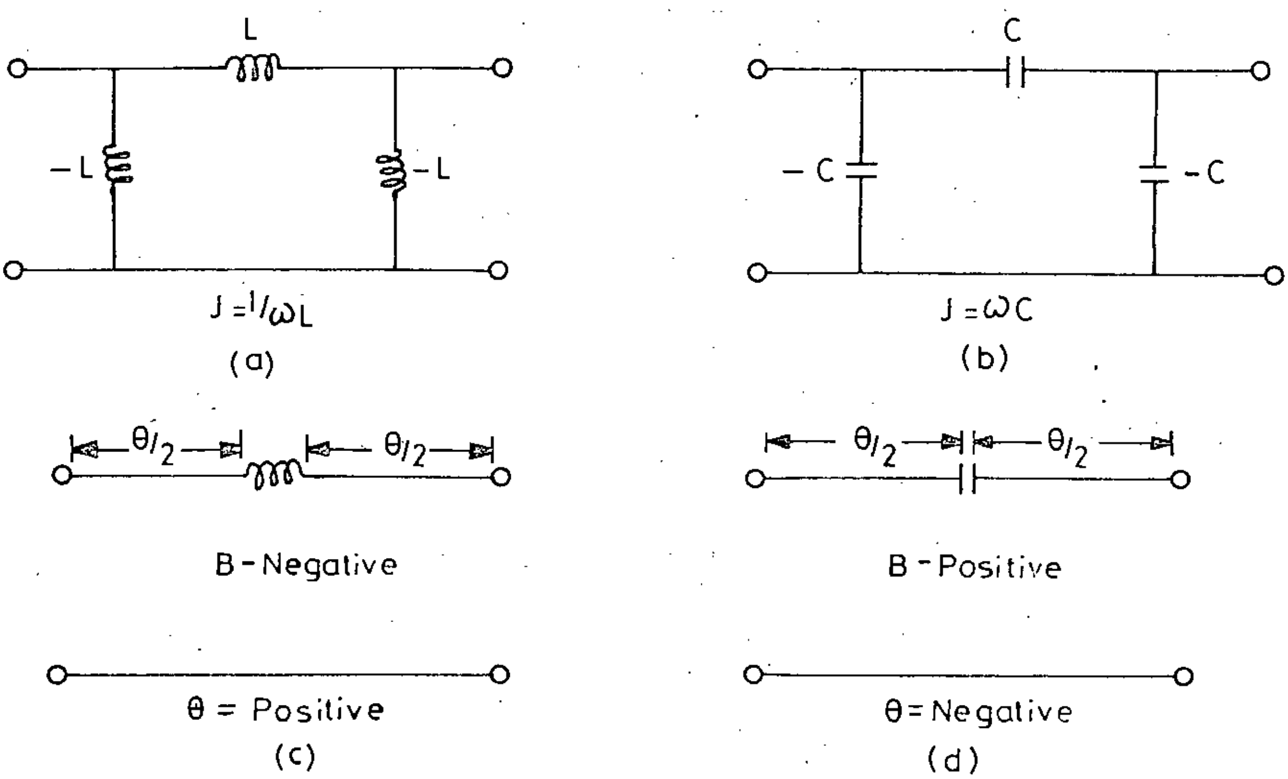

<u>Figure 2.7.</u> Four lumped element J- inverter circuits.

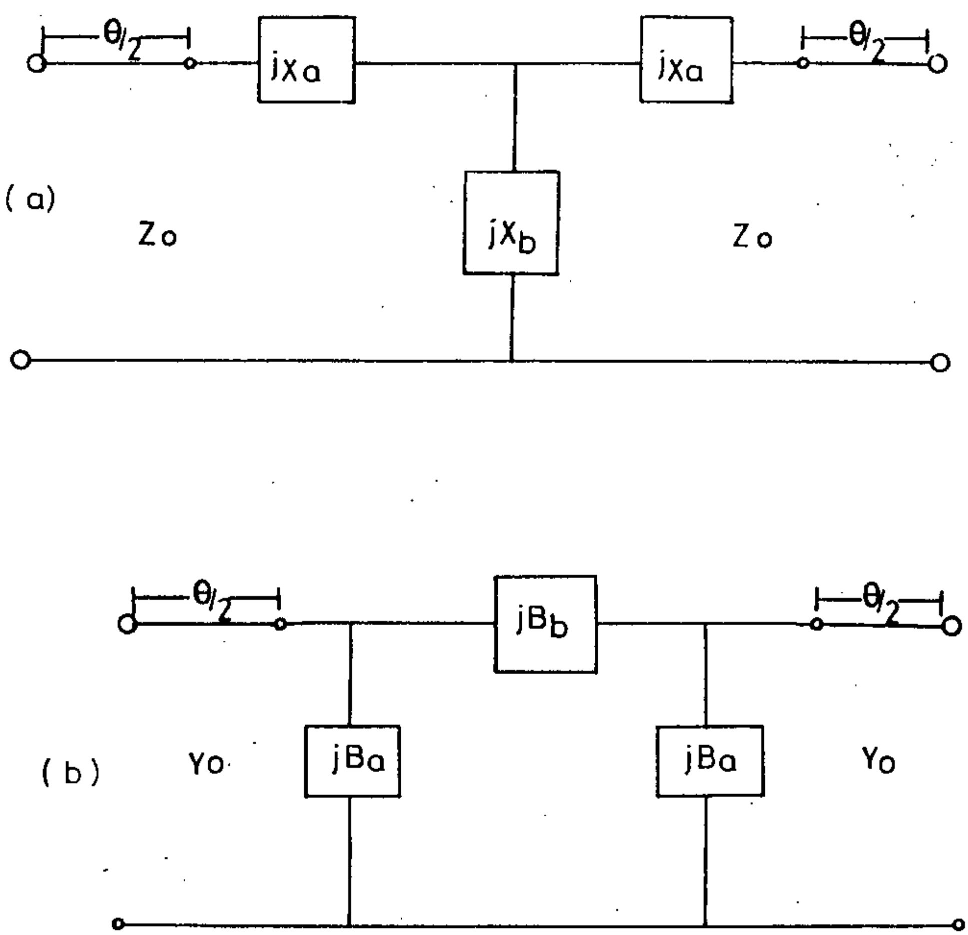

Figure 2.8. Two circuits representing inverter properties of certain discontinuities in transmission lines.

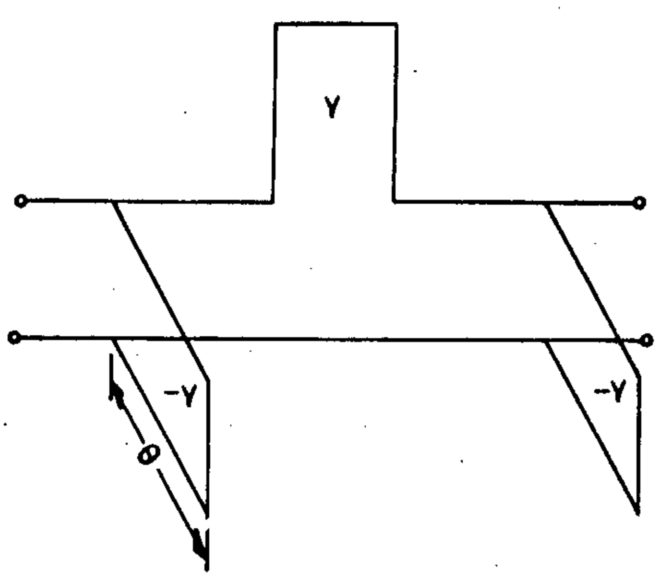

Figure 2.9. An admittance inverter formed by stubs of electrical length θ.

representation of the circuits of figure 2.6 and the inverter parameters J's are the image admittances of the inverter networks.

Figure 2.8 shows two more generalized circuits which may operate as inverters. These circuits are useful for computing the impedance inverting properties of certain types of discontinuities in transmission lines.

Another special form of admittance inverter composed of transmission line stubs of positive and negative characteristic admittance is shown in figure 2.9. The negative admittances of the stubs are in practice absorbed into adjacent lines of positive admittances.

A number of other circuits will operate as impedance or admittance inverters. The necessary requirements are that their image impedance must be real in the frequency band of operation, and that their image phase be some odd multiple of ±90 degrees.

2.6 Summary

The definitions and properties of admittance inverters as well as impedance inverters have been presented. Necessary equations have been presented which will enable one to convert a lowpass prototype into equivalent networks containing admittance inverters. Some useful practical forms of inverter networks have also been presented.

Chapter 3

Interdigital lines and their equivalent circuits

3.1 Introduction

It is necessary at this stage to explain the behaviour of coupled TEM lines in interdigital configuration since this will be the ultimate geometry of the filter under discussion. A main line of rectangular cross-section between two parallel ground planes is the type of TEM lines which will be used for fabricating these interdigital lines. Bolljahn and Matthaei [2] first indicated that interdigital lines have excellent bandpass filter properties. In order to make such a bandpass filter an array of coupled interdigital lines is needed. In this chapter analyses of a pair of interdigital lines and an array of interdigital coupled lines are presented. With the help of these circuits the equivalent circuits of two types of interdigital bandpass filters are also presented.

3.2 A pair of interdigital lines and its equivalent circuit

Figure 3.1(a) shows a schematic diagram of a pair of interdigital lines having two coupled lines of same cross-section. It may be seen that the two lines are alternately short and open circuited at their ends. Like other TEM parallel coupled lines, these interdigital lines are also parallel coupled and they are placed midway between a pair of parallel ground planes. This may be clearly seen from the cross sectional view of a pair of such interdigital lines presented in figure 3.1(c). This figure also shows the self capacitances and the different odd- and even- mode fringing capacitances. Further information on these capacitances will be presented in chapter 6.

Like other coupled lines here also one can obtain even- and odd- mode admittances or impedances [7] using these capacitances. The electrical equivalent circuit of the structure of figure 3.1(a) is available in references [18][19][26] and is presented in figure 3.1(b). For application in filters the electrical length of each short-circuited shunt stub and open-circuited connecting line

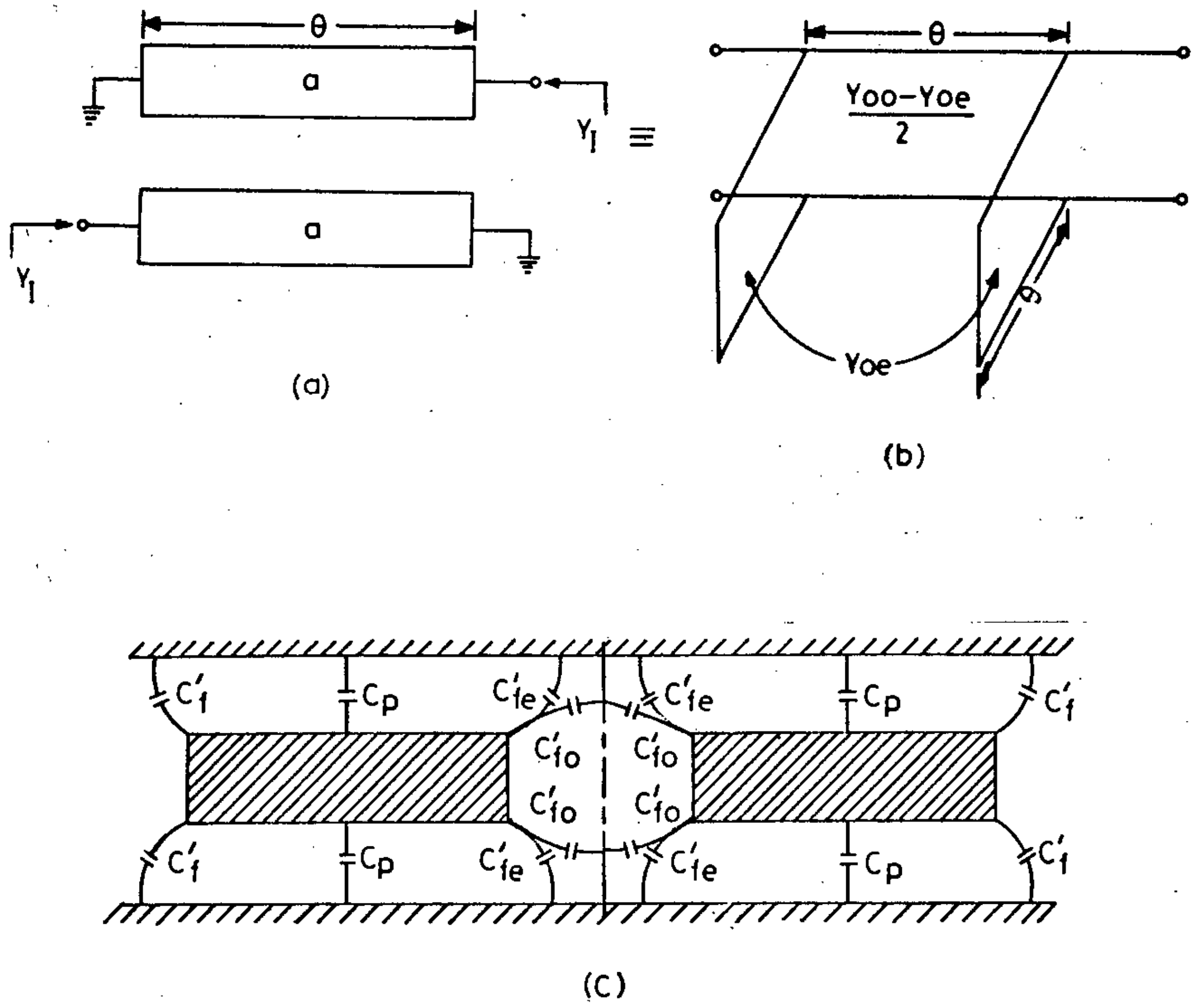

Figure 3.1. A pair of interdigital coupled lines of equal widths. (a) The main lines of two coupled lines of electrical length θ in interdigital geometry. (b) Equivalent circuit of (a). (c) Cross-section of (a) showing the various capacitances.

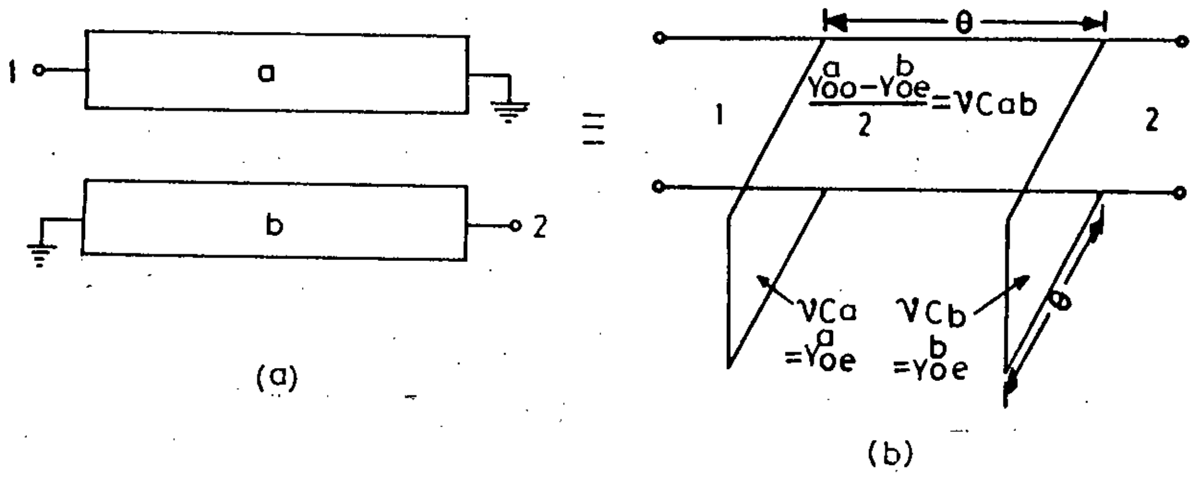

Figure 3.2. A pair of interdigital coupled lines of unequal widths. (a) The main lines of the two coupled lines of electrical length θ. (b) Equivalent circuit of (a).

of the circuit of figure 3.1(b) is quarter- wave at midband frequency. The characteristic admittances of shunt stubs and the connecting line are related to the odd- and even- mode admittances Y_{oo} and Y_{oe} respectively of the coupled lines. The characteristic admittance of each shunt stub is Y_{oe} and that of connecting line is $(Y_{oo} - Y_{oe})/2$.

A more generalized picture may be obtained if the two coupled lines of a pair of intertdigital lines are considered to be of different widths. This is shown in figure 3.2. The characteristic admittance of the two shunt connected short-circuited stubs for this case are [18][19] $Y_{oe}{}^{a}$ and $Y_{oe}{}^{b}$ and the characteristic admittance of the connecting line is $(Y_{oo}{}^{a} - Y_{oe}{}^{a})/2$. The lengths of shunt stubs as well as the connecting lines are same and equal to θ.

3.3 An array of interdigital lines and its equivalent circuit

Figure 3.3(a) shows an array of interdigital lines. In this case the widths of the lines may not be equal but the thickness (t) of all the lines are same. The various capacitances of this array of parallel coupled lines are shown in figure 3.3(b). Now for obtaining the electrical equivalent circuit of figure 3.3(a), we may first consider that the section between lines 2 and 4 exist i.e., only lines 2,3 and 4 exist in this array. Now, we may consider this section to be constructed with two equivalent sections. Each of these equivalent sections can now be seen as similar to the network of figure 3.1(b). On this basis the equivalent circuits for the line sections S_{23} and S_{34} are presented in figures 3.4(a) and 3.4(b). The characteristic admittances are also shown in figure 3.4. So the complete equivalent circuit of the section containing the three line array may now be obtained as shown in figure 3.4(c) by combining the two equivalent circuits of figure 3.4(a) and 3.4(b). Thus the characteristic admittance Y_3 of the shunt stub 3 has two components so that

$$Y_3 = (Yoe)_{23}^{s} + (Y_{oe})_{34}^{s} \qquad (3.1)$$

Thus the equivalent circuit of the array of interdigital lines of figure 3.3(a) can be obtained by following the above

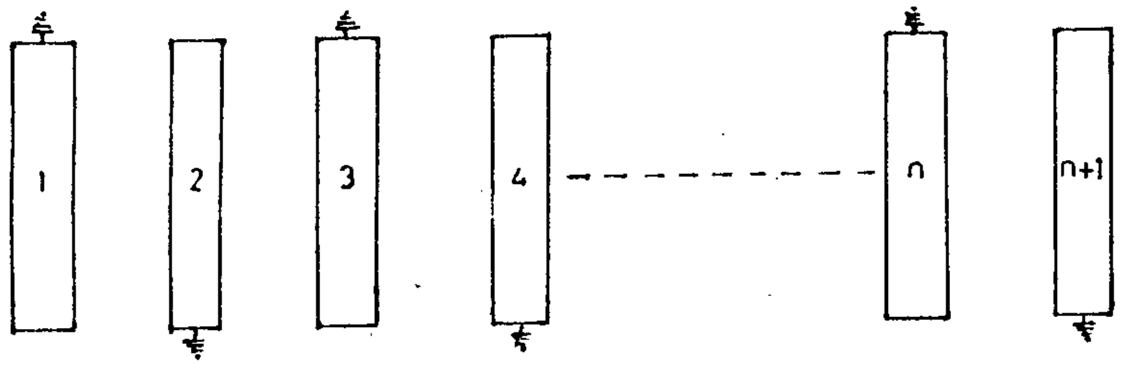

(a)

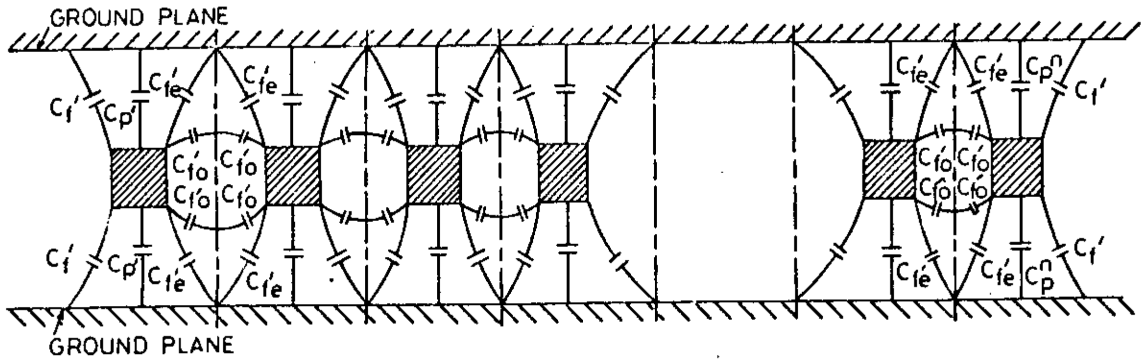

(b)

Figure 3.3. An array of interdigital coupled lines. (a) The main lines of the interdigital array. (b) Cross-sectional view of the coupled line array showing odd-mode, even-mode and fringing capacitances.

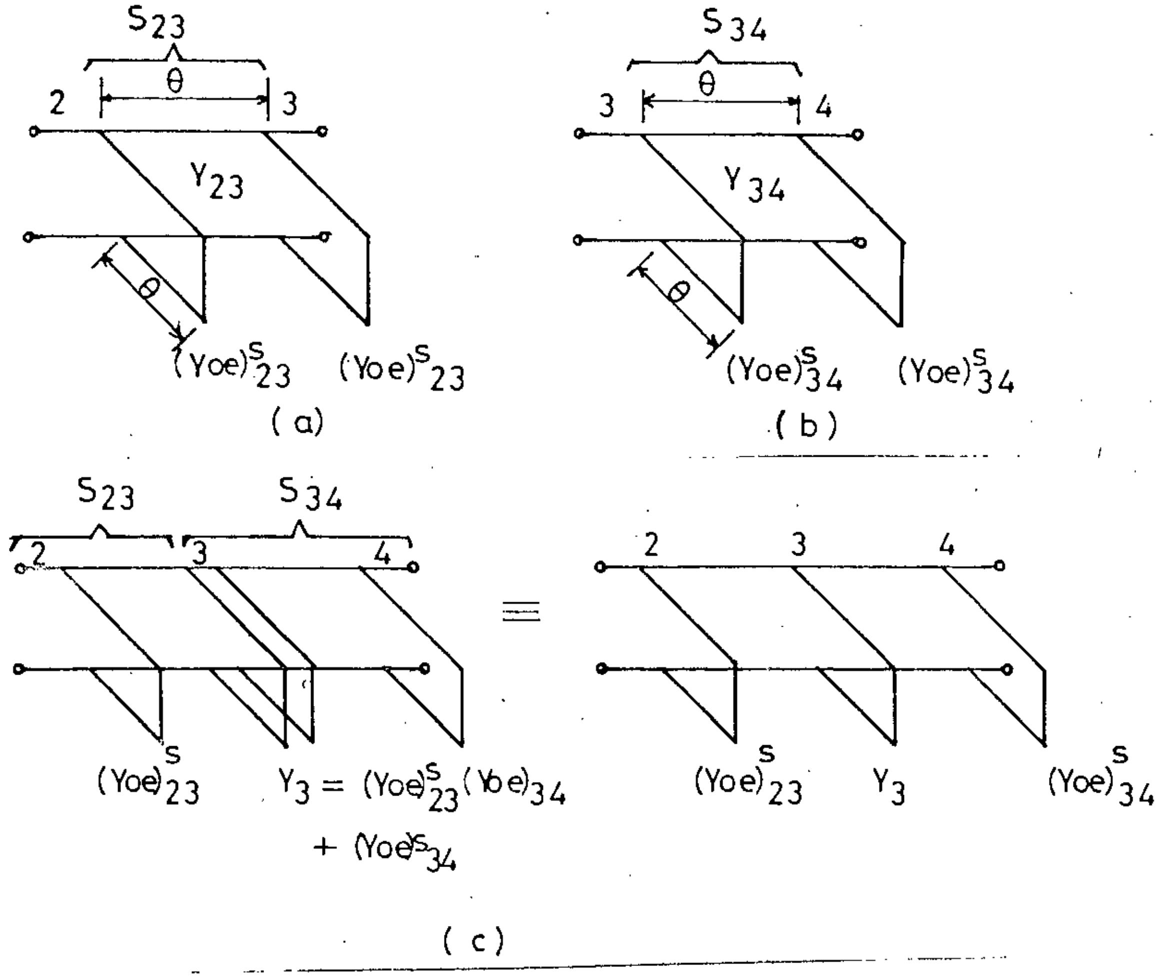

Figure 3.4. Development of equivalent circuit of a three coupled line section of an array of interdigital coupled lines. (a) The equivalent circuit of the interdigital section S_{23}. (b) The equivalent circuit of the interdigital section S_{34}. (c) Combined equivalent circuit of sections S_{23} and S_{34}

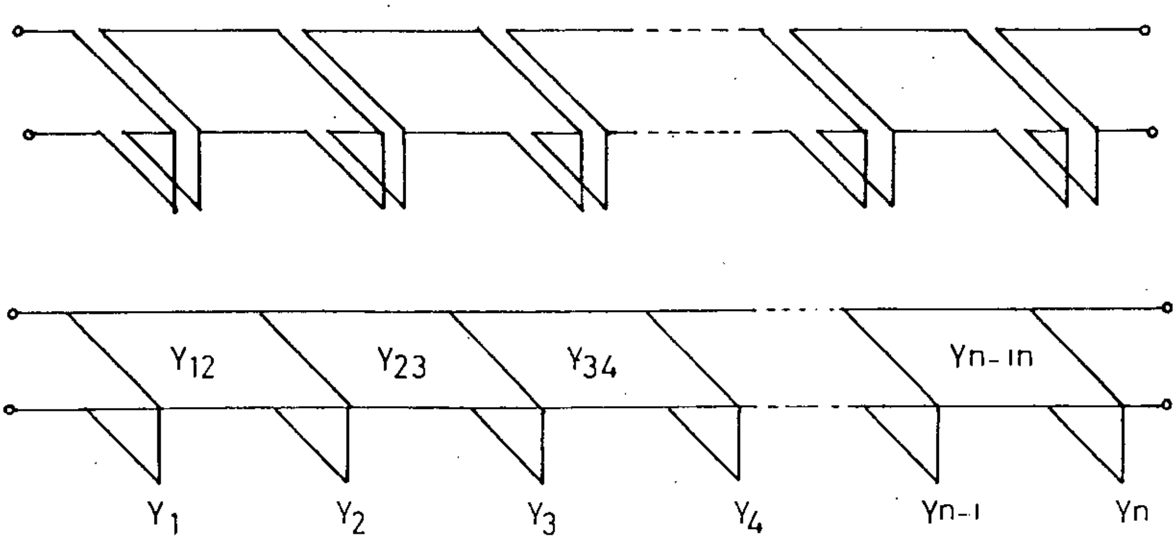

Figure 3.5. Equivalent circuit of the array of interdigital coupled lines of figure 3.3.

procedure. Figure 3.5 shows the complete equivalent circuit for the array.

3.4 Bandpass filter using an array of interdigital coupled lines

The equivalent circuit of figure 3.5 suggests that such an array of interdigital coupled lines will act as a bandpass filter if appropriate matching networks are added at the input and output ends. It has been shown by Matthaei [3] that by employing the arrangement of figure 3.5 one can achieve narrow band filter while the arrangement of figure 3.6(b) can give wideband filters.
From figure 3.3 and 3.6 one may observe that the interdigital filter structure is basically formed out of two comb-geometry structures. That is, the interdigital structure of figure 3.3 and 3.6 may the thought of made by interleaving two comb-line structures.

From the equivalent circuits of figure 3.7 it is now possible to understand that each line elements in the interior sections of the interdigital filters may be called a resonator supporting TEM-mode of propagation. Theoretically it is necessary that all resonators be made quarter- wave- length long at the midband frequency f_0. Coupling is achieved here through fringing fields between adjacent elements. For the structure shown in figure 3.6(a), the terminating elements i.e., the input and output lines of both ends act as impedance transformers rather than resonator. The second filter structure shown in figure 3.6(b) is similar to the structure shown in figure 3.6(a) except the input and output sections. In this second structure, the terminating lines are open-circuited instead of short-circuited and act as impedance transformers as well as resonators. The two short-circuited side walls are made apart exactly a quarter- wave- length long at the midband frequency f_0.

As mentioned above, theoretically the length of each resonator element should be equal to the separation of the two opposite ground side-walls. If this is done, practically both ends of each line are short circuited (instead of alternate shorts and opens) and the interdigital bandpass filter becomes a short circuited combline bandpass filter without reactive loading [2]. As a result, the bandwidth of such filter would shrink to zero .

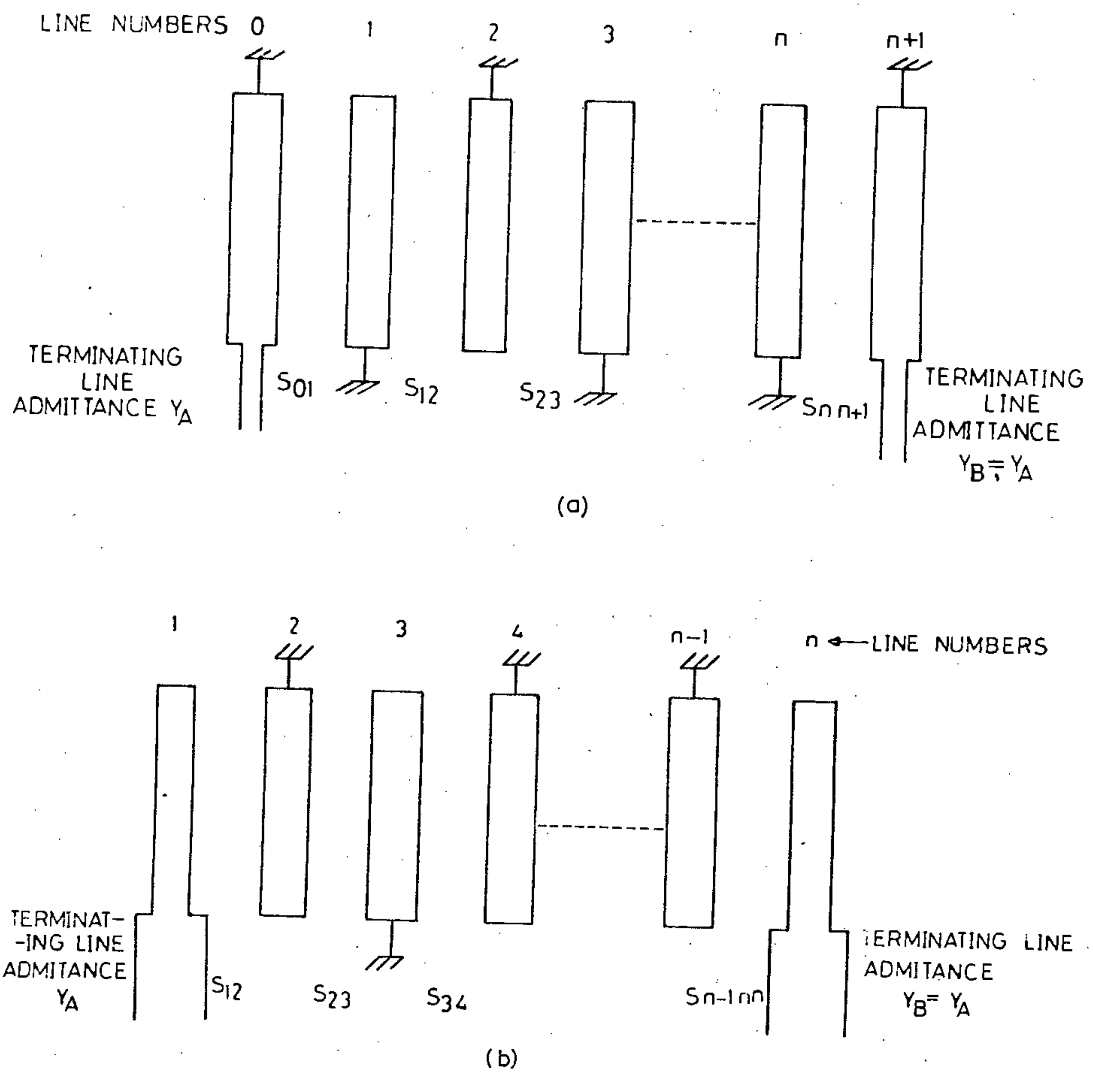

Figure 3.6. Schematic diagram showing the main lines of the two types of interdigital bandpass filters. (a) Interdigital bandpass filter with short circuited terminating lines for narrow to moderate bandwidth. (b) Interdigital bandpass filter with open circuited terminating lines for wide bandwidth.

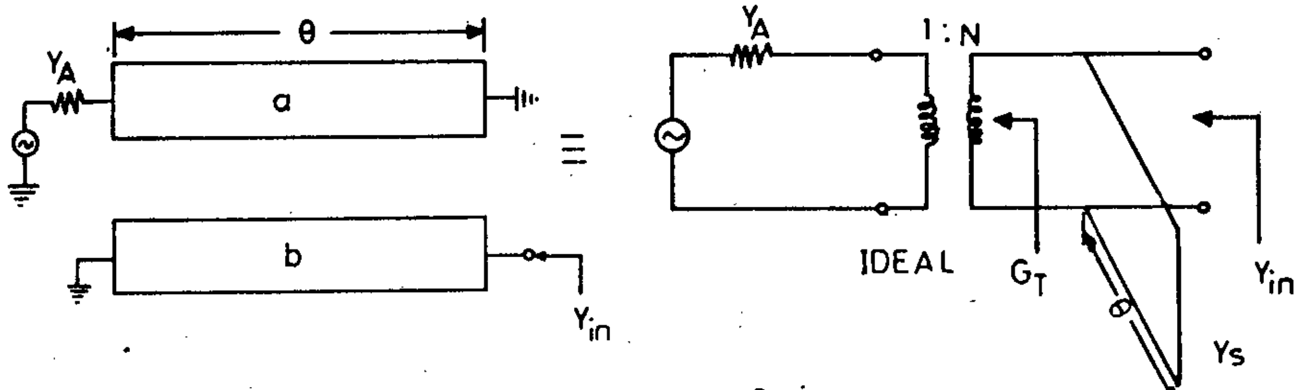

Special Constraint : $Y_{oe}^{a} + Y_{oo}^{a} = 2Y_A$

$$Y_{oo}^{a} = Y_A[\,G_T/Y_A + 1]$$
$$Y_{oe}^{b} = Y_s - Y_A[1 - G_T/Y_A] + Y_{oe}^{a}$$
$$Y_s = Y_A[N^2 - 1]/N^2 + Y_{oe}^{b} - Y_{oe}^{a}$$

N = Turn ratio

$$= 2Y_A/(Y_{oo}^{a} - Y_{oe}^{a})$$
$$G_T = Y_A/N^2$$

(a)

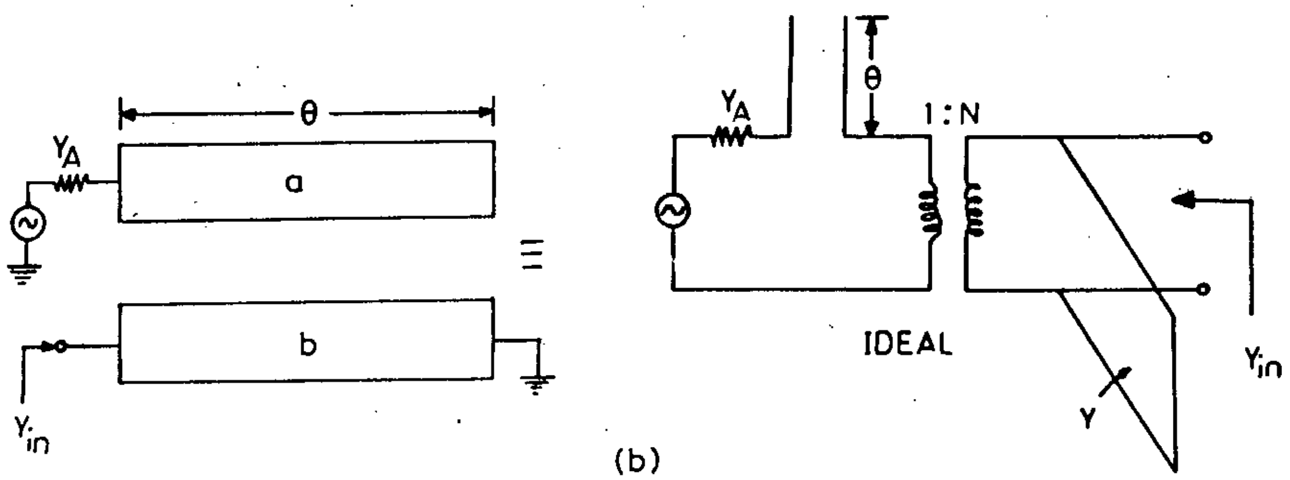

(b)

Figure 3.7. Equivalent circuits of the input output terminating sections. (a) Terminating section containing short circuited terminating lines and its equivalent circuit. (b) Terminating section containing open circuited terminating lines and its equivalent circuit.

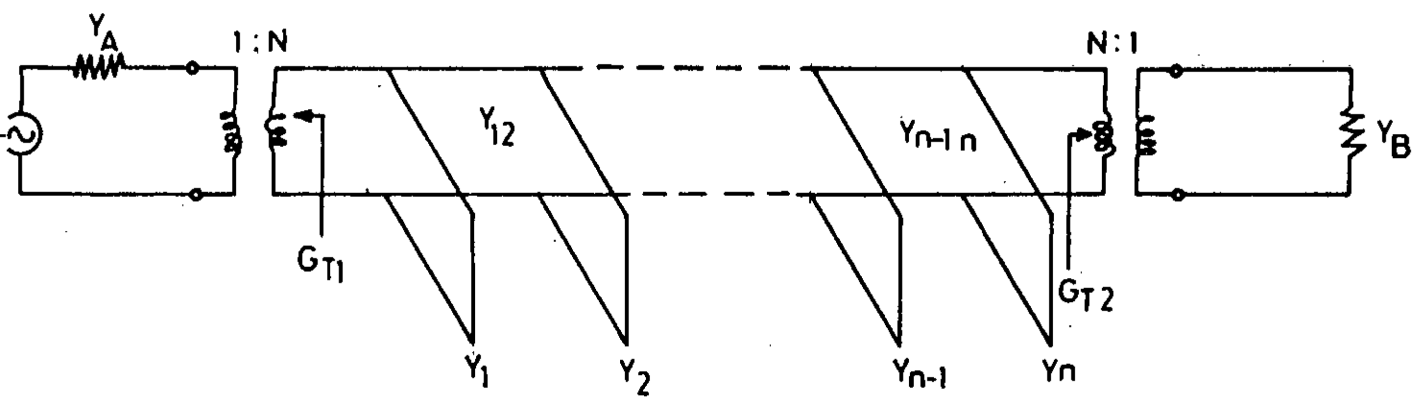

Figure 3.8. Equivalent two- wire circuit representation of the interdigital filter structure of figure 3.6(a).

band width i.e., the filter would go to stop-band at all frequencies.

To avoid this practical difficulty, resonator line-elements of interdigital filter are foreshortened at the open circuited ends by a small amount. The capacitance formed between the open-circuited end and the grounded side-walls maintain the resonant frequency at f_0. Satisfactory analytical method for determining the amount of foreshortening of the resonator length could not yet be established. An approximate method presented by Cohn [7] may be used to meet this situation.

3.5 Equivalent circuits of an interdigital filter

For obtaining the equivalent circuits of an interdigital filter it is necessary to add the equivalent circuits of the input and output tranformer matching and connecting sections to the equivalent circuit of the interdigital array of figure 3.5.

It is seen from the two interdigital banpass structures (figure 3.6) that they have different electrical connections at their terminating ends. The equivalent circuits of terminating sections for both type of filters are also different except that both the equivalent circuit contain ideal transformer. Our interest is mainly with section of figure 3.6(a). The equivalent circuit for the input/ output section of this structure is available in [18][19] and presented in figure 3.7. For the interior sections the equivalent circuit of figure 3.5 may be accepted. So by combining the equivalent circuit of figure 3.5 with the input/ output section equivalent circuits of figure 3.7 one can obtain the equivalent circuit of figures 3.8.

3.6 Summary

Starting with the equivalent circuits of a pair of coupled interdigital lines the equivalent circuit of an array of coupled interdigital lines has been developed. Using the known equivalent circuits of the input/ output terminating transformer sections the equivalent circuit of one type of interdigital bandpass filter have been presented. The necessity of foreshortening of the open circuited ends of the resonator elements has been explained.

Chapter 4

Insertion-loss characteristic and lowpass to bandpass transformation for interdigital filters

4.1 Introduction

The analytical expression for power loss ratio and insertion loss of a filter are presented. The insertion loss function for Chebyshev response of a lowpass prototype is presented. A transformation which transforms the lowpass insertion loss characteristic to bandpass insertion loss characteristic is also presented. This transformation gives a criteria for the choice of filter complexity n.

4.2 Power loss ratio and insertion-loss of a bandpass filter

Consider a lossless filter network connected between a source having internal resistance R and a load of resistance R as shown in figure 4.1. For this filter the power loss ratio P_{LR} is defined as the available power (incident power) divided by the actual power delivered to the load. If the incident power is P_i, the reflected power is $\rho^2 P_i$ and the power delivered to the load is $(1-\rho^2)P_i$ where ρ is the magnitude of reflection coefficient.

Therefore

$$P_{LR} = P_i/(1-\rho^2)P_i = 1/(1-\rho^2) \tag{4.1}$$

and $\rho = \sqrt{(P_{LR}-1)/P_{LR}}$ (4.2)

The insertion loss, measured in decibels, is

$$A = 10 \log_{10} P_{LR} \tag{4.3}$$

when the terminating load impedance equals the internal impedance of the generator at the input end. In general, the insertion loss is defined as the ratio of the power delivered to the load when connected directly to the generator to the power delivered when the filter is inserted. For a lossless filter and for the conditions stated above the insertion loss characteristic of a filter is the same as the attenuation characteristic.

It has been shown by Collin [30] that the power loss ratio may be expressed in terms of the input impedance parameters as

$$P_{LR} = 1 + M(\omega^2)/N(\omega^2) \tag{4.4}$$

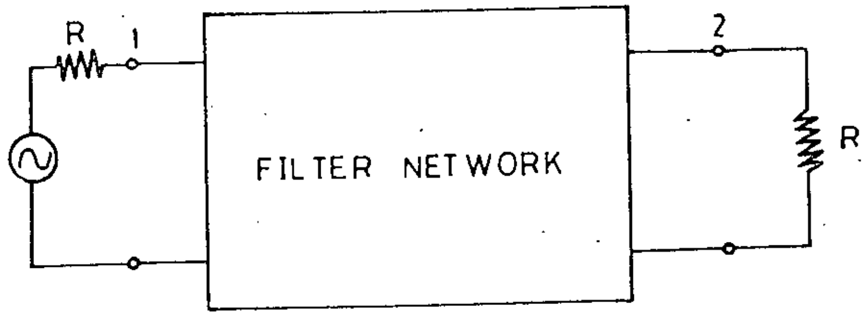

Figure 4.1. A circuit for defining power loss ratio and insertion loss.

As shown by Collin [30] $N(\omega^2)$ must be an even polynomial in ω so that we can write $N(\omega^2) = Q(\omega)^2$. Next denoting $M(\omega^2)$ by the even polynomial $P(\omega^2)$ we can write

$$P_{LR} = 1 + P(w^2)/Q(\omega)^2 \tag{4.5}$$

From equation (4.3) and (4.5) it is obvious that the insertion loss characteristic of a filter depends on the choice of the two polynomials $P(\omega^2)$ and $Q(\omega)^2$.

4.3 Chebyshev polynomial for power loss ratio

There are virtually an unlimitted number of different forms that could be specified for the power-loss ratio and be realized as a physical network. However,many of these networks could be anticipated to be very complex and hence of little practical utility. The power loss ratios that have been found most useful for microwave filter design are those that give a maximally flat response (Butterworth response) and those that give an equal ripple or Chebyshev response in the passband. For Butterworth response $Q(\omega)^2 = 1$ and $P(\omega^2) = k^2(\omega/\omega_c)^{2N}$ and for Chebyshev response $Q(\omega)^2 = 1$ and $P(\omega^2) = k^2T_N{}^2(\omega/\omega_c)$ where, $T_N(\omega/\omega_c)$ is the Chebyshev polynomial of degree N.

Figures 4.2(a) and (b) show the two attenuation characteristics of a lowpass prototype filter for Butterworth and Chebyshev responses. A bandpass filter characteristics for Chebyshev response is presented in figure 4.3. Because of the differences in the two characteristics, the design method for the two cases will be different. Therefore, for

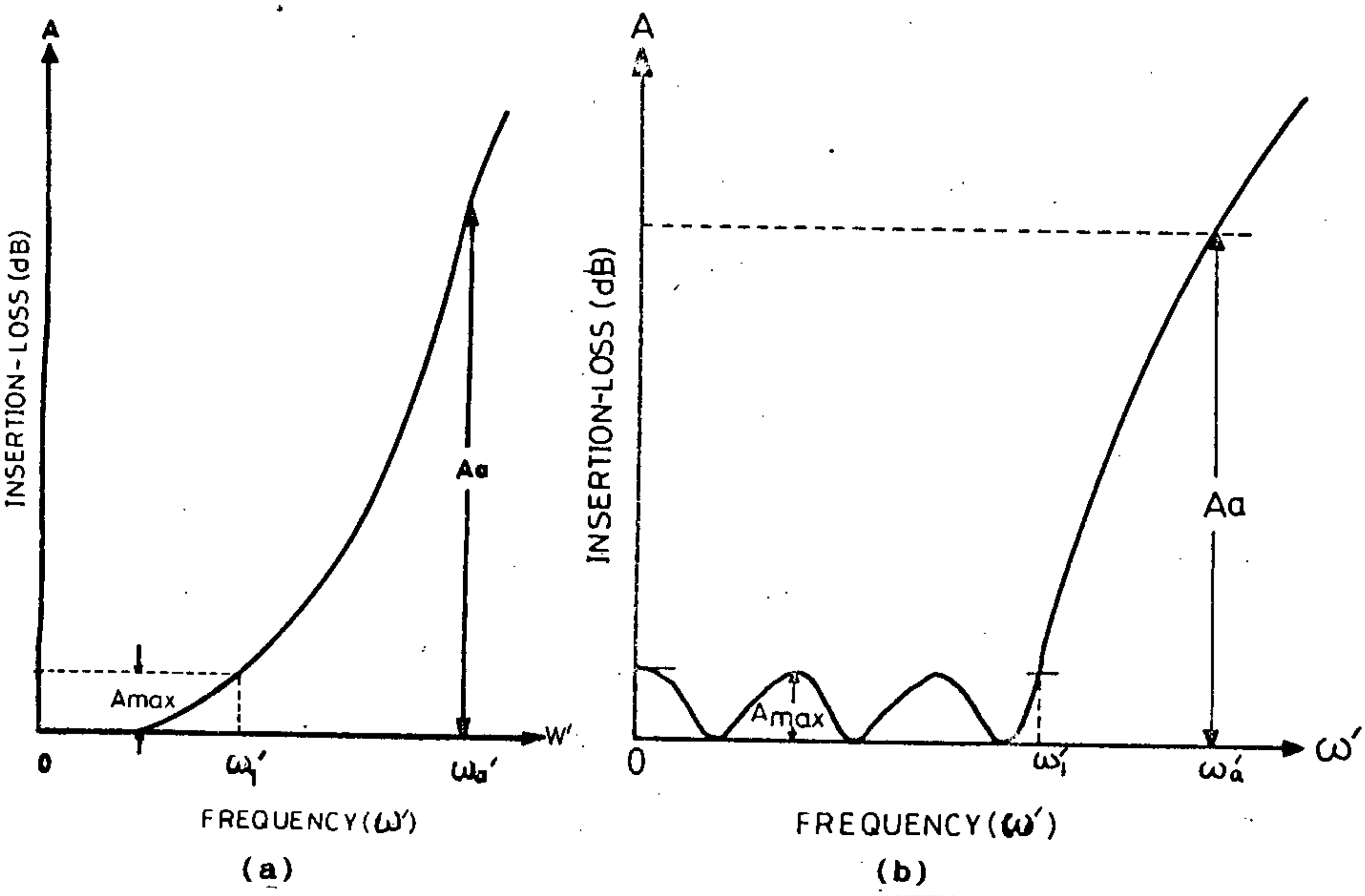

__Figure__ __4.2.__ Insertion loss characteristic of a lowpass filter. (a) For Butterworth response. (b) For Chebyshev response.

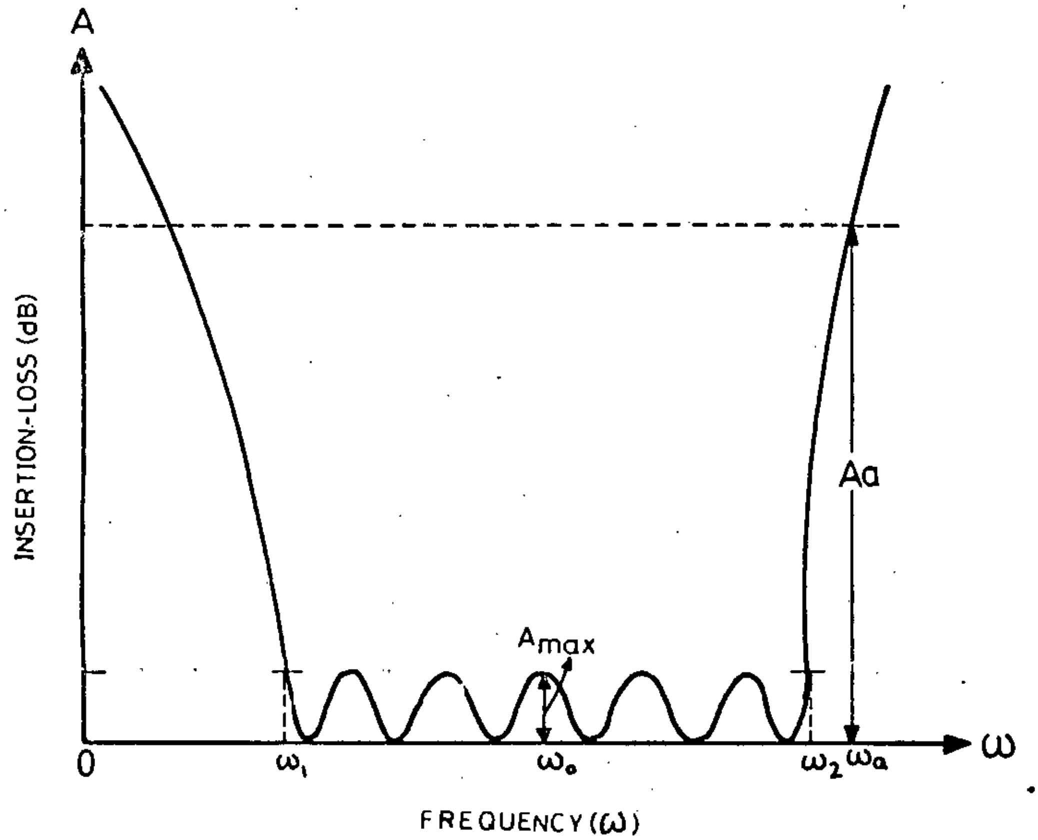

__Figure__ __4.3.__ Chebyshev Insertion loss characteristic of a bandpass filter.

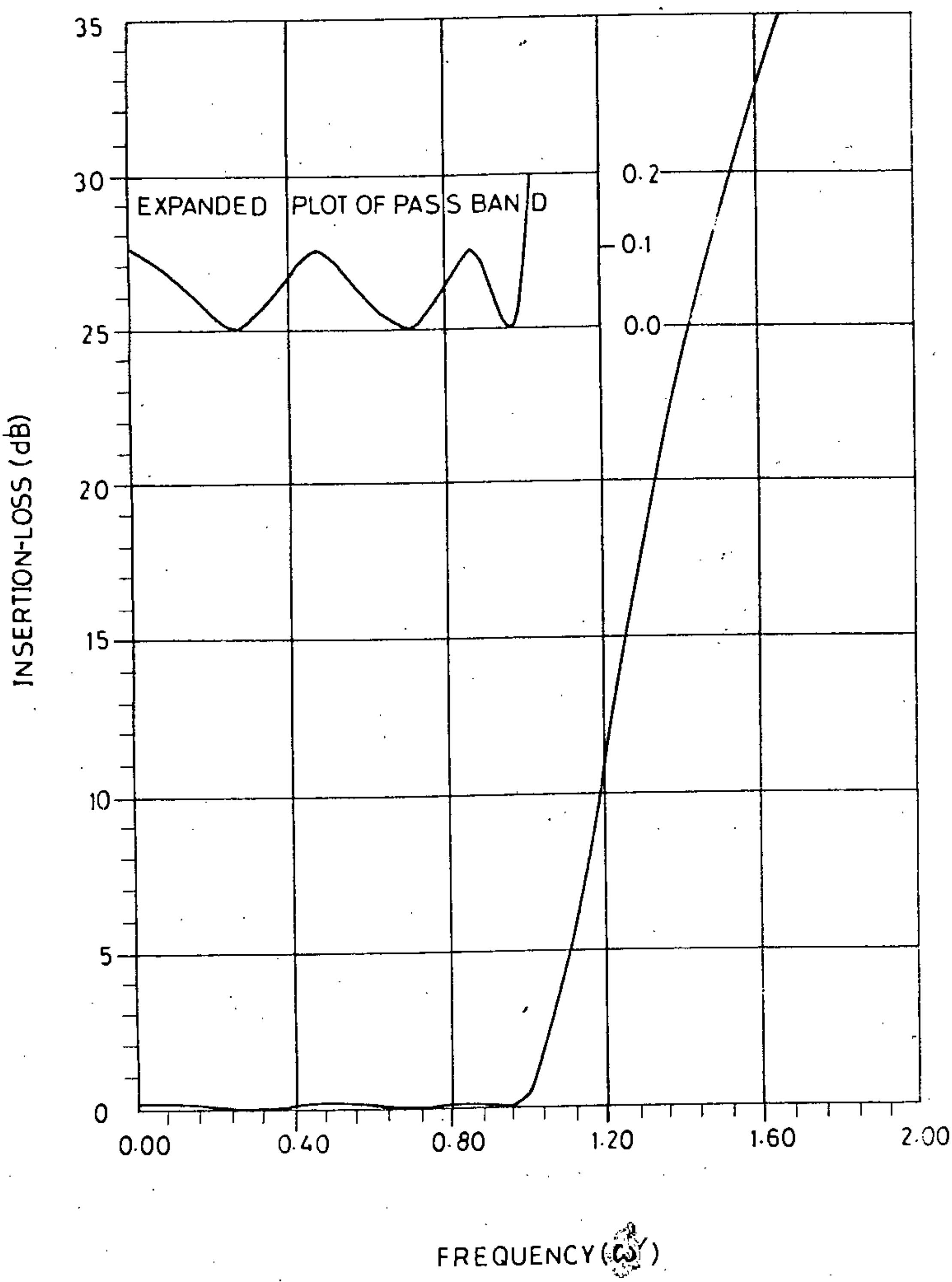

Figure 4.4. The computed insertion loss characteristic of a Chebyshev lowpass prototype filter having n=6 and A_{max}=0.1dB.

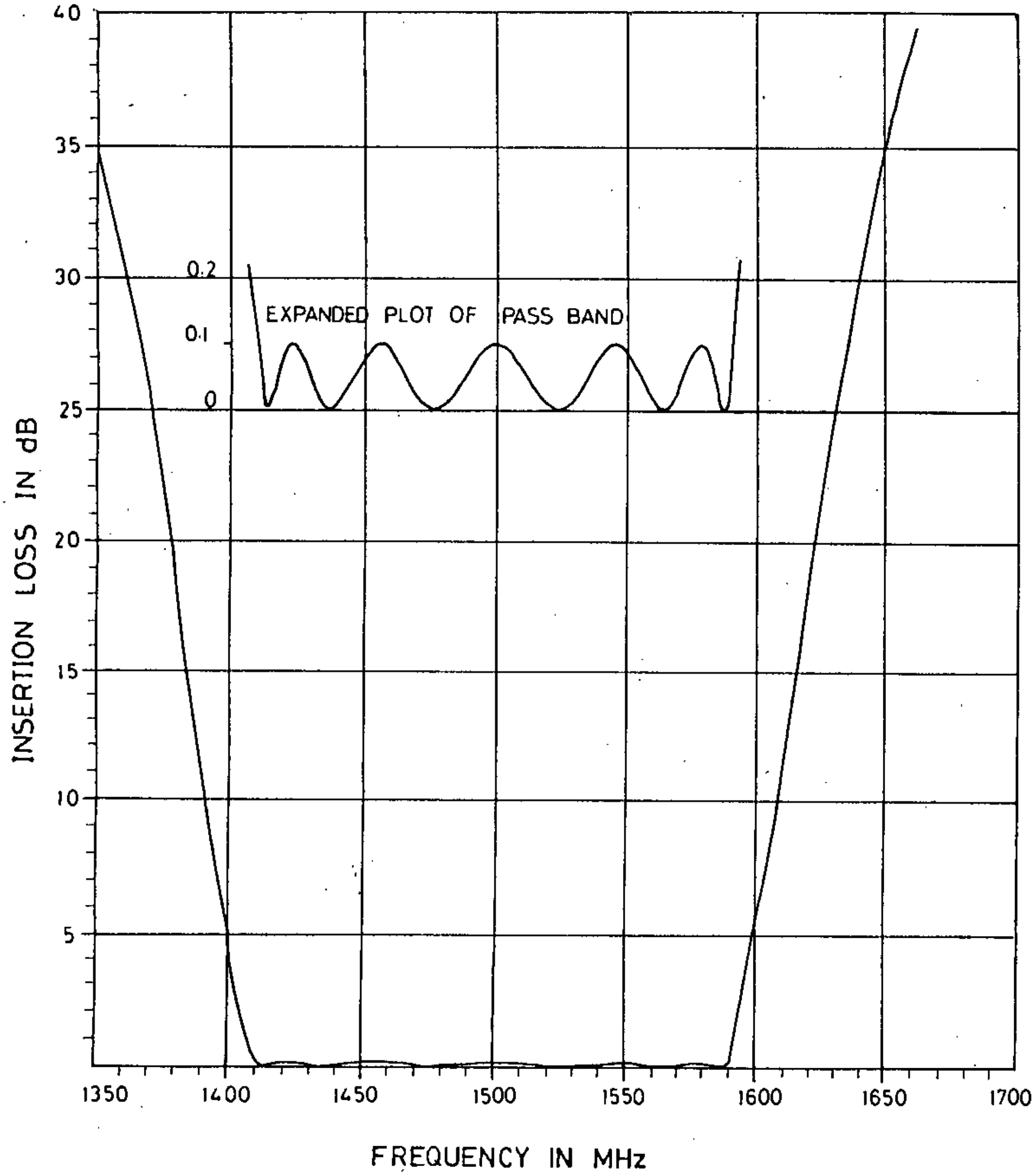

<u>Figure 4.5.</u> The computed bandpass insertion loss characteristic obtained after appling the lowpass-bandpass frequency transformation of equation (4.17) to the lowpass characteristic of figure 4.4. The center frequency is 1.5GHz and the bandwidth is 12%.

designing a bandpass filter, the expected type of response is to be selected first. The present work is based on Chebyshev characteristics.

The insertion-loss characteristic equation (4.3) can be expressed in a more generalized form [1] as

$$A = 10\log_{10}[1 + r^2 C_n^{\,2}(\Omega)] \text{ dB} \tag{4.6}$$

where, r = ripple factor, Ω = normalized frequency, n = number of resonators also known as filter complexity number, and $C_n(\Omega)$ = odd/even function of degree n for the response characteristics.

If A_{max} is the maximum permissible passband insertion loss of the lowpass prototype, then equation (4.6) becomes

$$A_{max} = 10\log_{10}(1 + r^2) \tag{4.7}$$

Hence, $$r = [\text{Antilog}_{10}(A_{max}/10) - 1]^{1/2} \tag{4.8}$$

Now, the insertion-loss characteristic for Chebysheve response of a prototype filter is

$$A = 10\log_{10}[1 + r^2\cos^2\{n \cos^{-1}(\omega'/\omega_1')\}] \quad \text{when } \omega' \le \omega_1' \tag{4.9}$$

and

$$A = 10\log_{10}[1 + r^2\cosh^2\{n \cosh^{-1}(\omega'/\omega_1')\}] \quad \text{when } \omega' \ge \omega_1' \tag{4.10}$$

4.4 Lowpass to bandpass frequency transformation

A lowpass prototype and its corresponding bandpass filter have identical insertion loss characteristics except that these characteristics possess the following relationships.

$$A_a(\omega'_a) = A_a(\omega_a) = A_a(\omega_b) \text{ dB} \tag{4.11a}$$

$$A_m(\omega') = A_m(\omega) \text{ dB in the passband} \tag{4.11b}$$

In general

$$A(\omega) = A(\omega') \text{ dB} \tag{4.11c}$$

Exact correspondence between the lowpass and bandpass characteristics can be obtained by using the lowpass to bandpass transformation [1]

$$\omega' = \mu_n F_n(\omega/\omega_0) \quad \text{and} \tag{4.12}$$

$$\mu_n = \frac{-\,\omega'_1}{F_n(\omega_2/\omega_0)} \tag{4.13}$$

Here $F_n(\omega/\omega_0)$ is called mapping function. The insertion-loss characteristic of a bandpass filter can now be obtained from the corresponding lowpass characteristic after defining a suitable mapping function. It may be mentioned here that the element values of a lowpass prototype filter network for particular values ofthe filter complexity number n and maximum insertion loss in the passband A_{max} can be obtained from [31].

4.5 Mapping function of the frequency transformation

The exact [1] mapping function $F_n(\omega/\omega_0)$ used in the frequency transformation of equation (4.8) has been given by Matthaei [1] as

$$F_n\left(\frac{\omega}{\omega_0}\right) = \frac{-\cos\dfrac{\pi\omega}{2\omega_\theta}}{\sqrt[n]{\left|\sin\dfrac{\pi\omega}{2\omega_0}\right|\left[\sin\dfrac{\pi(\omega-\omega_\infty)}{2\omega_0}\right]^2\left[\sin\dfrac{\pi(\omega-2\omega_\theta+\omega_\infty)}{2\omega_0}\right]^2}} \tag{4.14}$$

where, ω_∞ = frequency at the point of infinite attenuation.

For narrow or moderate bandwidth, equation (4.14) can be simplified [1] as

$$F_n\left(\frac{\omega}{\omega_0}\right) = \frac{-\cos\dfrac{\pi\omega}{2\omega_\theta}}{\sqrt[n]{\left|\sin\dfrac{\pi\omega}{2\omega_0}\right|}} \tag{4.15}$$

Equation (4.15) can further be simplified [1] with good accuracy as

$$F_n(\omega/\omega_0) = (\omega/\omega_0 - 1) \tag{4.16}$$

For narrow as well as moderate bandpass filters, the simplified mapping function of equation (4.16) may be used [1]. According to Matthaei [1] the result thus obtained shows excellent agreement to that obtained by using the mapping function of equation (4.15). For designing wide band filters equation (4.14) may be used [1].

Using the simplified mapping function of equation (4.16) the lowpass to bandpass frequency transformation of equation (4.12) becomes

$$\omega' = (2\omega'_1/W)\,|(\omega - \omega_0)/\omega_0| \tag{4.17}$$

where, $W = (\omega_2 - \omega_1)/\omega_0$ (4.18)

4.6 Determination of number of resonators

To determine the number of resonators n required for designing a Chebyshev bandpass filter, the following equation has been suggested by Matthaei [1].

$$n \geq \frac{\cosh^{-1}[\sqrt{\{(\text{antilog}_{10}(A_a/10) - 1)/r^2\}}]}{\cosh^{-1}(\omega_a'/\omega_1')} \tag{4.19}$$

where, ω_a', ω_1' and A_a are defined in figures 4.2 and 4.3. This equation can be obtained from equation (4.10).

As indicated in [1] the smallest integer n satisfying the above equation would be the appropriate number of resonators.

4.7 Summary

The definition of power loss ratio and insertion-loss of a filter have been presented. The insertion loss function with Chebyshev polynomials is shown. A lowpass to bandpass frequency transformation containing a mapping function has been presented. A simplified form of the mapping function has been presented to facilitate computations which can produce results with good accuracy. A formula has been presented for obtaining the filter complexity number n of a filter for a prescribed slope of the characteristic in the passband to stopband transition region.

We now take the example of a lowpass prototype filter for a Chebyshev characteristic having n=6 and A_{max}=0.1dB. The plot of the insertion loss characteristic of this filter against normalised frequency is chosen in figure 4.4. The computed bandpass characteristic obtained by appling the lowpass to bandpass transformation of equation (4.17) for a bandwidth of 12% (W=0.12) and for a centre frequency of 1.5GHz is shown in figure 4.5. The computer programmes used for obtaining these two plots are presented in Appendix A.1.

Chapter 5

Derivation of design equations of interdigital filters

5.1 Introduction

In chapter 2, it has been shown that a lumped lowpass prototype for Chebyshev response can be converted into either a network containing J- inverters with shunt capacitances or another network containing K- inverters with series inductances. On the other hand in chapter 3 it has been shown that an interdigital array of parallel coupled TEM lines has bandpass filter property. Also, in chapter 3, a two-wire equivalent circuit has been presented for an interdigital filter. Relationships between the modified lumped lowpass circuit, containing the J- inverters, of chapter 2 and the two-wire equivalent circuit of the distributed interdigital bandpass filter of chapter 3 will be established in the first part of the present chapter. These relationships or correspondences will be the basis for deriving necessary equations for designing the bandpass interdigital filter from the corresponding lumped lowpass prototype. The remaining part of this chapter deals with developing the design equations of interdigital bandpass filters.

5.2 Relationships between the modified lowpass prototype and the interdigital filter structure

For convenience the modified lowpass prototype having admittance inverters of chapter 2 is shown in figure 5.1 and the equivalent two-wire network of the interdigital filter structure of chapter 3 is presented in figure 5.2. On the basis of the required specifications of a bandpass filter usually a lowpass prototype filter is first selected. Based on the selected lowpass prototype it is now possible to obtain the modified prototype whose generalized version is shown in figure 5.1. For realizing such a filter in interdigital form having bandpass characterististics, it is now necessary to establish analytical relationships between the modified prototype of figure 5.1 and the equivalent two-wire representation of the interdigital filter of figure 5.2. This will provide a direct method of synthesis of the interdigital bandpass filter from its corresponding lumped lowpass prototype. According to Matthaei [1] the above mentioned analytical relationships can be obtained by forcing a number of correspondences between the modified lowpass prototypes of figure 5.1 and the equivalent circuit of the parallel coupled interdigital filter structure of figure 5.2. The correspondences are to be forced between section s'_{kk+1} of the modified prototype and section s_{kk+1} of the interdigital structure. These correspondences [1] are listed below.

A. For interior sections:

(i) The image phase of the parallel coupled sections when $\omega = \omega_0$ must be the same as the image phase of the prototype sections when $\omega' = 0$.

(ii) The image admittance/impedance of the parallel coupled sections when $\omega = \omega_0$ be the same (within scale factor h) as the image admittances/ impedances of the corresponding prototype sections when $\omega' = 0$.

(iii) The image admittances/impedances of the parallel coupled sections when $\omega = \omega_1$ must be the same (within scale factor h) as image admittances/ impedances of the corresponding prototype sections when $\omega' = \omega_1'$.

B. For the end sections:

(i) $Re[Y_{in}(j\omega_0)] = Re[Y_{in}(j\omega_1)]$ for the parallel coupled terminating sections, just as $Re[Y_{in}(j0)] = Re[Y_{in}(-\omega_1')]$ for terminating circuit of the prototype.

(ii) $Im[Y_{in}(j\omega_1)]/Re[Y_{in}(j\omega_1)]$ must equal B'/G' = $Im[Y_{in}(-j\omega'_1)]/Re[Y_{in}(-j\omega'_1)]$ computed from the prototype.

Here, it should be noted that the design of end sections of interdigital filter have additional degrees of freedom. In the following sections, design equations for narrow-band as well as wide-band bandpass filter have been derived analytically.

By applying the above correspondences it is now possible to derive the required design equations.

5.3 Derivation of design equations for the interdigital bandpass filter

In this section design equations will be derived for interdigital bandpass filters. We recall the interdigital filter structure of figure 3.6(a). It has been observed from this filter structure that the internal coupled sections of this filter have interdigital structures with quarter- wave long resonator lines at midband

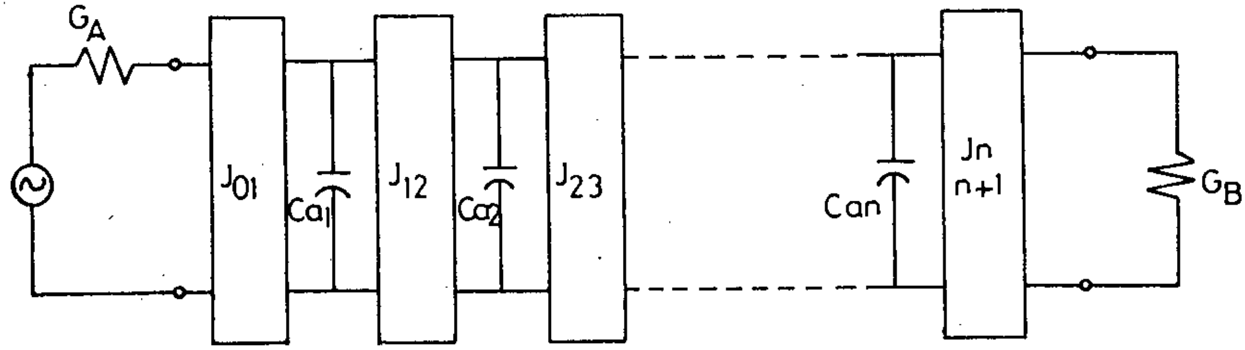

Figure 5.1. The modified lowpass prototype for Chebyshev response having J- inverters and shunt capacitances.

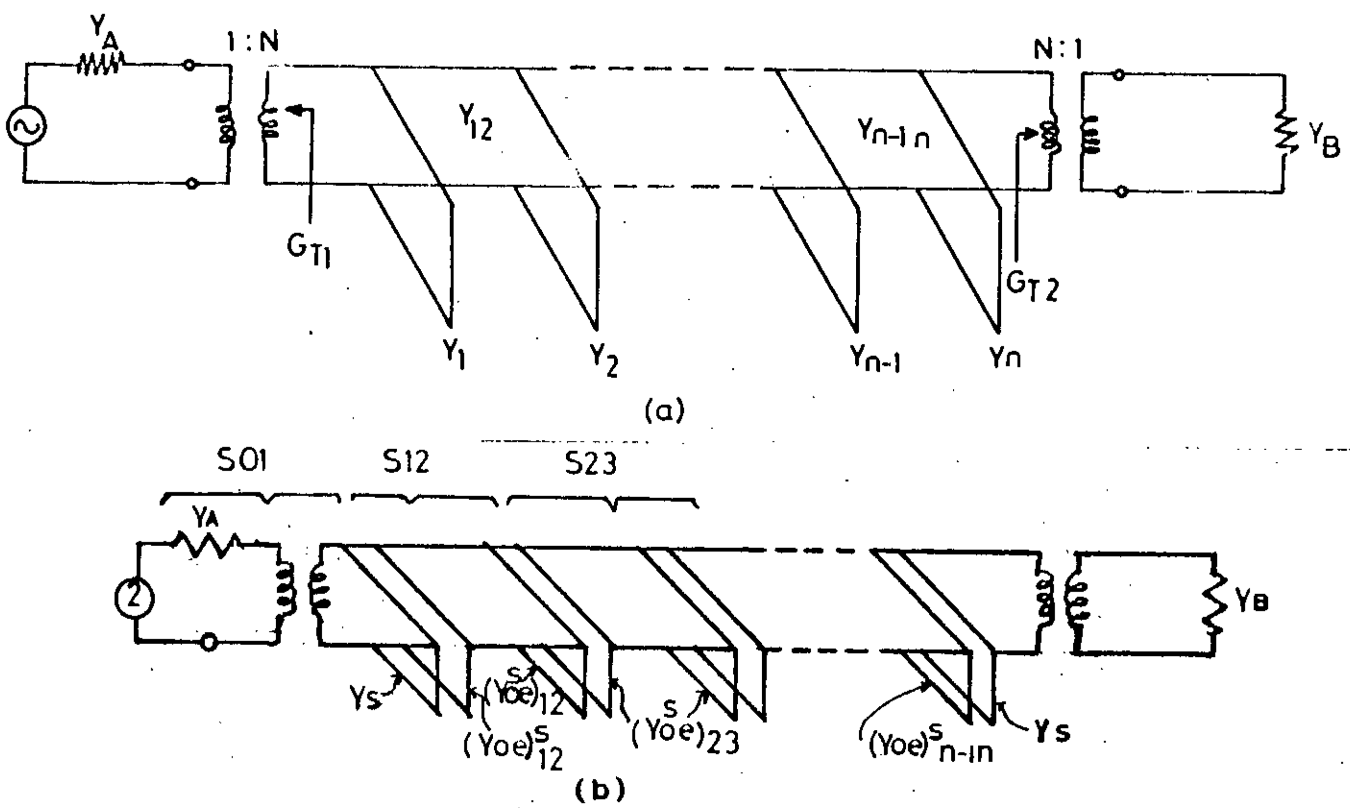

Figure 5.2. Two wire equivalent circuit of the interdigital bandpass filter structure of figure 3.6(a). (a) The complete equivalent circuit. (b) The equivalent circuit broken into symmetrical sections.

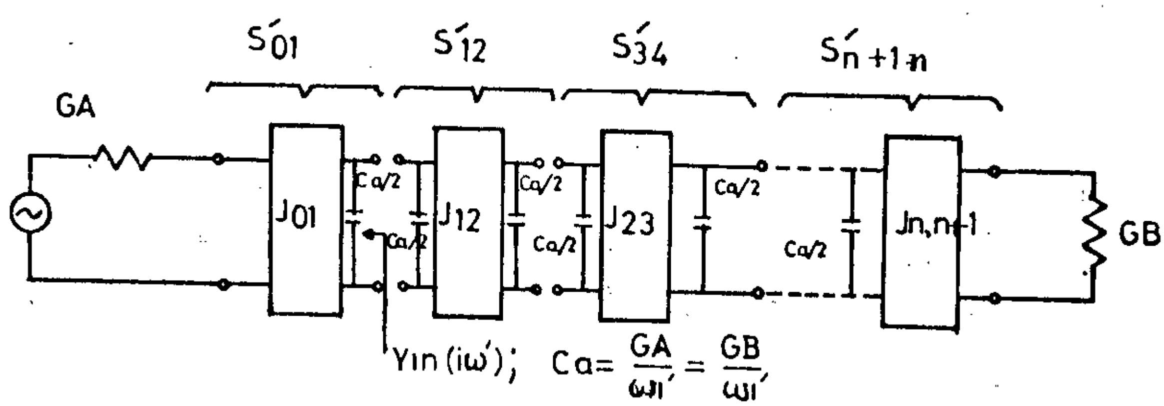

Figure 5.3. Modified lowpass prototype of figure 5.1 broken into suitable sections for deriving the design equations.

frequency. It may be observed that the input/ output line elements of the filter of figure 3.6(a) are short circuited at the ends. Here the input output lines work as admittance tranformation lines only.

Consider the filter structure of figure 3.6(a) and the corresponding two-wire equivalent circuit of figure 5.2. The modified lowpass prototype of figure 5.1 consisting of admittance inverters will now be used. For convenience the modified lowpass prototype of figure 5.1 is next broken into identical sections as shown in figure 5.3 so that the image parameters of the various sections of the modified prototype can easily be compared with that of the corresponding sections of the network of figure 3.8(a).

We start by assuming the input and output terminating conductances, G_A and G_B, of the modified lowpass prototype of figure 5.1 to be equal (which is practical). Similarly we assume the input and output terminating admittances of the interdigital bandpass filter (figure 3.8(a)) as equal, i.e., $Y_A = Y_B$. In fact we may assume

$$Y_A = Y_B = G_A = G_B = Y_0 \tag{5.1}$$

It is possible to choose the capacitances C_{a1}, C_{a2}, C_{a3},....C_{an} of the modified lowpass prototype of figure 5.1 to be equal. For convenience we make this choice so that

$$C_{a1} = C_{a2} = C_{a3} = \ldots\ldots.. = C_{an} = C_a \tag{5.2}$$

This is needed to break the interior sections of the modified prototype of figure 5.1 into symmetrical sections so that the new network becomes as shown in figure 5.3. We may fix the value of C_a equal to Y_A/ω'_1 so that

$$C_{ak}\Big|_{k = 1 \text{ to } n} = C_a = Y_A/\omega'_1 \tag{5.3}$$

Using the value of C_{ak} of equation (5.3) in equations (2.15),(2.8) and (2.14) of J_{01}, J_{kk+1} and J_{nn+1} of chapter 2 we get

$$J_{01}/Y_A = 1/\sqrt{(\omega'_1\, g_0\, g_1)} \tag{5.4a}$$

$$J_{kk+1}/Y_A\Big|_{k = 1 \text{ to } n-1} = 1/\{\omega'_1\, \sqrt{(g_k g_{k+1})}\} \tag{5.4b}$$

$$J_{nn+1}/Y_A = 1/\sqrt{(\omega'_1 g_n g_{n+1})} \tag{5.4c}$$

Jones and Bolljahn [11] showed that the image admittance and image phase of a pair of interdigital parallel coupled lines (figure 3.1(a)) can be written as

$$Y^I = \sqrt{\{[Y_{oo}-Y_{oe}]^2-[Y_{oo}+Y_{oe}]^2\cos^2\theta\}}/(2\sin\theta) \tag{5.5a}$$

$$\text{and} \quad \beta^I = \cos^{-1}\left[\frac{(Y_{oo} + Y_{oe})}{(Y_{oo} - Y_{oe})} \cos\theta \right] \tag{5.5b}$$

where, $\theta = (\pi\omega)/(2\omega_0)$. The admittances Y_{oo} and Y_{oe} are the odd- mode and even- mode admittances of the pair of coupled lines. Equations (5.5a) and (5.5b) may now be applied for the interior sections (i.e., sections s_{12} to s_{n-1n}) of the interdigital bandpass filter of figure 3.6(a). Thus the image impedance and image phase of the interior sections of the parallel coupled interdigital lines can be written in terms of odd- mode and even- mode admittance as

$$Y^I_{kk+1}(\omega) = \frac{[\{(Y_{oo})_{kk+1} - (Y_{oe})_{kk+1}\}^2 - \{(Y_{oo})_{kk+1} + (Y_{oe})_{kk+1}\}^2 \cos^2\theta]^{1/2}}{2\sin\theta} \tag{5.6a}$$

$$\text{and} \quad \beta_{kk+1} = \cos^{-1} \frac{(Y_{oo})_{kk+1} + (Y_{oe})_{kk+1}}{(Y_{oo})_{kk+1} - (Y_{oe})_{kk+1}} \cos\theta \tag{5.6b}$$

where, $\theta = (\pi\omega)/(2\omega_0)$ and $k = 1,2,3\ldots n$.

From the modified lowpass prototype of figure 5.1 we can obtain the expressions for image admittance Y^i_{kk+1} and phase β'_{kk+1} (in the pass band) for each of the prototype interior sections s'_{12} to s'_{n-1n} as

$$Y^i_{kk+1}(\omega') = J_{kk+1}\sqrt{[1 - \{\omega'(C_a/2)/J_{kk+1}\}^2]} \text{ and,} \tag{5.7a}$$

$$\beta'_{kk+1}\Big|_{\omega' \le J_{kk+1}/(C_a/2)} = \sin^{-1} [\omega'(C_a/2)/J_{kk+1}] \pm \pi/2 \tag{5.7b}$$

Here, the choice of $\pm\,\pi/2$ in equation (5.7b) depends on wheather the inverter of the section is taken to have + 90 degrees phase shift.

First we see that correspondence A(i) of section 5.2 is fulfilled if the + sign is chosen.

For fulfilling correspondence A(ii) the image admittance $Y^I_{kk+1}(\omega)$ at $\omega=\omega_0$ is to be equated with the image admittance $Y^i_{kk+1}(\omega')$ at $\omega'=0$. Therefore, putting $\omega=\omega_0$ in equation (5.6a) and $\omega'=0$ in equation (5.7a) and equating the right hand sides of these two equations we get

$$J_{kk+1} = [(Y_{oo})_{kk+1} - (Y_{oe})_{kk+1}]/2 \tag{5.8}$$

Next, in order to meet the conditions of correspondence A(iii) we replace ω by ω_1 in equation (5.6a) and ω' by ω_1' in equation (5.7a) and equate the right hand side of these two equations. This gives

$$J^2_{kk+1}[1 - \{(\omega_1'C_a/2)/J_{kk+1}\}^2] = \frac{[(Y_{oo})_{kk+1} - (Y_{oe})_{kk+1}]^2 - [(Y_{oo})_{kk+1} + (Y_{oo})_{kk+1}]^2\cos^2\theta_1}{4\sin^2\theta 1} \tag{5.9a}$$

where, $\theta_1 = (\pi\omega_1)/(2\omega_0)$

Now, putting the value of C_a from equation (5.2) in (5.9a)

$$(Y_{oo})_{kk+1}(Y_{oe})_{kk+1} = Y_A^2\tan^2\theta_1/4 \tag{5.9b}$$

From equations (5.8) and (5.9b) we get

$$\frac{(Y_{oo})_{kk+1} + (Y_{oe})_{kk+1}}{2Y_A} = \sqrt{[(J_{k+1}/Y_A)^2 + (\tan^2\theta_1)/4]} \tag{5.9c}$$

We denote the right hand side of equation (5.9c) by N_{kk+1} so that

$$N_{kk+1} = \sqrt{[(J_{kk+1}/Y_A)^2 + \tan^2\theta_1/4]} \tag{5.9d}$$

This permits us to rewrite equation (5.9c) as

$$[(Y_{oo})_{kk+1} + (Y_{oe})_{kk+1}]/2Y_A = N_{kk+1} \tag{5.10}$$

From equations (5.8) and (5.10) the odd-mode and even- mode admittances are obtained in terms of J_{kk+1} and N_{kk+1} as

$$(Y_{oo})_{kk+1} = [N_{kk+1} + J_{kk+1}/Y_A]Y_A \tag{5.11a}$$

$$(Y_{oe})_{kk+1} = [N_{kk+1} - J_{kk+1}/Y_A]Y_A \tag{5.11b}$$

At this stage we introduce an admittance scaling factor h for the odd and even- mode admittances in the interior sections so that equations (5.11a) and (5.11b) become

$$(Y_{oo})_{kk+1} = hY_A[N_{kk+1} + J_{kk+1}/Y_A] \tag{5.12a}$$

$$(Y_{oe})_{kk+1} = hY_A[N_{kk+1} - J_{kk+1}/Y_A] \tag{5.12b}$$

In order to derive the equations for the characteristic admittances Y_1, Y_2, ... of the shunt stubs of figure 5.2 we recall that each of these stubs appeared due to the shunt connection of two stubs of two adjacent sections as shown in figure 3.4. Thus in a generalized way the equation for the characteristic admittance of each of the shunt stubs for the interior sections of the filter may be written in terms of the even-mode admittances of the adjacent sections as

$$Y_k = Y^S_{k-1k} + Y^S_{kk+1} \tag{5.13a}$$

i.e., $Y_k = (Y_{oe})_{k-1k} + (Y_{oe})_{kk+1}$ (5.13b)

Using equation (5.12b) for putting the values of $(Y_{oe})_{k-1k}$ and $(Y_{oe})_{kk+1}$ in equation (5.13b)

$$Y_k = Y_A h[N_{k-1k} - J_{k-1k}/Y_A + N_{Kk+1} - J_{kk+1}/Y_A] \tag{5.14}$$

where, k=2,3...n-1. Equation (5.14) gives the admittances of the shunt stubs except the two shunt stubs on the input and output ends (i.e., stubs 1 and n) of the filter .

From figure 3.2 of chapter 3 and following Matthaei [1] the equations for admittances Y_{kk+1} of the connecting lines of each section of figure 5.2(a) can be written as

$$Y_{kk+1} = [(Y_{oo})_{kk+1} - (Y_{oe})_{kk+1}]/2 \tag{5.15a}$$

From equations (5.12a) and (5.12b)

$$Y_{kk+1} = hY_A J_{kk+1}/Y_A \tag{5.15b}$$

Using the relation between the characteristic admittance and the self capacitance per unit length of a line it is possible to write for the stub admittances

$$Y_k|_{k=2 \text{ to } n-1} = vC_k \tag{5.16a}$$

where $v = 1/\sqrt{(\mu\epsilon)}$ is the velocity of wave propagation. Putting the value of Y_k of equation (5.14) in equation (5.16a) we get

$$C_k/\epsilon = (\eta_0 Y_A h/\sqrt{\epsilon_r})[N_{k-1k} - J_{k-1k}/Y_A - N_{kk+1} - J_{kk+1}/Y_A] \tag{5.16b}$$

Similarly the characteristic admittances of the connecting lines of each interior sections can be written in terms of the mutual capacitance per unit length as

$$Y_{kk+1} = vC_{kk+1} \tag{5.17a}$$

Putting the value of Y_{kk+1} of equation (5.15b) in equation (5.17a) we get

$$C_{kk+1}/\epsilon = (\eta_0 Y_A h/\sqrt{\epsilon_r})[J_{k\ k+1}/Y_A] \tag{5.17b}$$

Equation (5.17b) is valid for k = 1,2,3,4 ....n-1.

For the remaining self capacitances C_0, C_1, C_n, C_{n+1}, and the mutual capacitances C_{01}, C_{nn+1} of the terminating input/ output sections (figure 3.8(a)), it is necessary to apply the special constraint indicated in figure 3.7(a). This is

$$Y^0_{oo} + Y^0_{oe} = 2Y_A \tag{5.18}$$

Thus from figure 3.7(a) it is possible to write the equtions for the self capacitance of the terminating line number 0 of figure 3.6(a) as

$$C_0/\epsilon = (\eta_0/\sqrt{\epsilon_r})Y^0_{oe} \tag{5.19a}$$

Enforcing the special constraint of equation (5.18) in the above equation we obtain

$$C_0/\epsilon = (\eta_0/\sqrt{\epsilon_r})[2Y_A - Y^0_{oo}] \tag{5.19b}$$

The odd-mode admittance Y^0_{oo} of element number 0 can be written as shown in figure 3.7(a) as

$$Y^0_{oo} = Y_A[\sqrt{(G_T/Y_A)} + 1] \tag{5.20a}$$

Here G_T is the conductance looking into the left as shown in figure 3.7(a) and 5.2(a). From figure 3.7(a) it may be observed that

$$G_T = Y_A/N^2 = Y_A h \tag{5.20b}$$

On the other hand, the conductance G'_T looking into the left of the prototype filter section of figure 5.1 is

$$G_T' = J^2_{01}/Y_A \tag{5.20c}$$

We now see that the conductance G'_T of the prototype filter multipled by admittance scale factor h will yield the conductance G_T of parallel coupled interdigital filter. This means

$$G_T = G'_T h = (J^2 01/Y_A)h \tag{5.20d}$$

Substituting the value of G_T in equation (5.20a), the odd-mode admittance Y^0_{oo} in terms of lowpass prototype parameters is

$$Y^0_{oo} = Y_A[1 + (J_{01}/Y_A)\sqrt{h}] = M_1 \tag{5.20e}$$

Here for convenience the term M_1 has been assumed as

$$M_1 = Y_A[1 + J_{01}/Y_A\sqrt{h}] \tag{5.21}$$

Now, replacing Y^0_{oo} of equation (5.19b) by M_1 the self capacitance per unit length of element 0 becomes

$$C_0/\epsilon = (\eta_0/\sqrt{\epsilon_r})[2Y_A - M_1] \tag{5.22}$$

Assuming symmetrical construction of the filter, the self capacitance per unit length of the element number n+1 can also be written as

$$C_{n+1}/\epsilon = (\eta_0/\sqrt{\epsilon_r})[2Y_A - M_n] \tag{5.23a}$$

where, $M_n = Y_A[(J_{nn+1}/Y_A)\sqrt{h} + 1]$ (5.23b)

The mutual capacitance C_{01} per unit length between two filter elements 0 and 1 at one terminating end

$$C_{01} = (\epsilon\eta_0/\sqrt{\epsilon_r})[Y^0_{oo} - Y^0_{oe}]/2 \tag{5.24a}$$

Applying the special constraint $2Y_A = Y^0_{oo} + Y^0_{oe}$ and replacing Y^0_{oo} by M_1 in the above equation we get

$$C_{01}/\epsilon = (\eta_0/\sqrt{\epsilon_r})[M_1 - Y_A] \tag{5.24b}$$

Following this, the mutual capacitance C_{nn+1} per unit length of the other end can be written in a similar way as

$$C_{nn+1}/\epsilon = (\eta_0/\sqrt{\epsilon_r})[M_n - Y_A] \tag{5.25}$$

Now, the characteristic admittance Y_1 of the shunt stub 1 of the equivalent circuit figure 5.2(a) can also be expressed as the summation of two components like Y_k. Therefore,

$$Y_1 = Y_s + (Y_{oe})_{12} \tag{5.26}$$

where, $(Y_{oe})_{12}$ is the even mode characteristic admittance of the stub 1 due to the contribution of the section S_{12} of the array. The other componet Y_s arises due to the coupling effect of section S_{01} as shown in the equivalent circuit of the terminating section of figure 3.7(a). In the figure the input admittance Y_{in} can be written as

$$Y_{in}(j\tilde{\omega}) = Y_A h - jY_s \cot\theta \quad (5.27a)$$

where $\theta = (\pi\tilde{\omega})/(2\tilde{\omega}_0)$

On the other hand, the input admittance of the terminating section of the broken prototype filter of figure 5.3 is,

$$Y_{in}'(j\tilde{\omega}') = J_{01}^2/Y_A + j\tilde{\omega}'C_a/2 \quad (5.27b)$$

Using equation (5.20d) we rewrite the above equation as

$$Y'_{in}(j\tilde{\omega}') = G_T/h + j\tilde{\omega}'C_a/2 \quad (5.27c)$$

Putting the value of G_T of equation (5.20b)

$$Y_{in}'(j\tilde{\omega}) = Y_A + j\tilde{\omega}'C_a/2 \quad (5.27d)$$

Now, applying correspondence B(ii) of section 5.2 for the terminating section we get

$$\mathrm{Im}[Y_{in}(j\tilde{\omega}_1)]/\mathrm{Re}[Y_{in}(j\tilde{\omega}_1] = \mathrm{Im}[Y_{in}(-j\tilde{\omega}_1')/\mathrm{Re}[Y_n'(-j\tilde{\omega}_1')$$

$$\text{or,} \quad -Y_s\cot\theta_1/(Y_A h) = (-\tilde{\omega}_1'C_a/2)/ Y_A$$

$$\text{or,} \quad Y_s = \tilde{\omega}_1'(C_a/2)h \tan\theta_1 \quad (5.27e)$$

Putting the value of C_a from equation (5.3)

$$Y_s = (1/2)\, Y_A h \tan\theta_1 \quad (5.27f)$$

Substituting the value of Y_s from equation (5.27f) in equation (5.26) we get

$$Y_1 = (1/2)Y_A h \tan\theta_1 + (Y_{oe})_{12} \quad (5.28)$$

Similarly for the n^{th} shunt stub

$$Y_n = (1/2)Y_A h \tan\theta_1 + (Y_{oe})_{n-1n} \quad (5.29)$$

Putting the value of $(Y_{oe})_{12}$ from (5.12b) in equation (5.28) the following equation is obtained

$$Y_1 = (Y_A h/2) \tan\theta_1 + Y_A h[N_{12} - J_{12}/Y_A] \quad (5.30a)$$

Again, the same characteristic admittance Y_1 of the parallel coupled section of the terminating end obtained from figure 3.7(a) is

$$Y_1 = Y_A (1 - 1/N^2) + Y^1_{oe} - Y^0_{oe} \quad (5.30b)$$

Using equations (5.20b), (5.20d), (5.18), (5.21) the above equation may be written as

$$Y_1 = M_1 - Y_A - (J_{01}^2/Y_A)h + Y^1_{oe} \quad (5.30c)$$

In order to obtain the self capacitance C_1 of the line the right hand sides of equations (5.30a) and (5.30c) are equated. This produces

$$Y^1_{oe} = Y_A h[(1/2)\tan\theta_1 + N_{12} - J_{12}/Y_A + (J_{01}/Y_A)^2] + Y_A - M_1 \quad (5.30d)$$

This means

$$C_1/\epsilon = (\eta_0/\sqrt{\epsilon_r})\{Y_A h[1/2\tan\theta_1 + N_{12} - J_{12}/Y_A + (J_{01}/Y_A)^2] + Y_A - M_1\} \quad (5.31)$$

Similarly, the self capacitance C_n of the n^{th} element is obtained as

$$C_n/\epsilon = (\eta_0/\sqrt{\epsilon_r})[(Y_A - M_n) + Y_A h\{(1/2)\tan\theta_1 + (N_{n-1n} - J_{n-1n}/Y_A + (J_{nn+1}/Y_A)^2\}] \quad (5.32)$$

For convenience it is now necessary to prepare a list of the equations for narrowband interdigital bandpass filter which will be used later for design purpose. This list of equations is presented below.

<u>Equations for the admittance inverters</u>

$$J_{01}/Y_A = 1/\sqrt{(g_0\, g_1\, \omega_1')} \quad (5.33a)$$

$$J_{kk+1}/Y_A \Big|_{k=1 \text{ to } n-1} = 1/\omega_1' \sqrt{(g_k g_{k+1})} \quad (5.33b)$$

$$J_{nn+1}/Y_A = 1/\sqrt{(g_n g_{n+1} \omega_1')} \quad (5.33c)$$

<u>The characteristic admittances of the shunt stubs</u>

$$Y_1 = Y_A h[1/2 \tan\theta_1 + N_{12} - J_{12}/Y_A] \quad (5.34a)$$

$$Y_k \Big|_{k=1 \text{ to } n-1} = Y_A h[N_{kk+1}/Y_A - J_{kk+1}/Y_A + N_{k-1k}/Y_A - J_{k-1k}/Y_A] \quad (5.34b)$$

$$Y_n = Y_A h[(1/2)\tan\theta_1 + N_{n-1n} - J_{n-1n}/Y_A] \quad (5.34c)$$

<u>The characteristic admittances of connecting lines</u>

$$Y_{kk+1}/Y_A \Big|_{k=1 \text{ to } n-1} = Y_A h(J_{kk+1}/Y_A) \quad (5.34d)$$

<u>The normalized self and mutual capacitances per unit length of the line elements</u>

$$C_0/\epsilon = (376.7/\sqrt{\epsilon_r})[2Y_A - M_1] \quad (5.35a)$$

$$C_1/\epsilon = (376.7/\sqrt{\epsilon_r})[Y_A - M_1 + hY_A\{\tan\theta_1/2 + (J_{01}/Y_A)^2 + N_{12} - J_{12}/Y_A\}] \quad (5.35b)$$

$$C_k/\epsilon \Big|_{k=2 \text{ to } n-1} = (376.7/\sqrt{\epsilon_r})[N_{kk+1}/Y_A + N_{k-1k}/Y_A - J_{kk+1}/Y_A - J_{k-1k}/Y_A] \quad (5.35c)$$

$$C_n/\epsilon = (376.7/\sqrt{\epsilon_r})[Y_A - M_n + hY_A\{\tan\theta 1/2 + (J_{nn+1}/Y_A)^2 + N_{n-1n} - J_{n-1n}/Y_A\}] \quad (5.35d)$$

$$C_{n+1}/\epsilon = (376.7/\sqrt{\epsilon_r})[2Y_A - M_n] \quad (5.35e)$$

$$C_{01}/\epsilon = (376.7/\sqrt{\epsilon_r})[M_1 - Y_A] \quad (5.36a)$$

$$C_{kk+1}/\epsilon\Big|_{k=1 \text{ to } n-1} = (376.7/\sqrt{\epsilon_r})Y_A h(J_{kk+1}/Y_A) \qquad (5.36b)$$

$$C_{nn+1}/\epsilon = (376.7/\sqrt{\epsilon_r})[M_n - Y_A] \qquad (5.36c)$$

where,

$$M_1 = Y_A[(J_{01}/Y_A)\sqrt{h} + 1] \qquad (5.37a)$$

$$N_{kk+1}\Big|_{k=1 \text{ to } n-1} = \sqrt{[(J_{kk+1}/Y_A)^2 + \tan^2\theta_1/4]} \qquad (5.37b)$$

$$M_n = Y_A[(J_{nn+1}/Y_A)\sqrt{h} + 1] \qquad (5.37c)$$

It may be observed that using equations (5.33a) - (5.33c) the values of self capacitances C_i (i=0,1,2,...n+1) of the parallel coupled lines and mutual capacitances $C_{j,j+1}$ (j=1,2,...n) between neighbouring lines of the interdigital lines can be obtained in terms of the lowpass prototype element values and other specifications of the bandpass filter. The values of these capacitances will be required to obtain the line dimensions of the interdigital bandpass filter.

5.4 Admittance scaling factor

The admittance scaling factor defined as h is necessary to maintain a convenient admittance level through out the interior sections of the interdigital bandpass filter. From the the figure 3.7 and figure 5.2, it is obvious that the characteristic admittance of the terminating input/ output sections of an interdigital filter may be fixed to any required value. The interior sections are designed from the prototype parameters. This is expected to produce a different admittance level for these sections. Therefore, the admittances of the interior sections obtained from lowpass prototype must be multiplied by the admittance scale factor h as used in the design equations. The admittance scaling factor h used in the design equations of section 5.3 is [3]

$$h = 1/N^2 \qquad (5.38)$$

where, N is the turns ratio of the ideal transformer in figure 3.7 and figure 5.2.

According to Matthaei [3], one of the prime considerations in the choice of h is, the line dimension must be such that the resonators will have a high unloaded Q. In the case of interdigital structure, optimum Q's are not known [3]. But it is known [3] that for air filled co-axial line resonators the optimum Q will result when the line impedance is about 76 ohms, and various approximate studies suggest that the optimum impedance for strip-line resonators is not greatly different. It is suggested [3] that, if the dielectric medium is air, for interdigital filter design h be so chosen that the following relationship is satisfied.

$$2C_{k-1k}/\epsilon + C_k/\epsilon + 2C_{kk+1}/\epsilon = 5.4 \text{ (around)} \qquad (5.39)$$

where, $k = n/2$ (for n even).

$= (n+1)/2$ (for n odd)

5.5 Summary

The equations for interdigital bandpass filter having short-circuited lines at the input and output lines have been derived. The useful equations necessary for designing this type of interdigital filter have also been listed separately. Using these equations it is now possible to obtain the self and mutual capacitances of the coupled lines of an interdigital filter which would ultimately allow us to obtain the line dimensions.

Chapter 6

Obtaining physical dimensions of interdigital filters

6.1 Introduction

In chapter 5, necessary equations for designing interdigital bandpass filters have been derived. It may be observed that these design equations contain the equations of self capacitances of interdigital filters and equtions for mutual capacitances between a line and its nearest neighbour. The self capacitances C_k are the static self capacitances formed between respective line and ground, while the mutual capacitances C_{kk+1} are the static mutual capacitances formed between two adjacent lines. It is now obvious that using the design equations of chapter 5 one can get the values of C_k's and C_{kk+1}'s for an interdigital filter. In order to fabricate a filter it is now necessary to find out ways of obtaining physical dimensions out of these two types of capacitances. In this chapter, the procedure of obtaining physical dimensions of parallel coupled lines, in the form of rectangular lines between ground planes, from self and mutual capacitances are described. The procedure involves the use of graphs and analytical expressions. The procedure is presented in a way so that this can be applied without any difficulty for obtaining physical dimensions of interdigital filters.

6.2 Static capacitances of parallel-coupled lines

6.2.1 Static capacitances of a pair of symmetrical parallel-coupled lines

Figure 6.1 shows a cross-section of a pair of parallel coupled rectangular bar transmission line of equal width w. The spacing between the parallel ground planes is 'b' and the two coupled lines are placed between the two ground planes. TEM-propagation through such structure can be described in terms of two orthogonal modes, usually denoted as even-mode and odd-mode [9][18]. For even-mode excitation, the even-mode capacitance C_{oe} to ground and for odd-mode excitation, the odd-mode capacitance C_{oo} to ground arise as shown in figure 6.1. It is to be noted here, both the bars are assumed to be wide enough that interactions between fringing fields at the inner sides of the

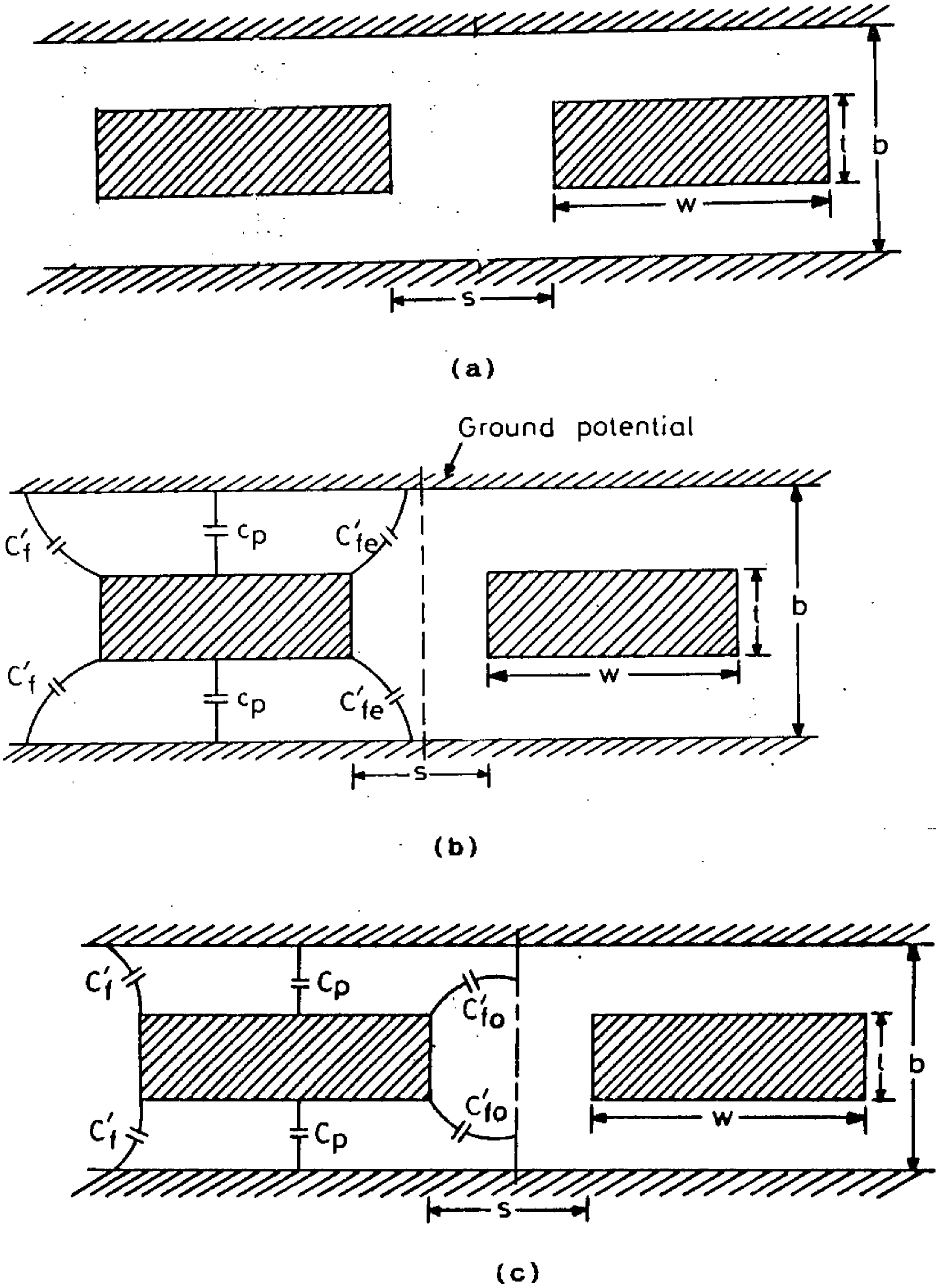

Figure 6.1. Two parallel-coupled rectangular bars having equal widths centred between ground planes. (a) Cross section of the coupled lines. (b) Capacitances for even-mode excitation. (c) Capacitances for odd-mode excitation.

bars are negligible or at least small enough to be easily corrected for[7],[9]. From figure 6.1 the equations for the total even-mode static capacitance C_{oe}/ϵ for one bar and the total odd-mode static capacitance C_{oo}/ϵ for one bar are

$$C_{oe}/\epsilon = 2\,[C_p/\epsilon + C_{fe}'/\epsilon + C_f'/\epsilon] \tag{6.1}$$

$$C_{oo}/\epsilon = 2\,[C_p/\epsilon + C_{fo}'/\epsilon + C_f'/\epsilon] \tag{6.2}$$

In the above equations, C_p denotes the parallel plate capacitance from the top or bottom side of one bar to the nearest ground plane; C_{fe}' denotes the capacitance to ground from one corner and half the associated vertical wall in the coupling region of a bar for even-mode excitation. Also C_{fo}' denotes the capacitance to ground from one corner and half the associtated vertical wall in the coupling region of a bar for odd-mode excitation and C_f' is the capacitance to ground from one corner and half the associated vertical wall away from the coupling region of a bar for any excitation as shown in figure 6.1.

The equations for inter- bar capacitance or mutual capacitance between two adjacent bars, $\Delta C/\epsilon$ can be written [9] as

$$\Delta C/\epsilon = (1/2)[C_{oo}/\epsilon - C_{oe}/\epsilon] \tag{6.3}$$

Putting the values of C_{oo}/ϵ from equation (6.1) and C_{oe}/ϵ from equation (6.2) in equation (6.3) we get

$$\Delta C/\epsilon = C_{fo}'/\epsilon - C_{fe}'/\epsilon \tag{6.4}$$

This shows that the inter-line capacitance can be expressed entirely in terms of fringing capacitances.

6.2.2 Static capacitances of an unsymmetrical pair of parallel-coupled lines

Consider a pair of parallel-coupled lines having unequal widths as shown in figure 6.2. In this figure, C_a is the capacitance per unit length between line 'a' and ground, C_{ab} is the capacitance per unit length between line 'a' and line 'b', and C_b is the capacitance per unit length between line 'b' and ground. Hence, the odd- and even-mode capacitance can be expressed in terms of line capacitances[9],[11],[18]. Thus,

$$C_{oo}^{a} = C_a + C_{ab}\ ; \quad C_{oe}^{a} = C_a \tag{6.5}$$

and for line b,

$$C_{oo}^{b} = C_b + C_{ab}\ ; \quad C_{oe}^{a} = C_b \tag{6.6}$$

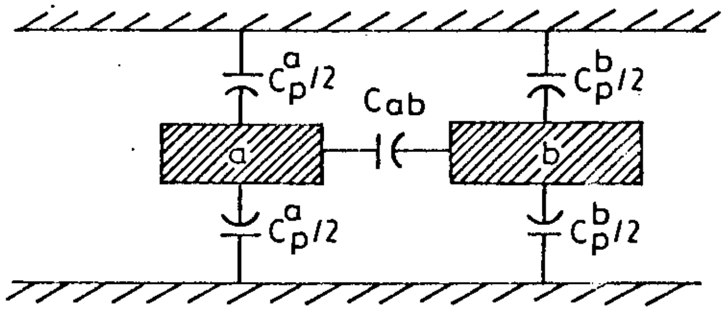

Figure 6.2. A pair of parallel-coupled lines having unequal widths showing the self and mutual capacitances.

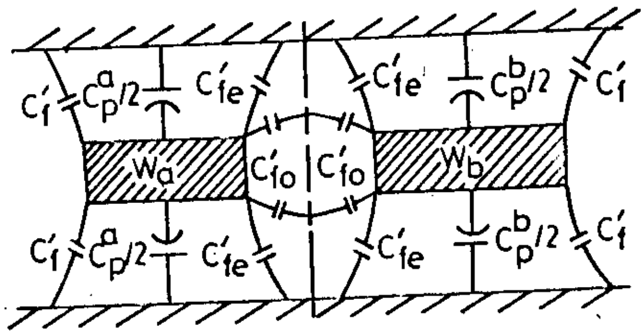

Figure 6.3. A pair of unsymmetrical rectangular bar parallel-coupled lines showing various capacitances.

These odd- and even-mode capacitances constitute odd- and even-mode admittances or impedances. The odd- and even-mode admittances for line 'a' and line 'b' are given [9][18] by

$$Y_{oo}^{a} = vC_{oo}^{a} = v(C_a + 2C_{ab}) \tag{6.7}$$

$$Y_{oe}^{a} = vC_{oe}^{a} = vC_a$$

and,

$$Y_{oo}^{b} = vC_{oo}^{b} = v(C_b + 2C_{ab}) \tag{6.8}$$

$$Y_{oe}^{b} = vC_{oe}^{b} = vC_b$$

From equations (6.7) and (6.8), the normalised self and mutual capacitances for line a and line b interms of odd- and even-mode admittances can be written as,

$$\frac{C_a}{\epsilon} = \frac{\eta_0 Y_{oe}^{a}}{\sqrt{\epsilon_r}} \tag{6.9}$$

$$\frac{C_b}{\epsilon} = \frac{\eta_0 Y_{oe}^{b}}{\sqrt{\epsilon_r}} \tag{6.10}$$

$$\frac{C_{ab}}{\epsilon} = \frac{\eta_0}{\sqrt{\epsilon_r}} \frac{(Y_{oo}^{a} - Y_{oe}^{a})}{2} \tag{6.11}$$

or, $$\frac{C_{ab}}{\epsilon} = \frac{\eta_0}{\sqrt{\epsilon_r}} \frac{(Y_{oo}^{b} - Y_{oe}^{b})}{2}$$

Here,

v = Velocity of light in the medium of propagation
= 1.18×10^{10} inches/sec.

η_0 = Intrinsic impedance for free space = 376.7 ohms

ϵ = dielectric constant = $0.225\epsilon_r$ μμf/inch.

For symmetrical parallel-coupled lines (i.e., $C_a = C_b$) odd-mode admittances are simply reciprocals to the odd-mode impedances, and analogously for even mode admittances and impedances. In case of unsymmetrical parallel-coupled lines, odd- and even-mode impedances are not simply reciprocals to the odd- and even-mode admittances. The reasons behind this is that when the odd- and even-mode admittances are computed, the basic definition of these admittances assumes that lines are being driven with voltages of identical magnitude with equal or opposite phase, while the currents in the lines may be of different magnitudes [11]. When the odd- and even-mode impedances are computed, the basic definition of these impedances assumes that the lines are being driven by the currents of identical magnitude with equal or opposite phases [11], while magnitudes of the voltages on the two lines may be different. These two sets of boundary conditions lead to different voltage-current ratios if the lines are unsymmetrical.

In figure 6.3, C_p^a is the parallel plate capacitance per unit length between one side of line 'a' and the adjacent ground plane, while C_p^b is the parallel plate capacitance per unit length between one side of line 'b' and the adjacent ground plane. The capacitance C_f' is the fringing capacitance per unit length for any of outer corners of the lines. The fringing capacitances per unit length at the inner corner of each line are designated C_{fe}' when the lines are excited in the even-mode; they are designated C_{fo}' when the lines are excited in the odd-mode. Here, both the lines are of same thickness and both are assumed to be wide enough so that interactions between the fringing fields at right and left sides of each bar (line) are negligible or at least small enough to be easily corrected for. On this basis, the fringing fields are same for both bars and their different capacitances C_a and C_b to ground are due entirely to different parallel plate capacitances C_p^a and C_p^b. For the structure shown in figure 6.3, the equations for self and mutual capacitances are [9]

$$C_a = C_{oe}^a = 2(C_p^a + C_{fe}' + C_f') \tag{6.13}$$

$$C_b = C_{oe}^b = 2(C_p^b + C_{fe}' + C_f') \tag{6.14}$$

and, $C_{ab} = (C_{fo}' - C_{fe}')$ (6.15)

Getsinger[9] presented some curves which relate the fringing capacitances to the thickness and spacing of parallel-coupled rectangular bar transmission lines. These curves are shown in figures 6.4, 6.5 and 6.6. Plots of both even-mode fringing capacitances C_{fe}'/ϵ and the mutual capacitance $\Delta C/\epsilon$ between bars as functions of bar thickness and spacing are presented [9] in figure 6.4, while similar plots for the odd-mode fringing capacitances C_{fo}'/ϵ are shown [9] in figure 6.5. Plots of fringing capacitance C_f'/ϵ from the outer edges of the bar as a function of thickness are presented [9] in figure 6.6.

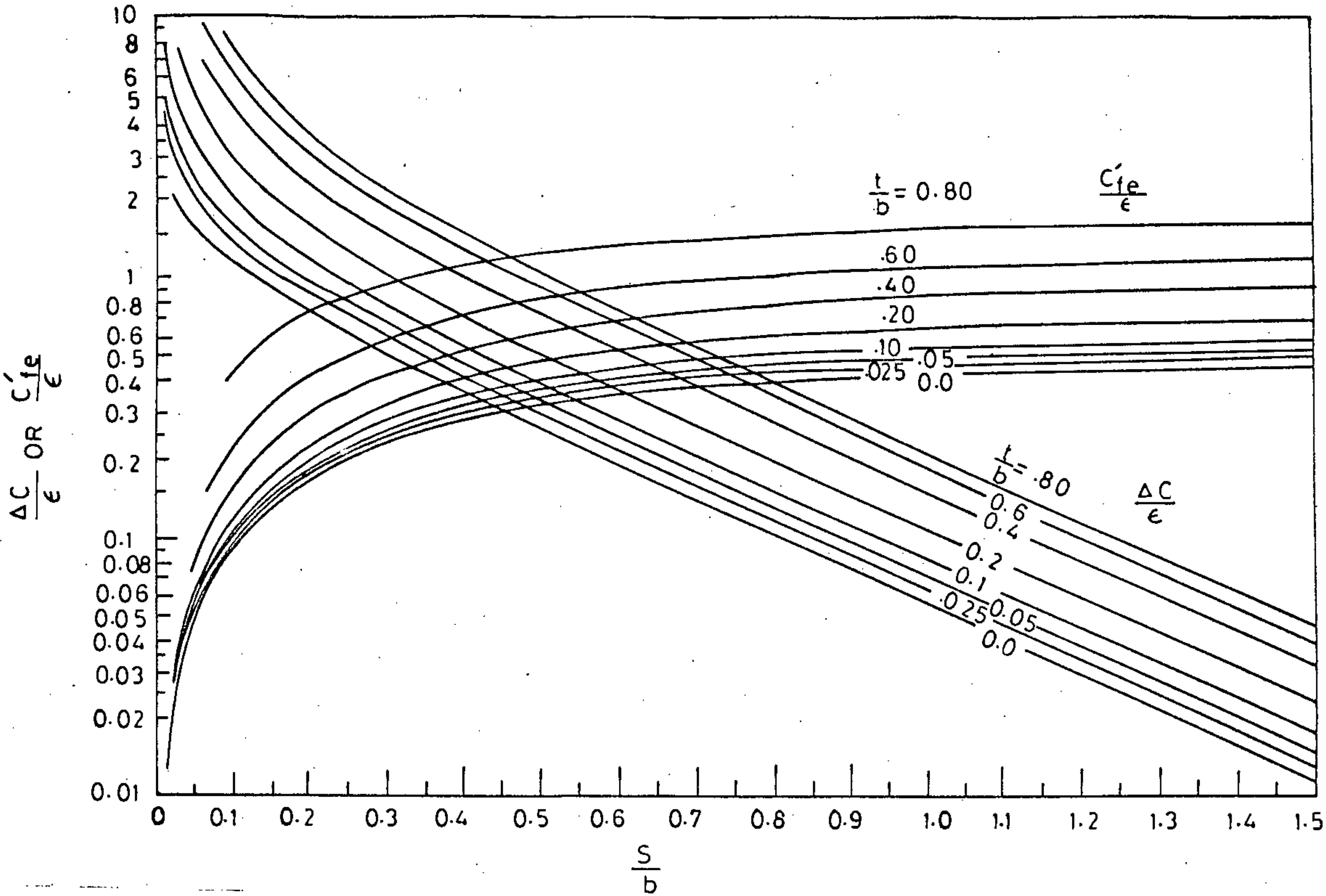

Figure 6.4. Plots of even-mode fringing capacitance C_{fe}'/ϵ versus spacing s/b and mutual capacitance $\Delta C/\epsilon$ versus spacing s/b of two coupled rectangular bars for various values of t/b.

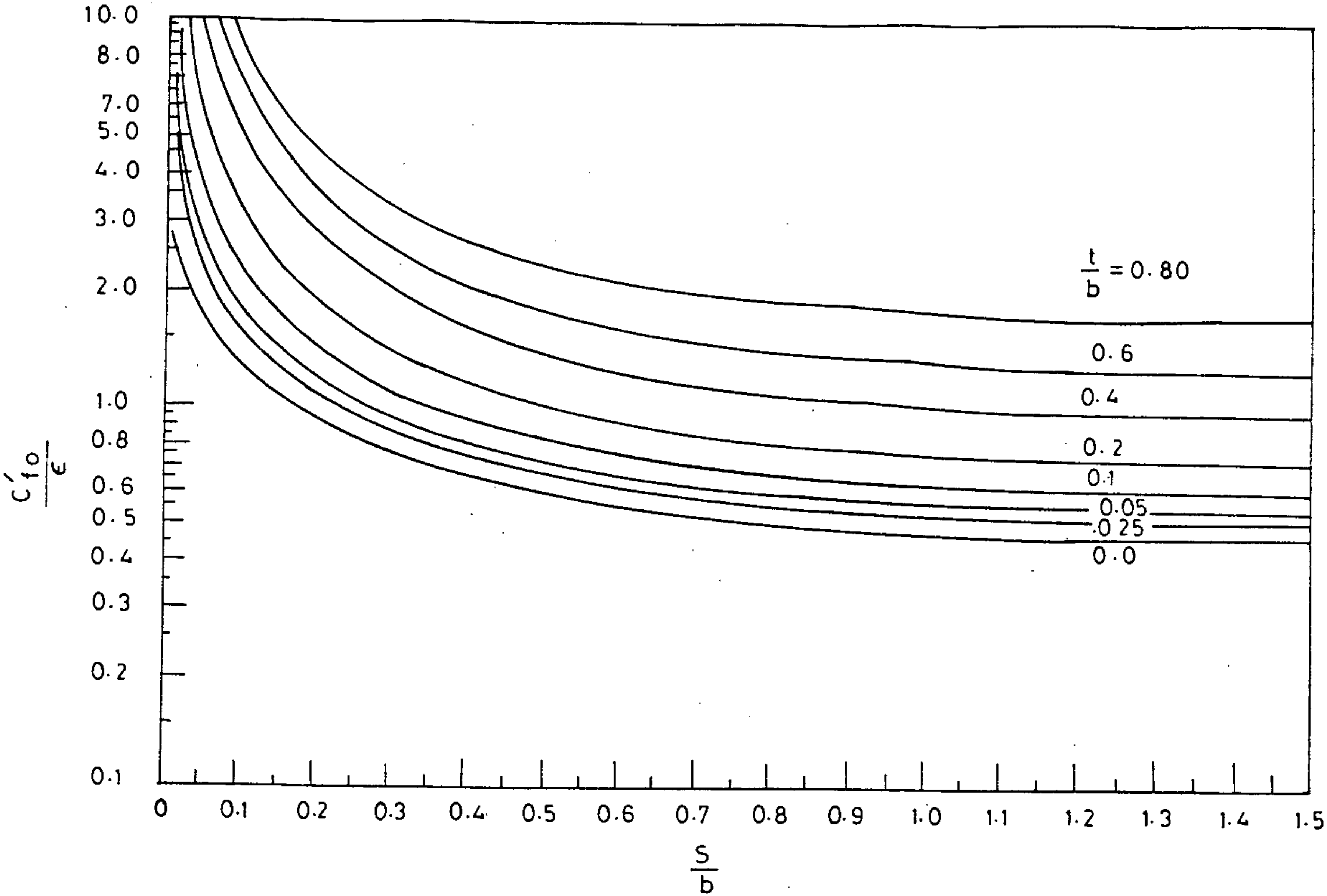

Figure 6.5. Plots of odd-mode fringing capacitance C_{fo}'/ϵ versus spacing s/b for two coupled rectangular bars.

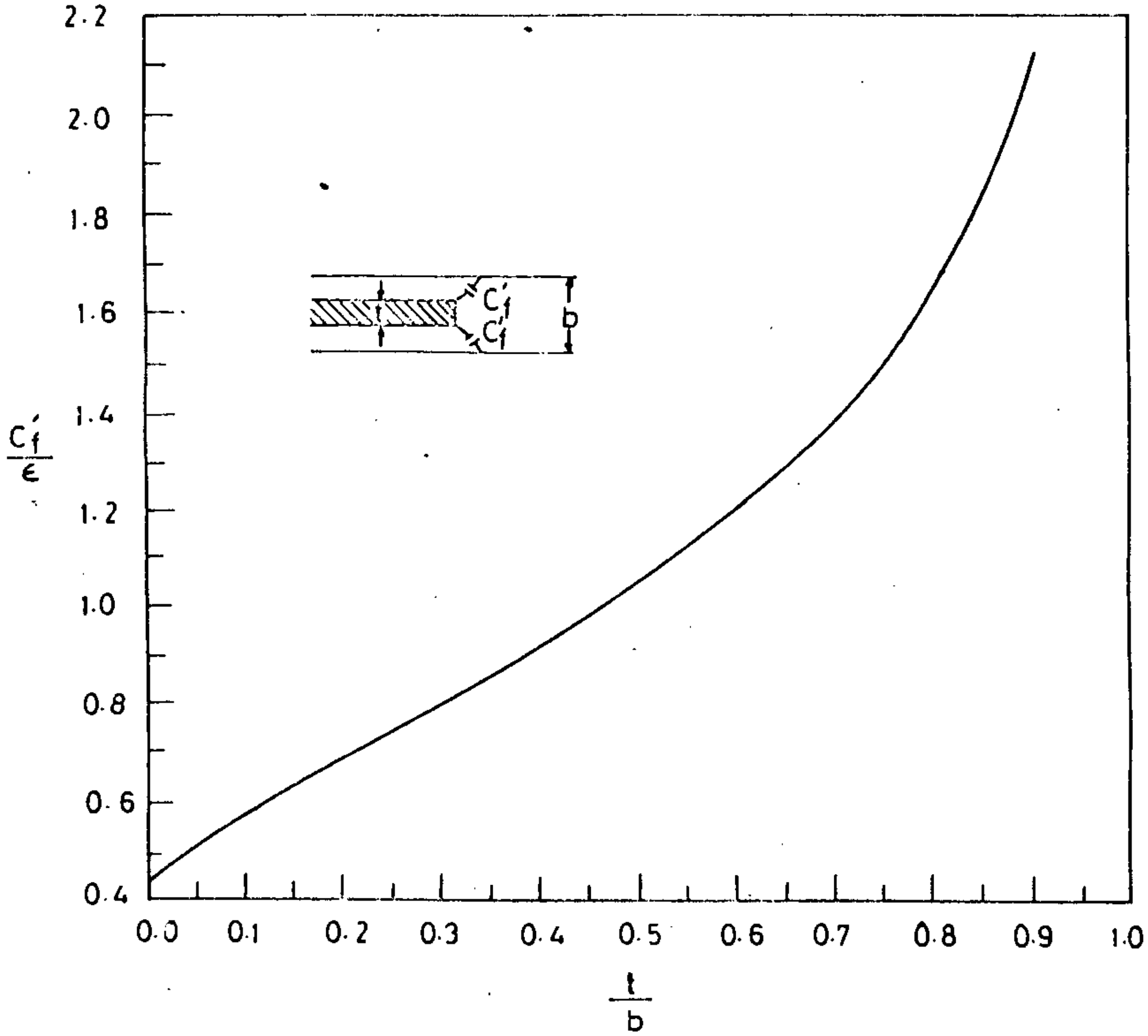

Figure 6.6. Plot of end fringing capacitance C_f'/ϵ versus thickness t/b for an isolated rectangular bar.

6.3 Determination of widths of unsymmetrical paralled-coupled rectangular bar lines

6.3.1 Widths of a pair of unsymmetrical parallel-coupled lines

By definition, the parallel plate capacitance C_p/ϵ per unit length of a line of figure 6.1 can be written as

$$C_p/\epsilon = \frac{w}{(1/2)(b-t)} \tag{6.16}$$

where, w = width of each bar, b = spacing between two ground planes and t = thickness of each bar. From equation (6.16) we can write

$$w/b = (1/2)(1 - t/b)\ C_p/\epsilon \tag{6.17}$$

Thus if the parallel plate capacitance of a line is known, then the width of the rectangular bar line can be obtained with the help of equation (6.17).

For unsymmetrical parallel-coupled lines shown in figure 6.3, using equations (6.13) and (6.14), the parallel plate capacitances C_p^a/ϵ and C_p^b/ϵ can be written as

$$C_p^a/\epsilon = 1/2[(1/2)\ C_a/\epsilon - C_{fe}'/\epsilon - C_f'/\epsilon] \tag{6.18}$$

and

$$C_p^b/\epsilon = 1/2[(1/2)\ C_a/\epsilon - C_{fe}'/\epsilon - C_f'/\epsilon] \tag{6.19}$$

Substituting the values of C_p^a/ϵ and C_p^b/ϵ in equation (6.17), the widths of line 'a' and 'b' may be written as

$$w_a/b = 1/2[1-t/b][1/2\ C_a/\epsilon - C_{fe}'/\epsilon - C_f'/\epsilon] \tag{6.20}$$

$$w_b/b = 1/2[1-t/b][1/2\ C_b/\epsilon - C_{fe}'/\epsilon - C_f'/\epsilon] \tag{6.21}$$

6.3.2 Widths of an array of parallel coupled lines

An interdigital filter consists of an array of parallel coupled lines of unequal widths. The cross-sectional view of such an array of parallel coupled lines is shown in figure 6.7. In this array of parallel coupled lines all the bars have the same t/b ratio. It is now necessary to generalize equations (6.20) and (6.21) in order to be able to compute the widths of the lines of this array of coupled lines.

In figure 6.7 the electrical properties of the lines have been characterised in terms of self capacitances C_k per unit length of each bar with respect to ground and mutual capacitances C_{kk+1} per unit length between adjacent bars k and k+1. This representation is not necessarily always highly accurate [9] but it is conceivable that a

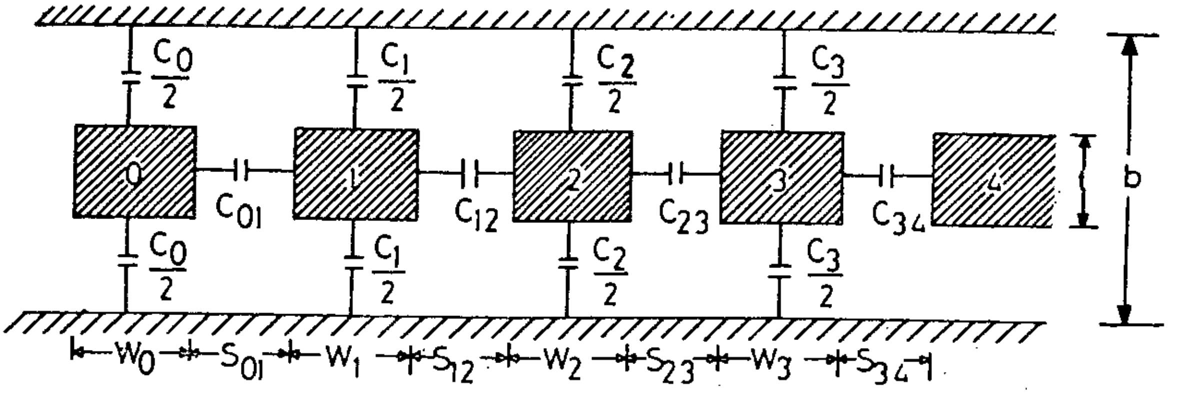

Figure 6.7. Cross-section of an array of unsymmetrical parallel-coupled lines showing various capacitances.

significant amount of fringing capacitance could exist between a given line element and, say, the line element beyond the nearest neighbour. However, at least for the geometry such as shown in figure 6.7, this representation gives satisfactory accuracy [9].

Since, fringing fields between adjacent two lines are considered to be same, the normalised self-capacitance C_k/ϵ for k^{th} bar can be written as

$$C_k/\epsilon = 2[C_p^{\,k}/\epsilon + (C_{fe}')_{k-1k}/\epsilon + (C_{fe}')_{kk+1}/\epsilon] \qquad (6.22)$$

Also the normalised self-capacitance per unit length for the end line 0 is

$$C_0/\epsilon = 2[C_p^{\,0}/\epsilon + (C_{fe}')_{01}/\epsilon + C_f'/\epsilon] \qquad (6.23)$$

$C_p^{\,k}$ and $C_p^{\,0}$ in the above equations are the parallel plate capacitance of the k^{th} line and 0^{th} line respectively. Now, extracting the values of $C_p^{\,0}$ and $C_p^{\,k}$ from equations (6.22) and (6.23) and putting these to the equation (6.17) we can write the expression for widths of k^{th} line and 0^{th} line as

$$w_k/b = (1/2)(1-t/b)[(1/2)C_k/\epsilon - (C_{fe}')_{k-1k}/\epsilon - (C_{fe}')_{kk+1}/\epsilon] \qquad (6.24)$$

$$w_0/b = (1/2)(1-t/b)[(1/2)C_0/\epsilon - (C_{fe}')_{01}/\epsilon - C_f'/\epsilon] \qquad (6.25)$$

These width formulas are sufficient to determine the width of each of the rectangular bar lines of the interdigital filter to be fabricated.

6.4 Use of Getsinger's graphs for computing physical dimensions

Plots of normalized mutual capacitance per unit length $\Delta C/\epsilon$ against spacing s/b between two parallel conductors as well as plots of associated normalized fringing capacitance per unit length C_{fe}'/ϵ against spacing s/b are available in figure 6.4. On the other hand, plots of normalized odd-mode capacitance C_{fo}'/ϵ against spacing s/b are available in figure 6.5. These plots are made for different values of t/b ratio. A plot of normalized end fringing capacitance C_f'/ϵ against t/b ratio is avaliable in figure 6.6. These plots have been taken from reference [9] of Getsinger.

If the mutual capacitance between two parallel coupled lines is known, the corresponding value of s/b for a chosen t/b ratio can be obtained from the plot of $\Delta C/\epsilon$ vs s/b of figure 6.4. For determining the widths of the lines (figure 6.7), the associated fringing capacitance C_{fe}'/ϵ or C_f'/ϵ have to be obtained first from the graphs of figure 6.4 and 6.6.

For computing the width w_k of k-th rectangular bar and the spacing s_{kk+1} between the k^{th} and $(k+1)^{th}$ lines (figure 6.7) the first step is to choose the values t (i.e. thickness of the bar) and b (i.e., distance between two parallel ground plates). This fixes the t/b ratio. Since,

$$(\Delta C/\epsilon)_{kk+1} = C_{kk+1}/\epsilon \tag{6.26}$$

the value of $(s/b)_{kk+1}$ and $(C_{fe}')_{kk+1}/\epsilon$ for the above mutual capacitance and selected t/b ratio can be obtained from the graphs of figure 6.4. Thus, the spacings s_{kk+1} between all the bars and also the associated fringing capacitances $(C_{fe}')_{kk+1}/\epsilon$ can be obtained. For a line of an interdigital filter the capacitance C_k/ϵ is obtained directly from the design equations of chapter 5 and the two fringing capacitance components $(C_{fe}')_{k-1k}/\epsilon$ and $(C_{fe}')_{kk+1}/\epsilon$ is obtained from figure 6.4 as discussed above. So the width W_k for the k^{th} line is then computed using eqution (6.24).

For obtaining the width of the input/ output lines of the array (line '0' figure 6.7), it is seen that the left side of the bar has no neighbour and the right side of the bar has a neighbouring line like other lines. For this case the fringing component C_f'/ϵ exists at the left side of the line '0' instead of the even-mode fringing capacitance C_{fe}'/ϵ. The width of this line is computed by following the procedure discussed above after obtaining the value C_f'/ϵ for th line using figure 6.6.

6.5 Width correction of relatively narrow width of rectangular bar

If the widths of the rectangular bar lines are wide enough th the interaction between the fringing fields at the inner sides of t bars may be neglected. In contrast to this, if the bar width w for line is too small, interaction of the fringing fields from the t edges will take place and, hence the decomposition of the tot capacitance into parallel plate capacitance and fringing capacitanc (which are based on infinite widths) will be no longer accurate [9 Cohn [7] has shown that for a single bar centred between parall planes, the error in total capacitance from interaction of t fringing fields is about 1.24 percent for $w/(b-t) = 0.35$. If a maxim error in total capacitance of approximately this magnitude is allowe then it is necessary that $(w/b)(1-t/b) > 0.35$.

Should this inequality be too restricting, it is possible to ma approximate corrections based on increase in the parallel pla capacitance to compensate for the loss of fringing capacitance due interaction of fringing fields. So, if it is found that the initi calculated value w/b is less than $0.35[1-t/b]$, then the correct width w'/b is obtained using the approximate formula

$$w'/b = \frac{0.07(1 - t/b) + w/b}{1.20} \tag{6.27}$$

Provided that $0.1 < [(w'/b)/(1-t/b)] < 0.35$

6.6 Summary

Analytical expressions for computing the widths of rectangul bar lines of an interdigital filter have been presented. Getsinger graphs for obtaining various fringing capacitances have be presented. Also, Getsinger's graphs for obtaining interbar spaci from mutual capacitances have been presented. Special treatments to given to the first and last (i.e., input and output) lines of a filt and for narrow-width lines have also been discussed.

Chapter 7

Design procedure of interdigital bandpass filters and design examples

7.1 Introduction

The procedure for designing interdigital bandpass filters, using the design equations derived and presented in chapter 5, is presented in this chapter. A design example is presented. Using the same lowpass prototype the results of design computation for various bandwidths with a range of 2% to 45% are also presented.

7.2 Design procedure

The following four steps are to be followed for designing interdigital bandpass filters.

Step 1 In this step a list of filter specification is prepared as shown below. If any of the required specification value is not available then a suitable value is to be assigned.

i) Type of function for response / characteristic (Chebyshev for the present case).

ii) Maximum passband insertion loss A_{max}. Alternatively maximum passband reflection coefficient.

iii) Steepness of the transition region between passband and stopband. Alternatively the value of insertion loss A_a at the specified frequency.

iv) Center frequency or midband frequency f_0 in Hz.

v) Fractional bandwidth (BW) W

vi) Terminating impedance $Z_0 = 1/Y_A = 1/G_A = 1/G_B$.

From the A_{max} mentioned in item (ii) above, the value of maximum reflection coefficient is to be obtained by using equations (4.1) and (4.3) of chapter 4. Also using the steepness value or the value of A_a and frequency the value of filter complexity number or resonator number n is to be computed by using equation (4.19) of chapter 4.

Step 2 For the filter under discussion the type of characteristic is Chebyshev. So for Chebyshev filter, for the filter complexity n and for the maximum passband reflection coefficient the lowpass prototype filter network parameters are obtained using filter catalogue of Saal [31]. Using these lowpass parameter values and using the equations presented in chapter 5 the inverter parameters J_{01}, J_{12}, J_{23}, ... J_{n-1n} for n-resonators are obtained. Using the equations provided in chapter 5 the self and mutual capacitance values of the coupled lines are obtained. The value of fractional bandwidth selected in step 1 will be used in this calculation . A computer program has been prepared to perform this part of computation work. The program is presented in Appendix A.2.

Step 3 A choice of ground plate spacing b and the thickness of each rectangular bar t is to be made at this stage. The distance between two grounded side walls along the length of the coupled lines is d = $\lambda_0/4$ inch. This value is computed for the selected center frequency of the filter.

Step 4 Using the self and mutual capacitance values of the interdigital coupled lines the widths of individual lines and the inter-line spacings are obtained by using Getsinger's graphs [9] and equations as described in chapter 6. The values of line thickness t and ground plane spacing b fixed in step 3 will now be useful, since for obtaining the line widths and inter-line spacings the value of t/b is needed. A computer program has been prepared to perform this part of computation work. The program is presented in Appendix A.3.

7.3 Design examples

A design example:

Step 1 The specifications of this filter are listed below.

i) Type of function for response / characteristic : Chebyshev.

ii) Maximum passband insertion loss Amax.= 0.1dB

iii) The value of insertion loss A_a =34.91dB at ω_a/ω_0 = 1.1.

iv) Center frequency or midband frequency f_0 = 1.5 GHz.

v) Fractional bandwidth (BW) W = 0.12

vi) Terminating impedance $Z_0 = 1/Y_A = 1/G_A = 1/G_B$ = 50 ohms.

From the given value of A_{max} = 0.1 dB the magnitude of reflection coefficient is obtained as ρ = 0.15 by using equations (4.1) and (4.13). Also from the given value of A_a = 34.91dB at ω_a/ω_0 = 1.1 the value of n is found to be 6.00025 by using equation (4.19). So the value of n = 6 is chosen.

Step 2 For Chebyshev filter having filter complexity n = 6 and for the maximum passband reflection coefficient of ρ = 0.15 the lowpass prototype filter network parameters are obtained using filter catalogue of Saal [31].

g_0 = 1.0000, g_1 = 1.1650, g_2 = 1.4040, g_3 = 2.0540, g_4 = 1.5180,
g_5 = 1.9000, g_6 = 0.8613, g_7 = 0.7391.
This lowpass prototype is shown in figure 7.1.

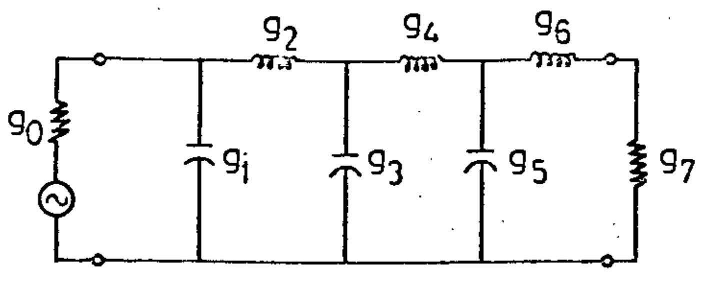

Figure 7.1. A Chebyshev Lowpass prototype filter for n=6, p=15%.

Using these lowpass parameter values and using the equations presented in chapter 5 the inverter parameters J_{kk+1}, the values of $N_{k,k+1}$ are computed. Next, the values of self and mutual capacitance values C_k, C_{kk+1} of the coupled lines are computed for this six resonator filter. The value of fractional bandwidth (W = 0.12) selected in step 1 is used in this calculation . A computer program has been prepared to perform this part of computation work. The program is presented in Appendix A.2.

Step 3 The ground plate spacing is chosen as b = 0.625 inch and the thickness of each rectangular bar is chosen as t = 0.187 inch. Thus the value of t/b = 0.187/0.625 = 0.2992. The distance between two grounded side walls along the length of the coupled lines is d = $\lambda_0/4$ inch. For the selected center frequency of 1.5 GHz of this filter d = 1.969 inch.

Step 4 Using the self capacitance values of the interdigital coupled lines obtained in step 3, the widths of individual lines are obtained for a t/b = 0.2992 by using Getsinger's graphs [9] and equations as described in chapter 6. Next, using the mutual capacitance values of the interdigital coupled lines the inter-line spacings are obtained for t/b = 0.2992 by using Getsinger's graphs [9] as described in chapter 6. A computer program has been prepared to perform this part of computation work. The program is presented in Appendix A.3.

The values of C_k, C_{kk+1}, J_{kk+1}, N_{kk+1}, w_k and s_{kk+1} obtained in the above steps are as follows:

Design example of interdigital bandpass filter for 12% bandwidth

k	C_k/ϵ	$C_{k,k+1}/\epsilon$	$J_{k,k+1}/Y_A$	$N_{k,k+1}$	w_k	$s_{k,k+1}$
0	5.8135	1.7205	0.9265	------	0.3908	0.1415
1	3.1832	0.3579	0.7819	5.34685	0.1430	0.4114
2	4.2562	0.2696	0.5889	5.32205	0.1768	0.4719
3	4.3424	0.2592	0.5663	5.31960	0.1733	0.4805
4	4.3424	0.2695	0.5888	5.32205	0.1733	0.4719
5	4.2563	0.3578	0.7817	5.34683	0.1768	0.4114
6	3.1834	1.7203	0.9263	-------	0.1460	0.1438
7	5.8137	------	------	-------	0.3952	-------

$h = 0.060758$ $M_1 = 0.02460$ $M_6 = 0.0246$ $Y_A = 0.02$ mho.

A drawing of this interdigital bandpass filter having Chebyshev characteristic, showing the various dimensions, is shown in figure 7.2.

In order to see the effect of variation of bandwidth on the line parameters of the above filter, 13 values of bandwidths within 2% to 45% have been considered. The line parameters computed for these 13 values of bandwidths are presented in Appendix C. From these values it has been observed that the width (w_1) of the resonator line next to the input line as well as the width (w_6) of the resonator line adjacent to the ouput line of the filter become smaller as the bandwidth is increased. Similar effect is observed for the interline spacings between lines 0 and 1 as well as lines 6 and 7. These can be

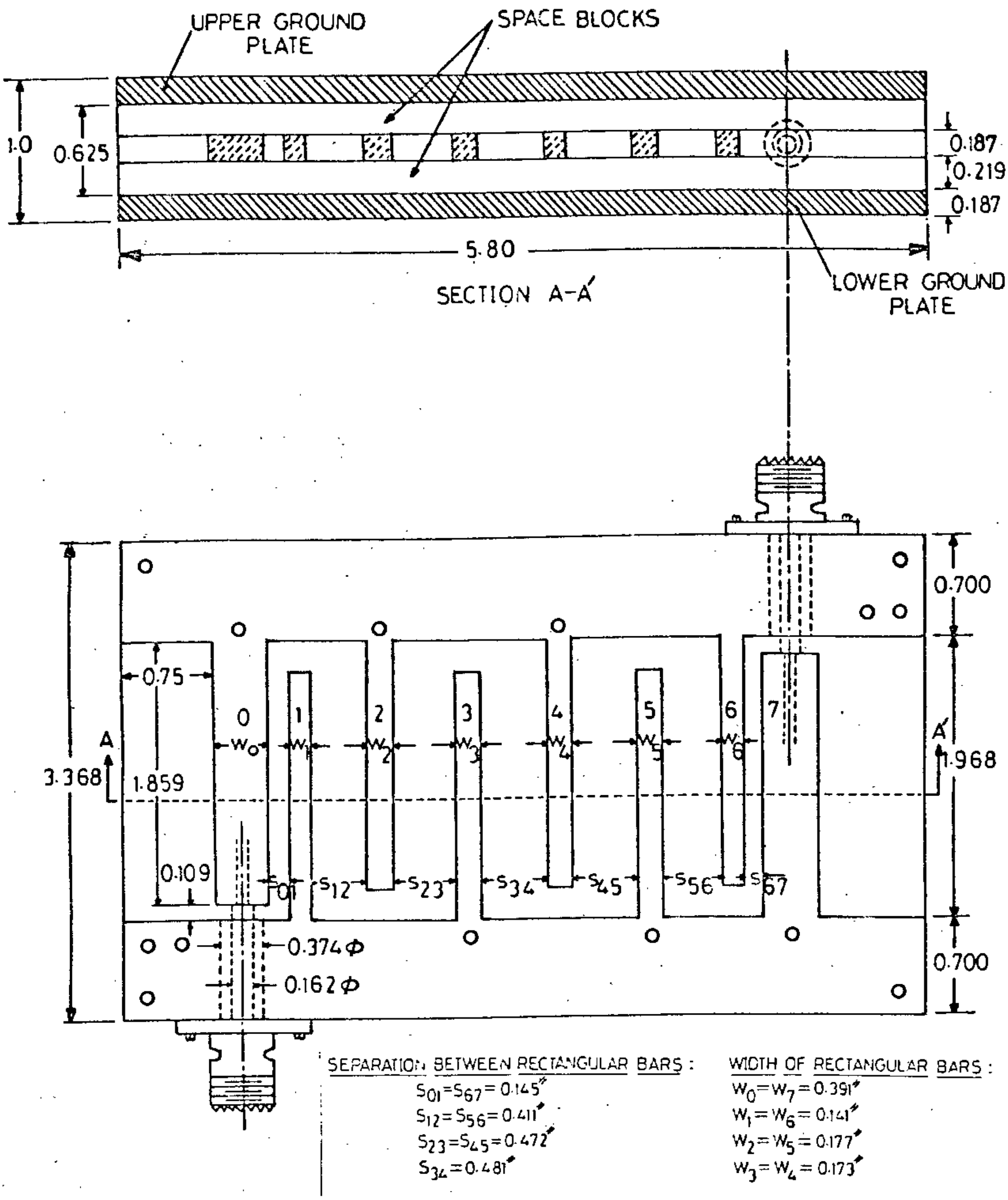

Figure 7.2. A drawing of the designed Chebyshev Interdigital Bandpass Filter for n=6 and 12% bandwidth showing the various dimensions.

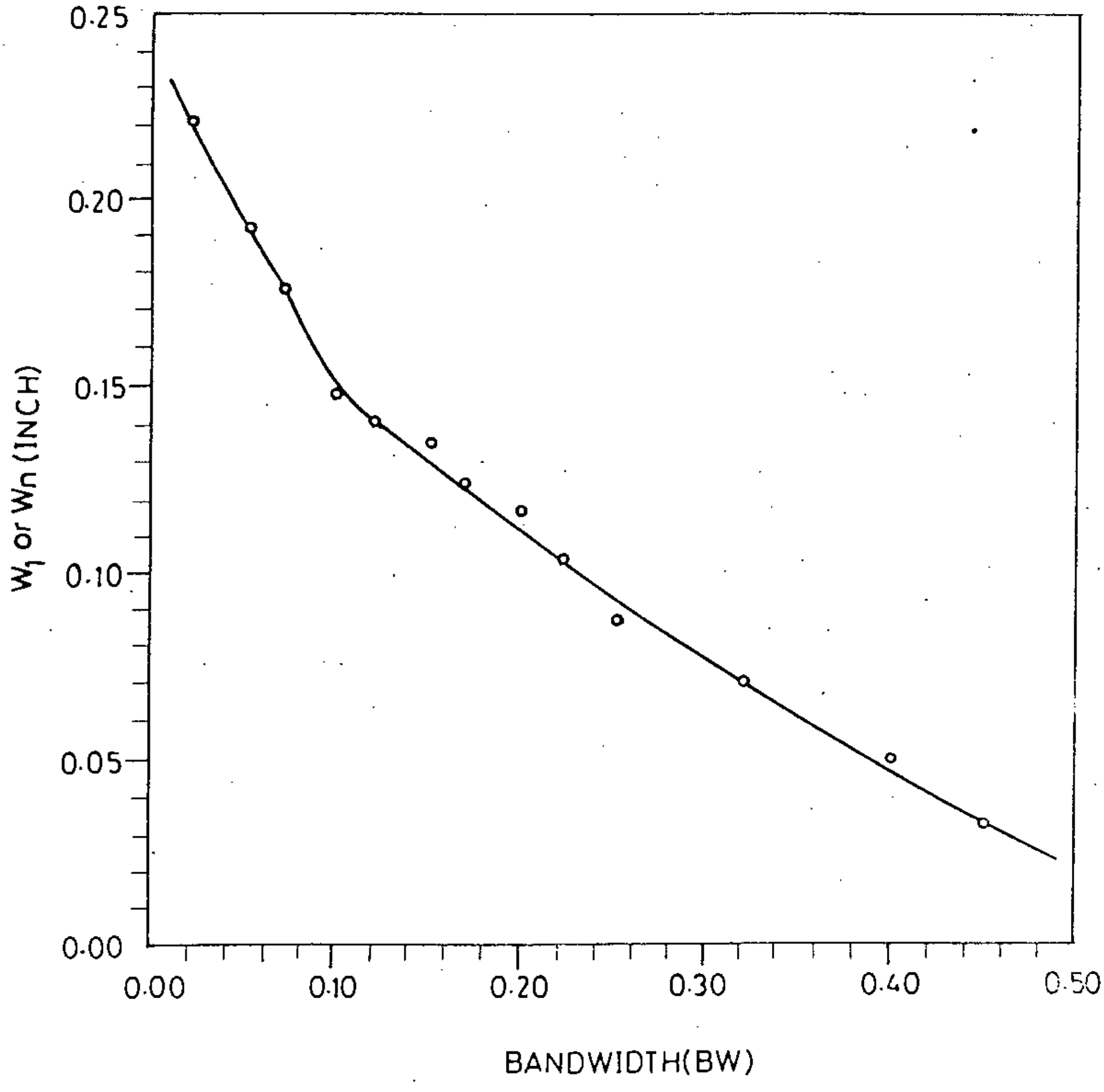

Figure 7.3. A plot of line width of line 1 versus bandwidth for the present design method.

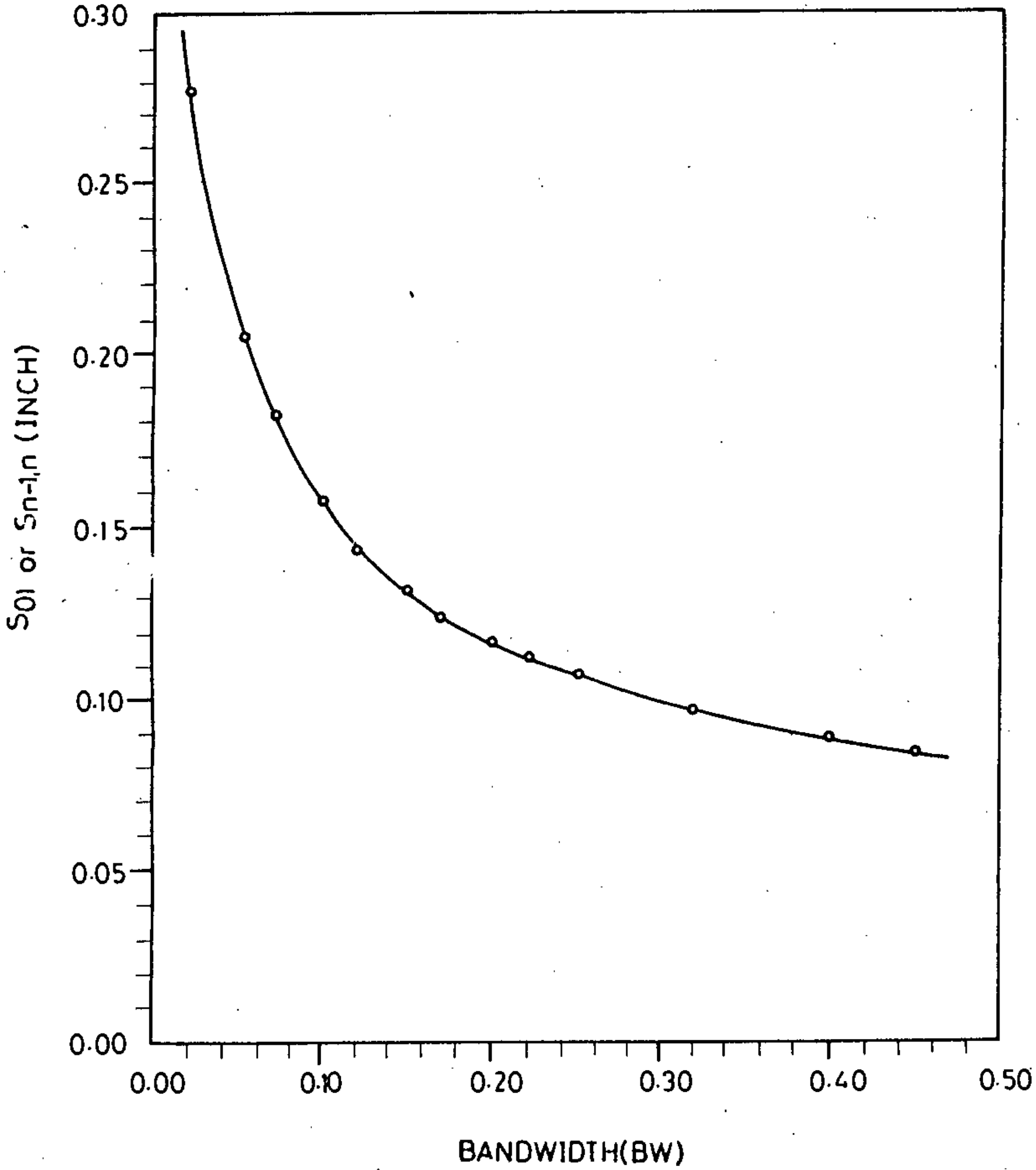

Figure 7.4. A plot of spacing betwen line 0 and line 1 versus bandwidth for the present design method.

observed from the curves of figures 7.3 and 7.4. At broader bandwidths such as 40% the line dimensions are difficult to fabricate. In fact the widths and interline spacings of all the lines become smaller with the increase in bandwidth. This makes us to believe that due to the above difficulties, the present design method is suitable for narrow-band but not good for broad-band filters.

7.4 Summary

The steps for designing interdigital bandpass filters have been presented. A design example having 6 resonators for 12% band width have also been presented. The line parameters of this design example have also been computed for 12 more bandwidths within the range of 2% - 45%. From these computations it has been observed that for broadband filters this design method produces dimensions which are difficult to fabricate. The method produces better dimensions for narrow-band filters.

Chapter 8

Fabrication of an experimental filter

8.1 Introduction

The process of fabricating an experimental interdigital bandpass filter is briefly presented in this chapter. The techniques involved in this process are also briefly outlined.

8.2 Method of fabrication

The design example presented in chapter 7 for 12% bandwidth is selected for fabrication. A drawing showing the plan of this filter with the top ground plate removed has been presented in figure 7.2. The cross-sectional view of this filter is presented in figure 8.1. From these two drawings it was figured out that the fabrication work will be done with 0.25 inch thick cold rolled brass plates. At the time of this work the 0.25 inch thick plate was one of the sizes available in the market.

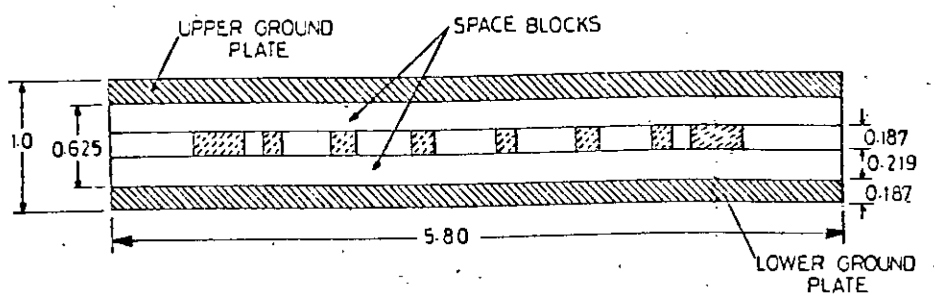

Figure 8.1. Cross-sectional view of the designed filter whose plan of the interdigital lines has been presented in figure 7.2.

From the cross-sectional view of figure 8.1 it is seen that the thickness of the main lines is $t = 0.187$ inch. It was decided that this thickness will be obtained by machining a 0.25 inch thick brass plate. For properly maintaining the vertical gaps with the ground plates, while the main lines are welded by gas flame to the ground walls, spacers are needed. These spacers maintaining vertical gap are of $(0.625 - 0.187)/2 = 0.219$ inch thickness. At least four additional spacers of 0.187 inch thickness are needed to maintain the inter-line spacings.

For fabrication, an interdigital bandpass filter may be divided into the following four parts.

(i) The bottom ground plate.

(ii) Spacers of thickness 0.219 inch maintaining permanent space between the main lines and the bottom ground plane. At least Two spacer bars are needed for two sides.

(iii) The interdigital main lines formed by interleaving two combline structures.

(iv) Spacers of thickness 0.219 inch maintaining permanent space between the main lines and the top ground plane

(v) The top ground plate.

From the drawing of figure 7.2 it may be observed that the dimension of the ground cover plates should be 5.9"x4". These two ground plates are made by smooth machining on both sides of two 0.25" thick brass plates. The length and width is taken at least 1/8" bigger than the required size in order to be able to give a final finished cutting of the completed filter. Brass plates has been found to have a tendency of bending while machining. So care must be taken so that the machining is done slowly and proper cooling arrangement is made during machining. Because of softness of brass care must be taken in subsequent handling of these plates so that no dent or surface bend appear.

Two spacer bars are next prepared by machining 0.25" thick brass plates. The size of these spacer bars is 5.8"x0.70"x0.219". The length and width of these bars shall also be taken 1/8" bigger than actual dimensions. These two spacers will be needed for mainitaining the bottom gap. So, two more identical spacers will be necessary for the top gap. These four spacers will remain as parts of the filter.

For obtaining the resonator lines (main lines), first, both the faces of a 2.5"x5.5"x0.25" brass plate are smoothly machined to bring down the thickness to 0.187". The 2.5" width dimension of the plate is then reduced, by machining both sides, down to (d - r) = 1.96"-0.2" = 1.76". The individual resonator elements are then produced by smoothly cutting out of this plate. Two combline structures will be formed by welding these resonator lines to two pieces of brass bars. These bars are identical to the four spacers mentioned above except that the thickness here is 0.187" instead of 0.219". Two such bars are prepared next. For placing the resonators of one comb structure and the corresponding grounding bar together during welding, temporary spacers are required for maintaining interline spacing. These spacers have the same thickness of 0.187". The lengths of these bars are made 1.96" and the widths are made to be equal to the interline gaps of the lines of the filter. After these spacers are made, the next job is to form the two comb structures by putting the temporary spacers in between the resonator lines. Actually the two comb structures are interleaved to form the interdigital structure and the assembly is done on a smooth surface metal base plate. After this the entire structure (i.e., the two comb structure in interleaved form) are tied together by wires.

The perpendicular junctions between the ends of the resonator lines and the ground bar are then joined by smooth gas welding. The gas welding is to be done in a number of steps. After the welding on one side the assembly is turned upside down on the baseplate for welding on the other side. Some finishing work with emery paper may be needed to remove surface irregularities at the junction due to gas welding. Actually if appropriate machines and tools were available then probably better finishing could have been obtained by cutting the total structure out of a single plate of 0.187" thickness.

After the welding work is done the temporary structures are not needed. However, these are needed during mounting of the complete filter structure. During this mounting, required permanent as well as temporary spacers are added in place to maintain the gap between the ground planes and the lines. The cover ground planes are then placed in position and at six places around the periphery of the filter light gas welding is performed so that the different layers of plates do not move during subsequent drilling work.

A number of drilled holes are made on two sides of the filter threads and arrangements are made for 3/16" dia countersunk brass screws. The screws are then fixed in position. A preliminary machined finish is given on the peripheral sides of the filter. During this finishing the light temporary fix welding applied will be cut. Two drilled holes of appropriate dimensions (0.374" for our case) are next cut for fitting the input and output coaxial connectors. The flange of each connector is fixed to the filter body by screws. RS 239

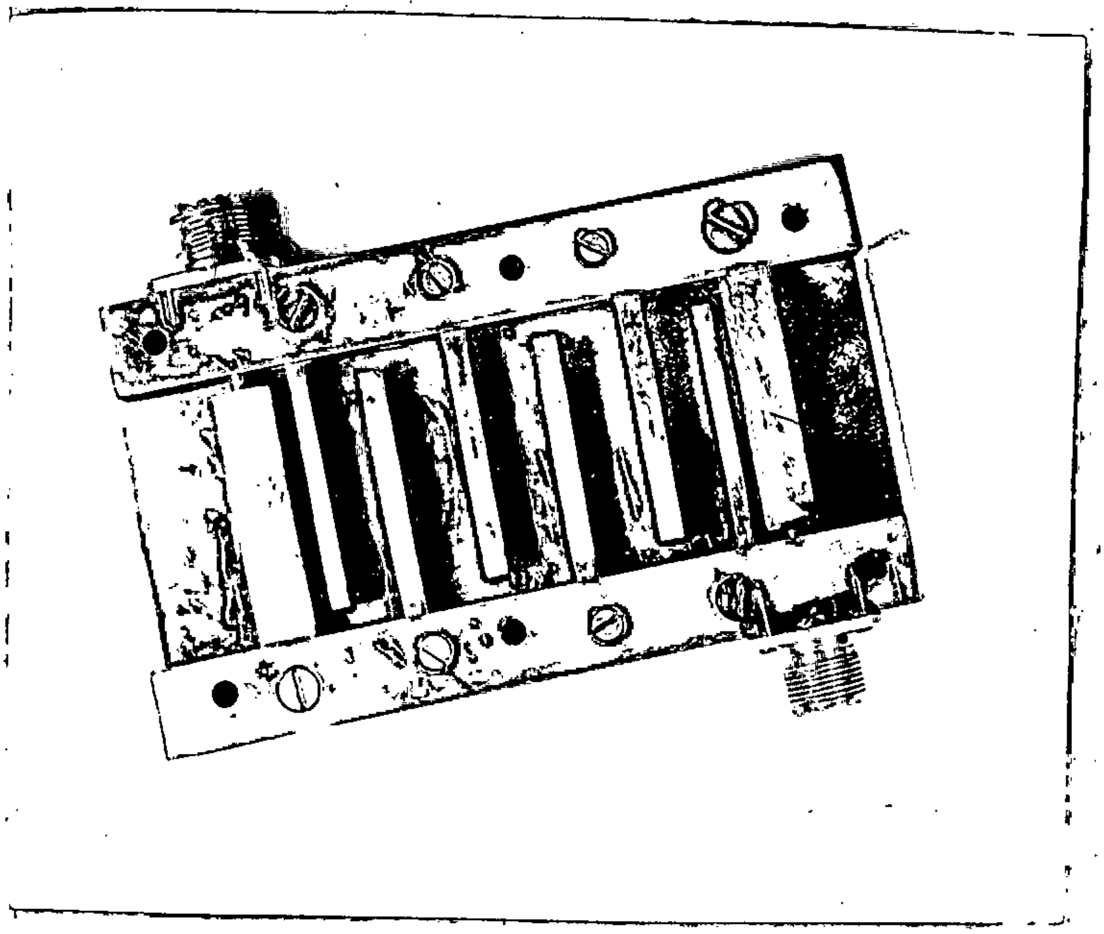

Figure 8.2. Photograph of a fabricated 12% bandwidth interdigital bandpass filter for Chebyshev characteristic. The designed center frequency is f_0 = 1.5 GHz.

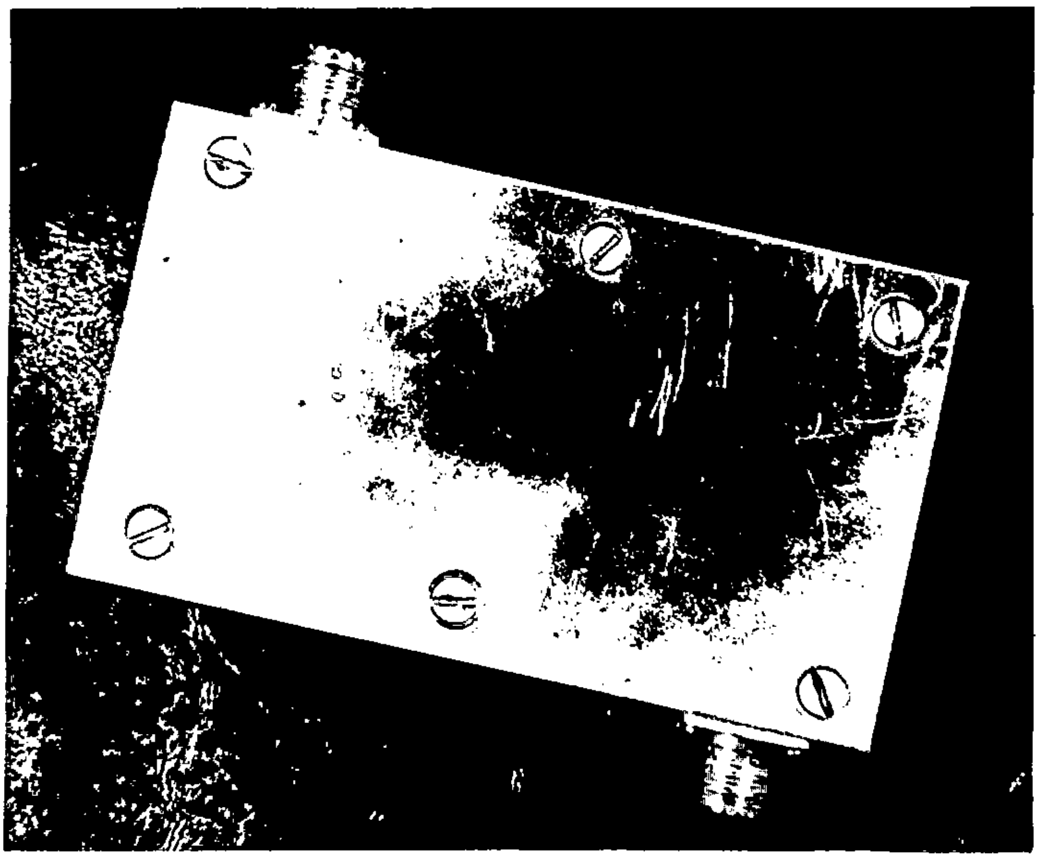

Figure 8.3. Top view of the fabricated filter.

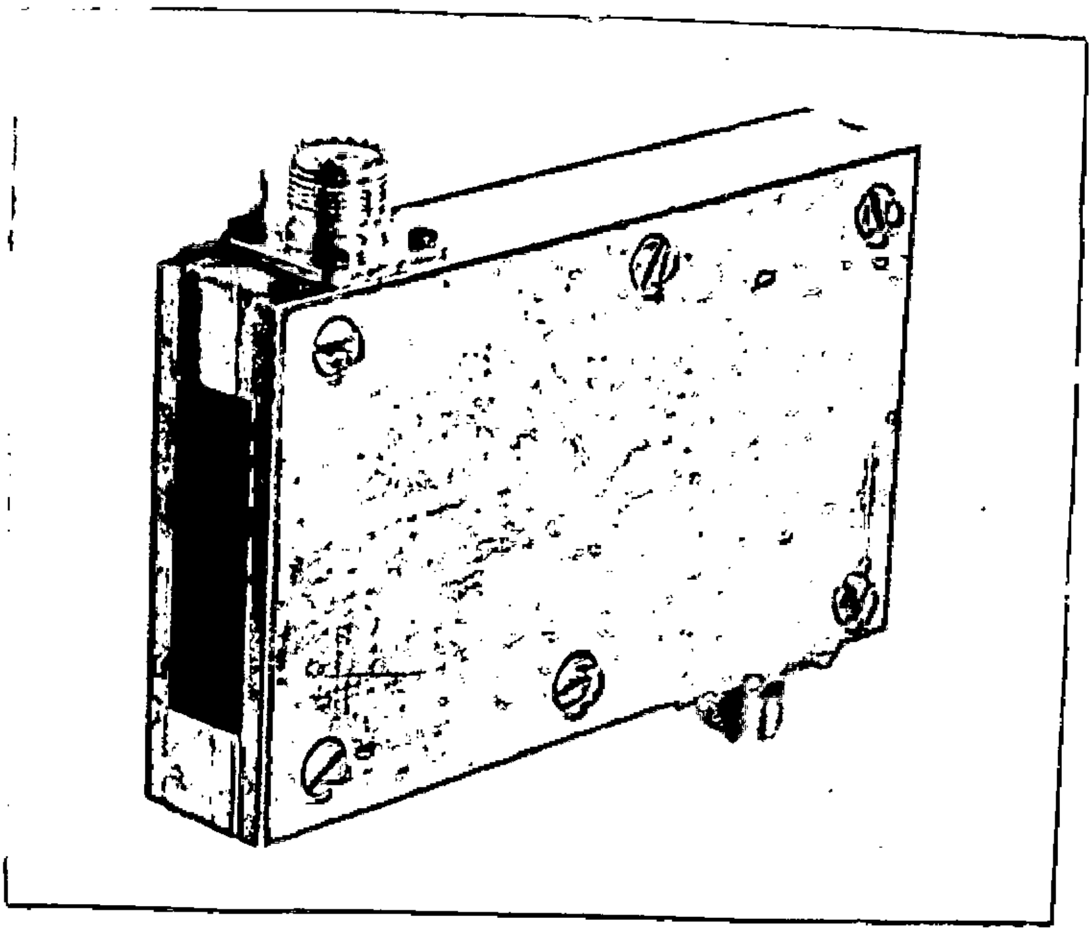

Figure 8.4. Photograph of the assembled filter.

connectors have been used. The protruding central conductor of this connector is .0625".

Before the final mounting of the coaxial connectors one of the cover plates is opened by unscrewing the screws. Arrangements are now made to fix some screws so that the filter structure remains fixed when the top cover plate is removed. The temporary spacers are then removed. The filter is then cleaned with acetone soaked tissues. The top cover plate is next placed in position, screws are fixed. At this stage a final light machining finish is given to the peripheral sides of the filter. The connectors are mounted after cleaning the connectors, connector holes, inside of the filter and outside of the filter with acetone soaked tissues. Acetone cleaning degreases the surfaces and removes the brass particles sticking to the surfaces. The filter is now ready for test and use.

An experimental filter has been constructed using this technique. The machining jobs of this fabrication were done in the machine shop of BUET and the gas welding jobs have been done in a market shop. The photograph of the experimental filter is presented in Figure 8.2. Actually one more filter was constructed before this one. The filter shown in figure 8.2 has been constructed to improve dimensional accuracy and finish over the filter made at first.

8.3 Summary

By machining of brass plates an experimental interdigital bandpass filter has been constructed. Fabrication process of this experimental interdigital bandpass filter has been discussed. For maintaining dimensional accuracy upto .0005" the presented method is expected to give nearly good result if the job is done meticulously. It is difficult to achieve good accuracy and good finish without attaining certain degree of skill in this fabrication job.

Chapter 9

Obtaining insertion loss characteristic of the experimental filter by microwave power measurement

9.1 Introduction

The procedure for measuring insertion losses of the experimental filter at discrete frequency points are described in this chapter. A number of plots of insertion-loss versus frequency for the various changes of physical dimensions of the filter are presented in this chapter.

9.2 Microwave power measurement at discrete frequencies using microwave power meter

A Hewlett Packard (HP) 430C microwave power meter, a HP-477B coaxial thermistor mount (bolometer) [23], a microwave signal generator were used for measuring average microwave power levels at discrete frequency points. The connection for this measurement set up requires a cable for connecting the bolometer with the power meter, a piece of microwave 50 ohms coaxial cable and connectors for connecting the microwave source with the filter under test or the bolometer as shown in figure 9.1. With this power meter it is possible to measure average power within the power range of 0.01mw - 10mw. The upper limit can be extended by adding precision fixed attenuators.

The bolometer used here contain a thermistor element which is a resistive device [23] capable of dissipating microwave power. The dissipation of microwave frequency signals causes thermal energy absorption which changes the resistance of the thermistor mount. The thermistor has a negative co-efficient of temperature and is constructed generally using a small amount of semiconducting material suspended by two fine wires. The HP-477B co-axial bolometer is designed to operate at 200 ohms resistance and with negative temperature co-efficient.

In the measurement set up, the bolometer forms one leg of a self balancing bridge of the power meter which balances operating resistance. The power meter contains such a bridge, a 10.8 KHz oscillator, a d.c. bias circuit and a meter circuit. At first, the output side of the bolometer is connected to the power meter, with a

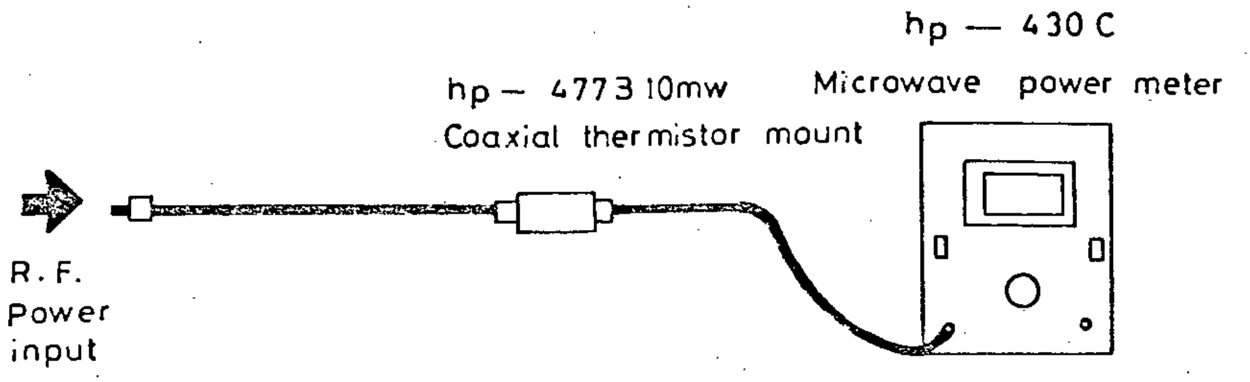

Figure 9.1. Measurement of microwave power of a microwave source at discrete frequency points with the help of a microwave power meter.

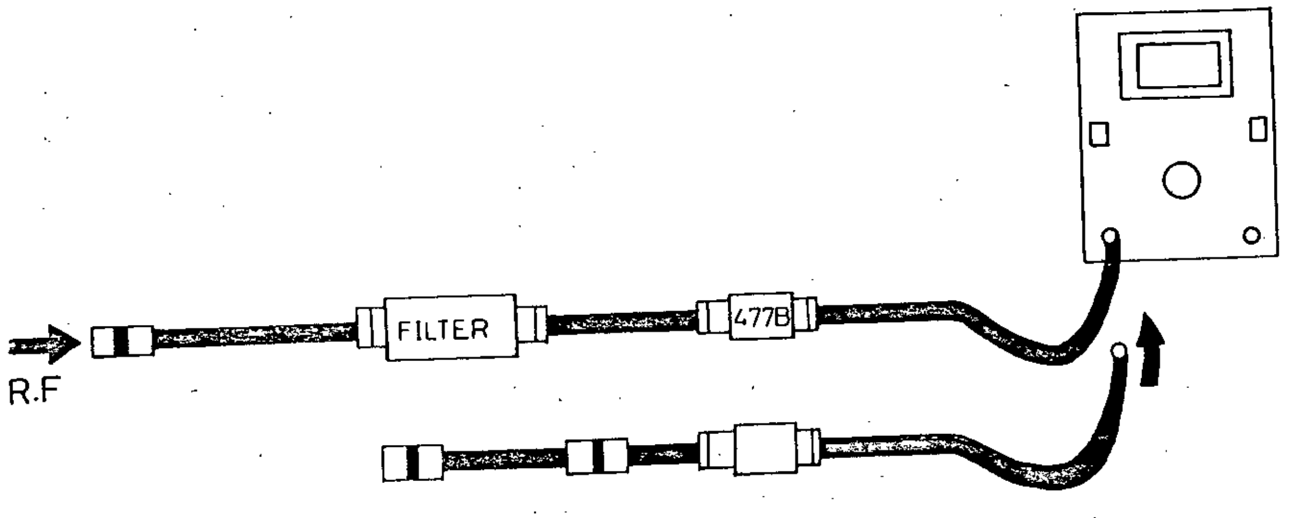

Figure 9.2. Measurement of input and output power of a microwave filter for obtaining power loss ratio at a particular frequency.

piece of coaxial cable having BNC connector at both ends, while keeping the bias switch of the power meter at OFF position. The input end of the bolometer is left open instead of connecting to the microwave source or filter. The bolometer is thus connected to the bridge circuit of the power meter.

Next the power range switch of the power meter is set to the required range. The biasing range switch is then turned on and set to the appropriate range so that the pointer of the meter remains near to zero. At this stage zero setting of the pointer can be obtained by the zero set knob. The thermistor mount bridge is balanced when the element changes from its cold resistance to its operating resistance. The change takes place as the element absorbs power from the oscillator and d.c. power from the bias circuit of the power meter.

A microwave signal generator with its built-in attenuator set to zero or minimum power output is connected with coaxial cable and connectors to the input side of the bolometer already connected to the power meter. The frequency of the microwave source is set to the center frequency of the filter (1.5 GHz in the present case). The built-in attenuator of the source is then increased slowly upto a point when the power meter indicates 75% of the maximum power. The frequency changing knob of the microwave source is then slowly rotated through the range of frequencies over which measurements will be done. For example in the present case the frequency range is appproximately 1.32GHz to 1.68GHz. While rotating the frequency knob if it is found that the power meter pointer never exceeds the maximum limit of the scale then the set up is now ready for measurement. Otherwise some readjustment of the attenuator of the microwave source would eliminate the problem.

Because of the dissipation due to absorption of microwave power from the external source, the thermistor changes its resistance which unbalances the bridge of the power meter. This action causes the output from the oscillator inside the power meter to decrease to accomodate the external microwave power through the thermistor element. The voltmeter circuit inside the power meter measures the amount of this power decrease from the oscillator of the power meter due to the presence of microwave signal from the external source and display the result of the measurement over a calibrated scale.

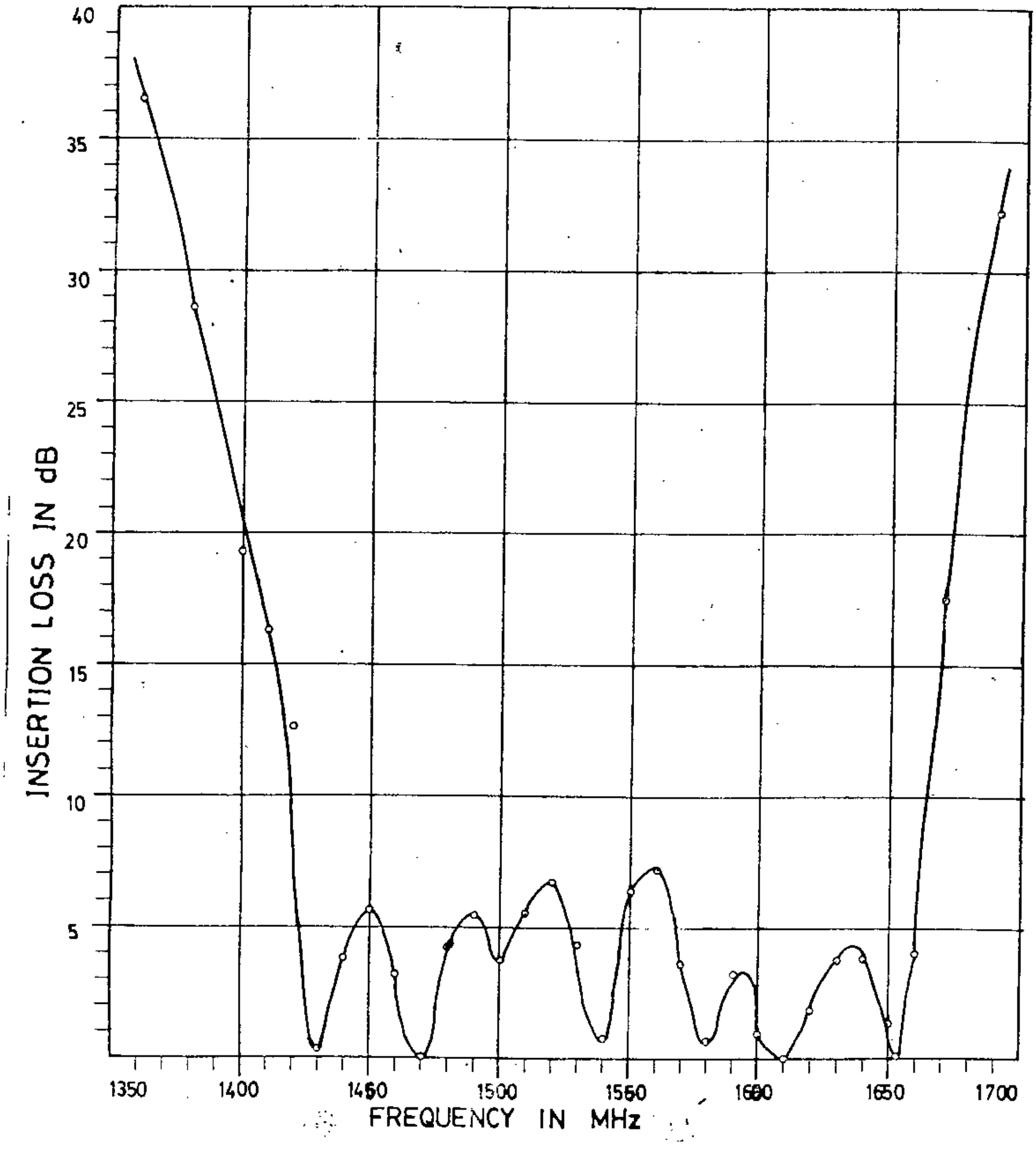

Figure 9.3. First plot of measured insertion loss against frequency of the experimental filter. The center frequency is f_o = 1.532 GHz, bandwidth = 218 MHz (14.22%) and A_{max} = 7.25 dB.

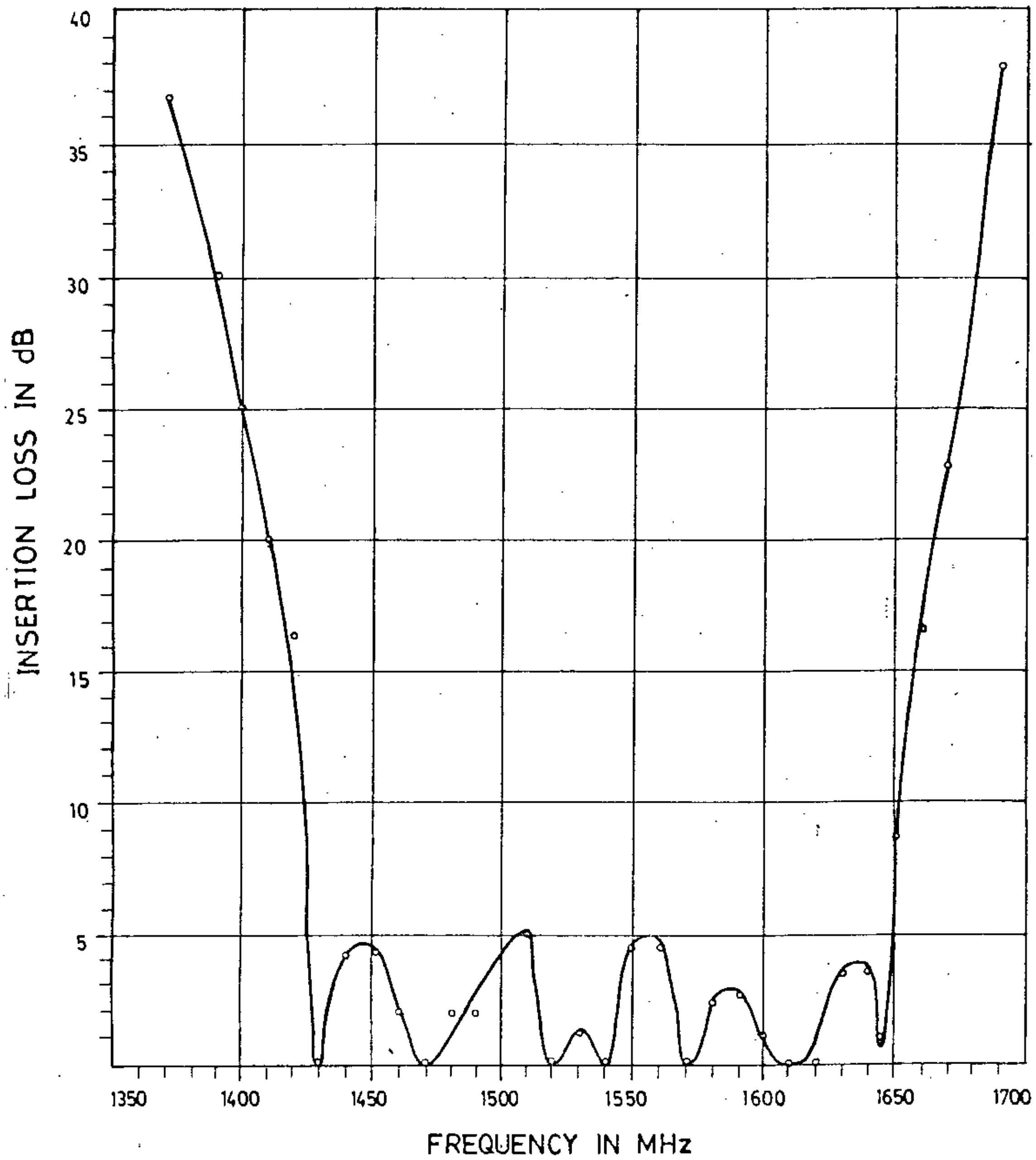

Figure 9.4. Plot of measured insertion loss against frequency of the experimental filter after adding 0.5mm thick brass shim to the coupled sides of input as well as output transformer element. The plot shows that the center frequency is f_o = 1.533 GHz, bandwidth = 225 MHz (14.67%) and A_{max} = 5.1 dB.

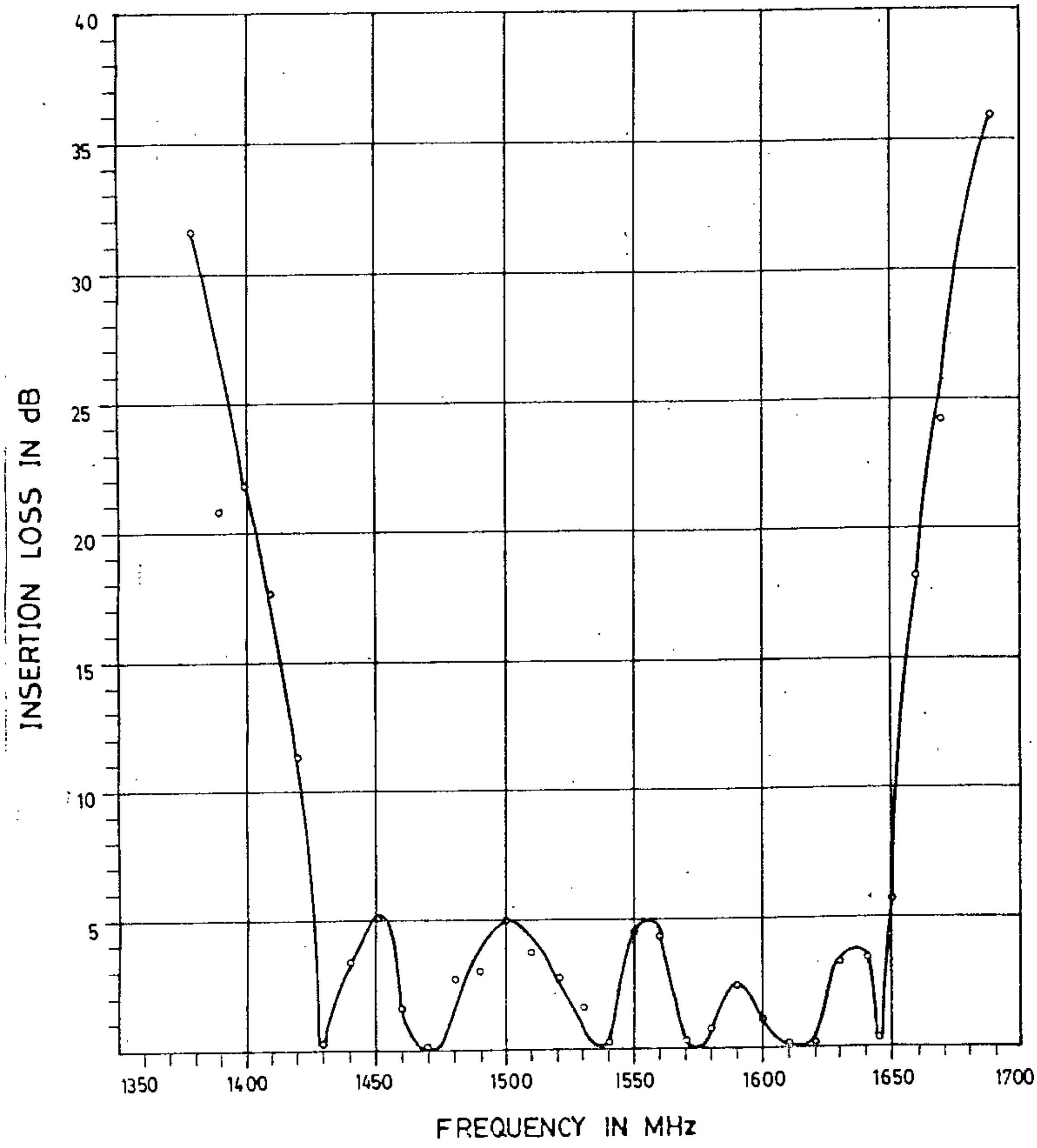

Figure 9.5. Plot of measured insertion loss against frequency of the experimental filter after adding 0.5mm thick brass shim to the coupled sides of input as well as output transformer element. The input and output connections were inter-changed during measurement. The plot shows that the center frequency is f_o = 1.533 GHz, bandwidth = 225 MHz (14.67%) and A_{max} = 5.1 dB.

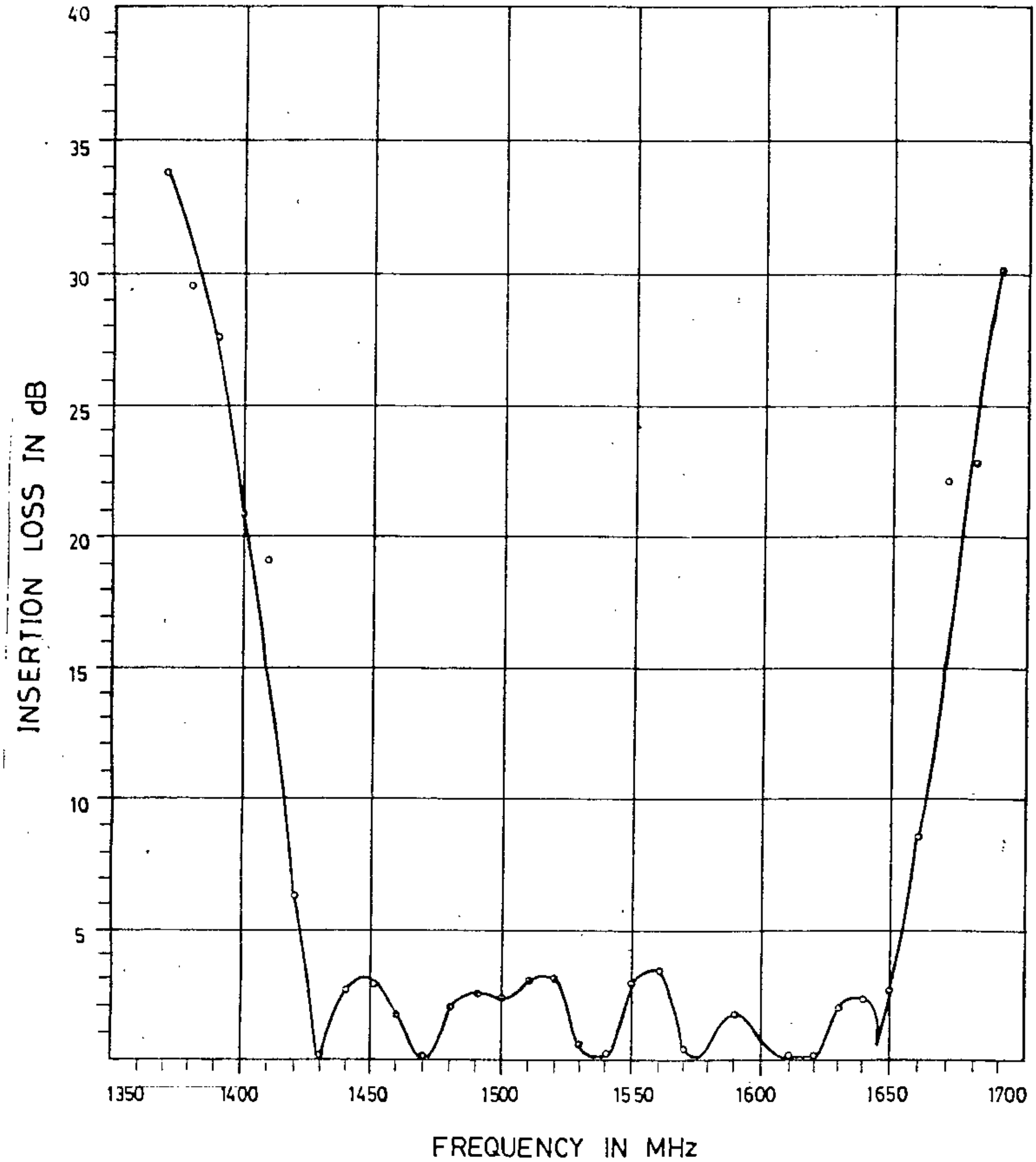

Figure 9.6. Plot of measured insertion loss against frequency of the experimental filter after adding 0.75mm thick brass shim to the coupled side of the input transformer element and 0.5mm thick brass shim to the coupled side of the output transformer element. The plot shows that the center frequency is f_o = 1.538 GHz, bandwidth = 223 MHz (14.48%) and A_{max} = 3.3 dB.

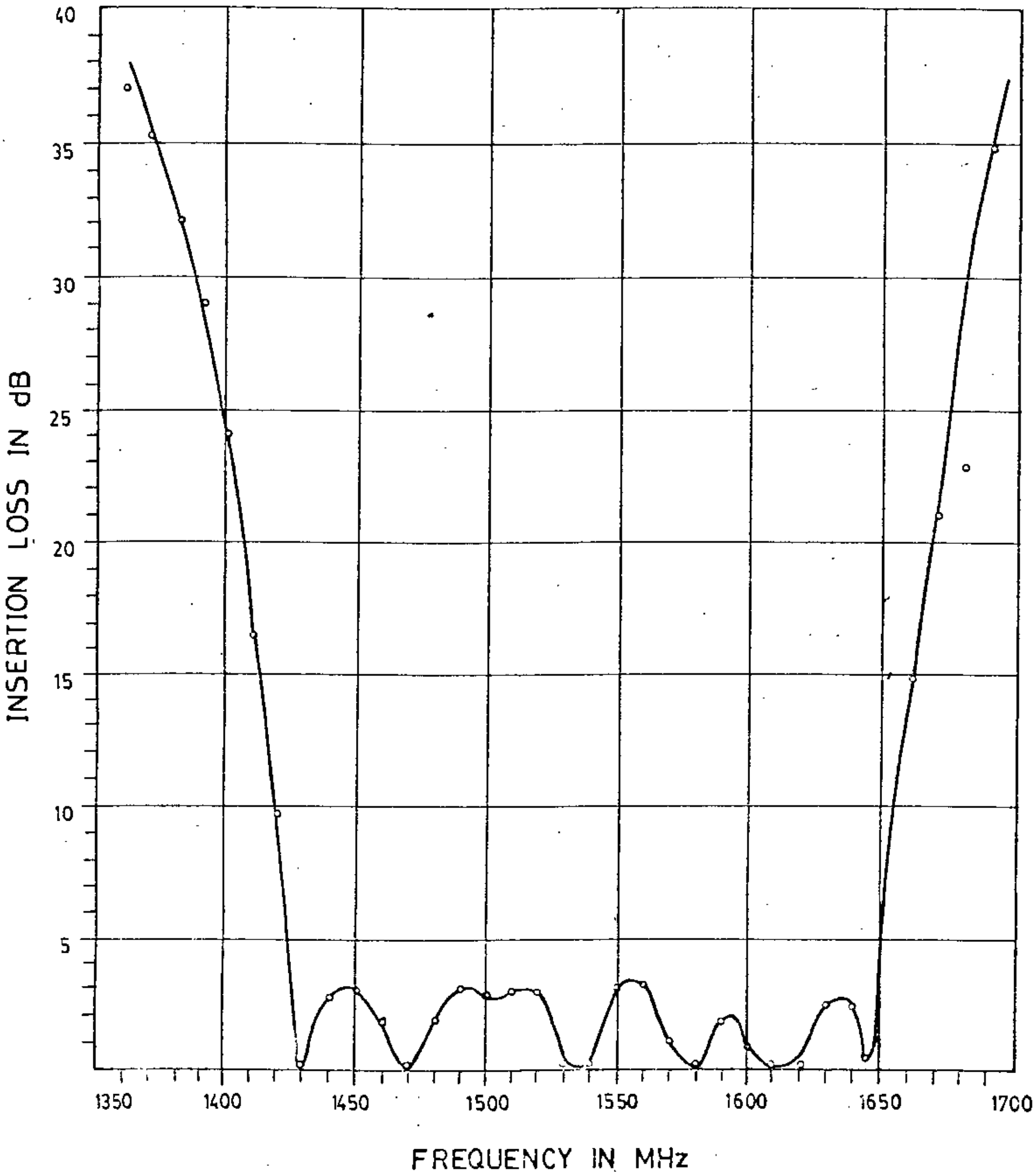

Figure 9.7. Plot of measured insertion loss against frequency of the experimental filter after adding 1.0mm thick brass shim to the coupled sides of input as well as output transformer element. The plot shows that the center frequency is f_o = 1.533 GHz, bandwidth = 225 MHz (14.67%) and A_{max} = 3.1 dB.

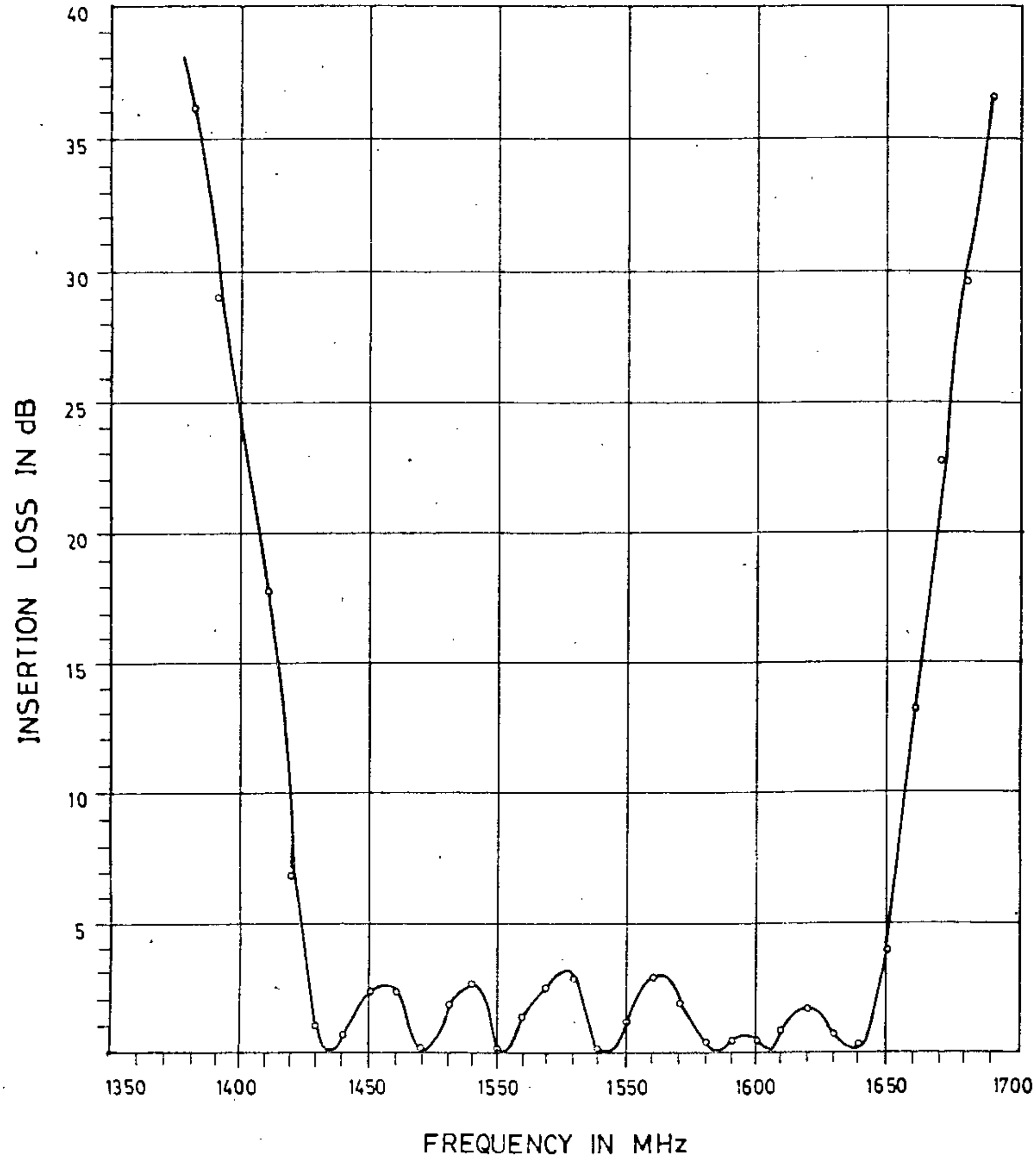

Figure 9.8. Plot of measured insertion loss against frequency of the experimental filter after adding 1.0mm thick brass shim to the coupled sides of input as well as output transformer element. The input and output connections were inter-changed during measurement. The plot shows that the center frequency is f_o = 1.535 GHz, bandwidth = 222.5 MHz (14.5%) and A_{max} = 3.0 dB.

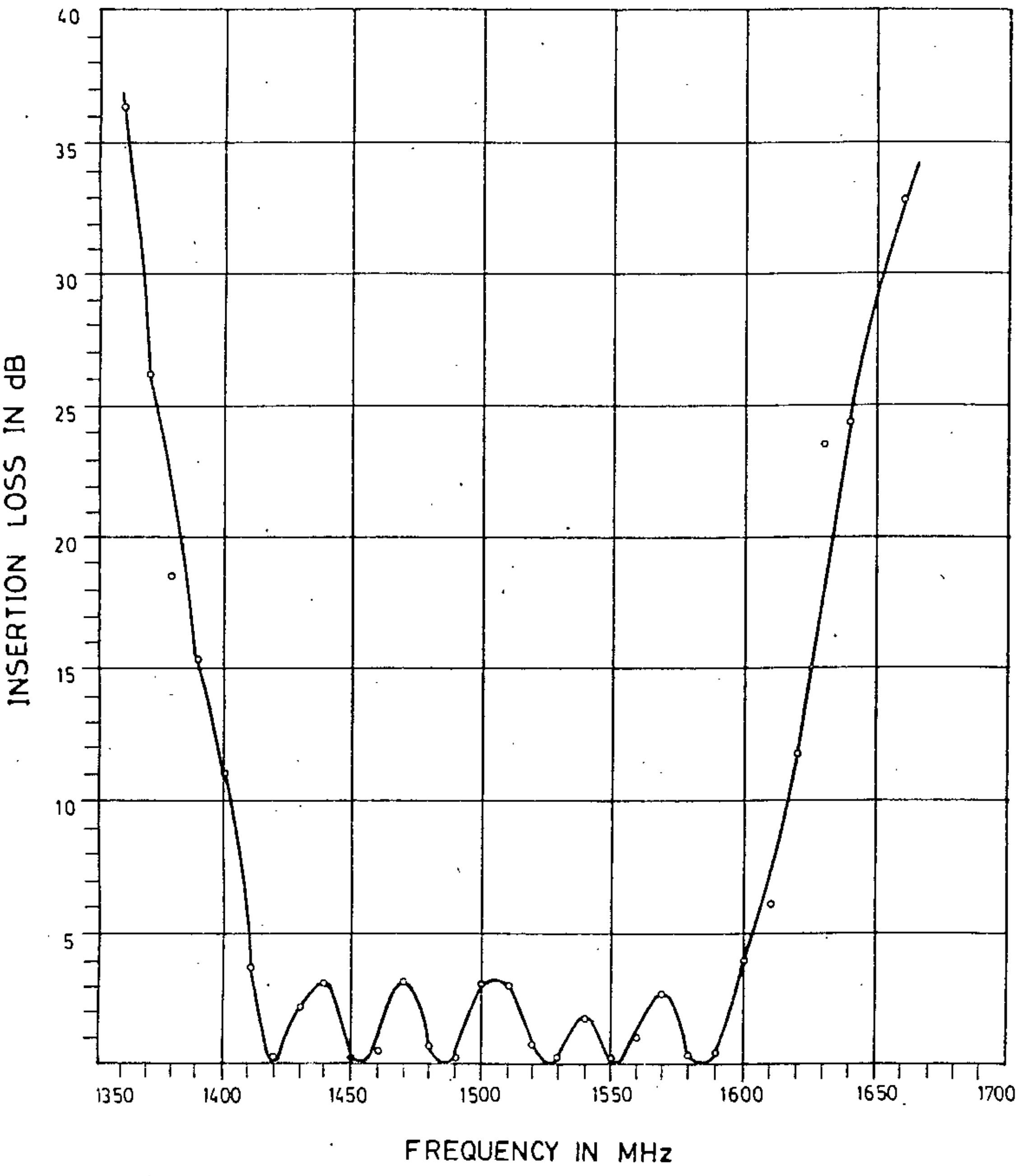

Figure 9.9. Plot of measured insertion loss against frequency of the experimental filter after reducing the shortening length of the resonators to 0.18" from 0.216". The plot shows that the center frequency is f_o = 1.502 GHz, bandwidth = 185 MHz (12.32%) and A_{max} = 3.1 dB.

9.3 Obtaining insertion loss characteristic of a filter

For obtaining the power loss ratio of the experimental filter, the source cable is connected to the input end of the filter and the input side of the bolometer is connected to the output of the filter as shown in figure 9.2. The power meter now gives the output power P_{out} of the filter at the frequency of measurement. Keeping the source frequency and all other adjustments same, another reading is taken after removing the filter from the circuit and connecting the connectors at the end of the source-cable directly to the bolometer. The power reading thus obtained is input power P_{in}. It is important that the connections to the filter is made with minimum number of connectors and adapters and that these are selected in a way so that the number of connectors remain the same during direct connection of the bolometer with the power meter. The reason for this is that the loss of a connector will add to the measurement if an additional connector is used. However, from the two measurements we get P_{out} and P_{in}. Thus we can obtain the power loss ratio by computing P_{out}/P_{in} at the frequency of measurement. In this way, readings of P_{out} and P_{in} are taken at the frequencies within the band of interest at small but equal intervals.

For taking readings at frequencies beyond both the sides of the passband, the power range switch is required to be changed. The reason being that at those frequencies the insertion losses of the filter are high and the output power readings are very small. Thus the power readings at all the frequencies are taken. From these readings we compute the power loss ratio P_{out}/P_{in} at each frequency. The corresponding values of insertion losses in dB are computed by using equation (4.1) and (4.3) of chapter 4. The values of insertion losses in dB are plotted against frequencies of measurement to produce the insertion loss characteristic of the filter under test.
The insertion loss of the experimental filter thus obtained is presented in figure 9.3 and the power measurement data are provided in Appendix C. From the insertion loss characteristic of figure 9.3 it may be observed that the achieved center frequency is 1.532 GHz instead of 1.5 GHz and the bandwidth is 14.22% instead of 12%. The ripple sizes inside the passband are found to be unequal.

The modern method of obtaining insertion loss characteristic of a filter is by using a network analyser. This system was not available in the laboratory at the time of this work. As a result the insertion loss characteristics were obtained using microwave power measurement data as described above.

9.4 Improvement of insertion loss characteristics of the experimental filter

To improve the insertion loss characteristic of the experimental filter one 0.5 mm thick brass shim was added to the coupled side of the input transformer element and another was added to the output transformer element. Power measurements were performed as before. The characteristic thus obtained is presented in figure 9.4. From this characteristic it may be observed that the center frequency and bandwidth of the filter remained more or less unchanged but the value of A_{max} has reduced by 2.15 dB. The input cable is next connected to the output port of the filter and the bolometer is connected to the input port of the filter. The characteristic obtained after power measurement is presented in figure 9.5. This characteristic is almost similar to the characteristic of figure 9.4 except some changes in the shapes of the ripples. This is expected since for this filter the input and output ports is expected to be same. In practice due to constructional defects some dissymetries arise which may cause differences in the behaviours of input and output ports.

In the second attempt of improvement, on the input side a 0.75mm thick shim was added after removing the 0.5mm shim while on the output side the existing 0.5mm brass shim was left unchanged. The power measurement procedure was repeated and the characteristic obtained is presented in figure 9.6. This shows significant improvement in terms of maximum insertion loss in the passband. The value of A_{max} is 3.3 dB in this case. The changes in bandwidth and center frequency are insignificant.

In the third attempt of improvement, the existing shims were replaced by 1mm shims on both input as well as output sides. The power measurement procedure was repeated and the characteristic obtained is presented in figure 9.7. This shows further improvement in terms of maximum insertion loss in the passband. The value of A_{max} this time is 3.1 dB. The changes in bandwidth and center frequency are almost negligible. By changing the input and output connection the value of

A_{max} was found to be 3.0 dB (figure 9.8) which exhibit slight improvement.

Next the length of the resonators were increased to have a length shortening of 0.18" instead of 0.216". The 1mm thick brass shims were present during this measurement. The characteristic obtained during this time is presented in figure 9.9. The value of A_{max} did not improve due to this change. The center frequency has come down to 1.5 GHz from 1.535 GHz and the bandwidth has reduced to 185 MHz (12.32%) from 222.5 MHz (14.5%). This is not unexpected since an increase in length of the resonators should lower down the center frequency and also the percentage bandwidth. After the experimental steps taken to improve the insertion loss characteristic of the experimental filter it is seen that the characteristic of figure 9.8 is the best one.

9.5 Summary

The technique of microwave power measurement used for obtaining the insertion characteristics of the experimental filter has been described. The insertion loss characteristics of the experimental filter obtained from the measurement of power-loss ratios at different frequencies have been presented. Better characteristics are expected if the mesasurements are done using a network analyser.

Chapter 10

Discussions and suggestions for future work

10.1 Discussions

A method for designing Chebyshev bandpass filters using parallel coupled TEM lines in interdigital configuration has been presented. Using this design method design calculations have been performed using a lowpass prototype having n=6 and ρ=15% for achieving a bandpass interdigital filter having center frequency of 1.5 GHz and 12% bandwidth. The design computations were repeated with the same lowpass prototype for 12 more values of bandwidths within the range of 2% to 45%. The purpose of this was to see whether this design method can be used for narrow as well as wide band filters. It has been observed that the dimensions of the filter becomes difficult to realize for 40% bandwidth and wider bandwidth values. At narrow bandwidth values dimensions were found to be good for physical realization. This indicates that the design method is suitable for narrow band filters and not suitable for broadband filters although theoretically there is no such limitation.

The 12% bandwidth design example was accepted for fabrication. The results of the fabricated filter produced close to the expected results except that the maximum attenuation inside the passband was more than expectation. The difficulties in fabrication are non-availability of appropriate machines, skilled technicians and appropriate devices for accurate measurement gaps and spacings. As a result the fabrication work had to be done in a crude manner. This resulted in errors in the resonator widths as well as inter-line spacings. At first a filter was fabricated and the insertion loss of the filter was obtained. The characteristic of the filter exhibited significant loss in the passband. In order to find the reason behind this the line widths and spacings were measured with a slide calliper and a scale. Dimensional errors of the order of 0.01 was observed on certain lines. Moreover it was found that most of the parallel coupled lines were not parallel.

So this filter was discarded and a new one was fabricated. Unfortunately, the desired perfection could not be obtained for the second filter also. However, some improvement of the maximum passband insertion loss was obtained. Later by adding shims on the input and output lines by trial and error method further improvement on maximum passband insertion loss could be achieved. In both the cases it was observed that the percentage bandwidth and center frequency of the experimental filters were close to the design values. It is thought that with appropriate machines such errors in the line widths and spacing should not arise.

There is a possibility that errors in the theoretical inter-line spacing had been introduced while obtaining these values from the graphs of Getsinger for a particular value of $\Delta C/\epsilon$. For reading the inter-line spacings interpolation of the plots had to be done. It would have been better if an enlarged photocopy of the graphs was used intead of using 1:1 copies.

At this stage it was thought worth while making little investigation by theoretical simulation. A computer program in BASIC was prepared for PCs to obtain the insertion loss characteristic of the two wire equivalent circuit of the interdigital filter. The characteristic admittance values were put from the design calculation. It was found that by increasing the amount r by which the resonator lengths are foreshortened the passband (hence the center frequency) of the filter moves towards right. This result fully coincides with the theoretical expectation. So it was obvious that the amount of foreshortening of length was not responsible for increased amount of passband loss.

Correction for the improvement of the experimental filter could have been done if TDR (time domain reflectometer) technique could be applied to see the locations and amount of impedance mismatch of the filter. It is suspected a good deal of reflections occurring at the input and output connections of the connectors is responsible for this increase in the maximum passband insertion loss. RS 239 connectors have been used for the filter which are not truely microwave connectors. So, it is thought that by using low VSWR microwave connectors and by eliminating the mismatches in the input and output it will be possible to achieve the desired results.

If this design method is used for narrowband filters then, in principle, the resulting filter should exhibit the following attractive features over other parallel coupled TEM line filters.

i) The filters are compact.

ii) The filters should have relatively relaxed manufacturing tolerences because of relatively large spacings between the resonator elements.

iii) The second pass-band is centered at three times the centre frequency of the first-pass band, and there is no possibility of spurious responses in between. (It is known that for filters with half-wave length parallel coupled resonators even slightest mistuning results in narrow spurious passbands at twice the frequency of first passband centere.)

iv) These filters can be fabricated in structural forms which are self-supporting so that dielectric material need not be used. Thus dielectric loss can be eliminated.

10.2 Suggestions for future work

It has been observed that for broad band interdigital filter the design method presented in this work produces dimension which are difficult to fabricate. This difficulty limits the application of this design method to narrow to moderate bandwidth filters only. Theoretically no such limitation have so far been found. This indicates that further work needs to be done to modify the design method so that this may become equally useful for wide band filter design without facing any practical difficulty.

Secondly, it is hoped that by following this work a design method may be developed by using alternative equivalent circuits or some other arrangements of the interdigital structure for broad band filter design.

It is well known that microstriplines are very popular now-a-days because of their light weight, compactness, low cost, easy of fast fabrication with very good accuracy in dimension, and suitability for MMIC application. Considering these it is worthwhile trying for modification of the design method for fabrication of interdigital filters using microstriplines.

References

[1] G. L. Matthaei, "Design of Wide-Band (and Narrow-Band) Band-Pass Microwave Filters on the Insertion Loss Basis," IRE Transactions on Microwave Theory and Techniques, vol. MTT-8, November 1960, pp.580-593.

[2] J. T. Bolljahn and G. L. Matthaei, "A Study of Phase and Filter Properties of Arrays of Parallel Conductors Between Ground Planes," Proceeding of the IRE, vol.50, March 1962, pp.299-311.

[3] G. L. Matthaei, "Interdigital Band-Pass Filters," IRE Transactions on Microwave Theory and Techniques, PGMTT-10, November 1962, pp.479-491.

[4] G. L. Matthaei, P. S. Carter Jr., and W. J. Getsinger, "Design Criteria for Microwave Filters and Coupling Structures," Stanford Research Institute, Menlo Park, California, Final Reptort, SRI Project 2326, Contract DA 36-039, Sc-74862, January 1961.

[5] S. B. Cohn, "Direct Coupled Resonator Filters," Proceedings of the IRE, vol.45, February 1957, pp.187-196.

[6] S. B. Cohn et. al., "Research on design criteria for microwave filters," Stanford Res. Inst., Menlo Park, Calif., Final Rept. SRI project 1331, Contract DA 36-039. Sc-64625. Ch. 4, June 1957.

[7] S. B. Cohn, "Parallel-Coupled Transmission Line Resonator Filters, " IRE Transactions on Microwave Theory and Techniques, vol. MTT-6, April 1958, pp.223-231.

[8] E. M. T. Jones, "Synthesis of Wide-Band Microwave Filters to Have Prescribed Insertion Loss", IRE Convention Record, pt.5, pp.119-128.

[9] W. J. Getsinger, "Coupled Rectangular Bars Between Paralell Plates," IRE Transactions on Microwave Theory and Techniques, vol. MTT-10, January 1962, pp.65-72.

[10] S. B. Cohn, "Shielded Coupled Strip-Transmission Line," IRE Transactions on Microwave Theory and Techniques, vol. MTT-3, October 1955, pp.29-38.

[11] E. M. T. Jones and J. T. Bolljahn, "Coupled Strip-Transmission Line Filters and Directional Couplers," IRE Transactions on Microwave Theory and Techniques, vol. MTT-4, April 1956, pp.75-81.

[12] S. B. Cohn, "Problems In Strip-Transmission Line," IRE Transactions on Microwave Theory and Techniques, vol. MTT-3, March 1955, pp.119-126.

[13] S. B. Cohn, "Characteristic Impedence of the Shielded Strip-Transmission Line," IRE Transactions on Microwave Theory and Techniques, vol. MTT-2, No. 2, July 1954, pp.52-57.

[14] P. N. Butcher,"The Coupling Imepdance of Tape Structures," Proceedings of the IEE (London), Pt. B, vol. 104, March 1957, pp.177-187.

[15] R. C. Fletcher,"A Broad-Band Interdigital Circuit for Use in Travelling-Wave Type Amplifiers," Proceedings of the IRE, vol.40, August 1952, pp.951-958.

[16] L. Weinberg, "Network Design by Use of Modern Synthesis Techniques and Tables," Research Labs. Hughes Aircraft Co. Culver City, California, Tech. Memo. 427, April 1956.

[17] Paul I. Richards, "Application of Matrix Algebra to Filter Theory," Proceedings of the IRE and Waves and Electrons, vol. 34, March 1946, pp. 145-150.

[18] G. L. Matthaei, L. Young, E. M. T. Jones, "Microwave Filters, Impedance Matching Networks and Coupling Structures," McGraw-Hill Book Company, Inc., New York, 1966, pp.144-161, 175-176, 187-188, 190-192 and 217-228.

[19] H. Ozaki and J. Ishii, "Synthesis of transmission line networks and the design of UHF filters," IRE Transactions on Circuit Theory, vol. PGCT-2, December 1955, pp.325-336.

[20] R. J. Wenzel, "Exact Theory of Interdigital Band-Pass Filters and Related Coupled Structures," IEEE Tranctions on Microwave Theory and Techniques, vol. MTT-13, No.-5, September 1965, pp.559-575.

[21] R. J. Wenzel, "Exact Design of TEM Microwave Networks Using Quarter-Wave Lines," IEEE Transactions on Microwave Theory and Techniques, vol. MTT-12, January 1964, pp.94-111.

[22] S. Gupta, D. Arora, S. B. Sarna and P. Lonkar, "Microwave Fundamentals", Khanna Publishers, Delhi, 1984, pp.154-169.

[23] S. F. Adam, "Microwave Theory and Applications", Hewlett Packard, Prentice Hall Ins., New Jersey, U.S.A., 1969.

[24] M. L. Sisodia, G. S. Raghuvashi, "Microwave Circuits and Passive Devices", Wiley Eastern Ltd., New Delhi, 1987, pp.127-227, 231-228 and 448-516.

[25] L. Weinberg, "Additional Tables for Design of Optimum Ladder Networks," J. Franklin Inst., vol.246, July and August 1957, pp.7-23 and 127-138.

[26] H. Ozaki and J. Ishii, "Synthesis of a class of stip line filters," IRE Trans. on Circuit Theory, vol. PGCT-5, June 1958, pp.104-109.

[27] G. L. Matthaei, "Comb-line band-pass filters of narrow or moderate bandwidth," Microwave Journal (USA), August 1963, pp.82-91.

[28] J. D. Rhodes, "The Stepped Digital Elliptic Filter," IEEE Transactions on Microwave Theory and Techniques, vol. MTT-17, No. 4, April 1969, pp.178-184.

[29] J. D. Rhodes, "The Half-Wave Stepped Digital Elliptic Filter," IEEE Transactions on Microwave Theory and Techniques, vol. MTT-17, No.-12, December 1969, pp.1102-1107.

[30] R. E. Collin, "Foundations for Microwave Engineering," McGraw-Hill International Book Company, pp.398-404 and 410-415.

[31] R. Saal, "Der Entwurf von Fitern mit helfe des Katalogues Normierter Tiefpasse." Telefunken Gmbh, Backnay Wurtemberg, W. Germany, 1964.

[32] A.I. Zverev, "Handbook of Filter Synthesis", John Wiley & Sons., New York, 1967.

[33] The Microwave Engineers' Handbook and Buyers' Guide, Brooklyn, Mass. Horizon House Microwave, Inc., 1963.

[34] E. G. Fubini, W. E. Fromm and H. S. Keen, "Microwave applications of high - Q strip components," IRE Convention Record pt. 8, March 1954, pp.98-103.

[35] E. H. Bradley, "Design and development of strip line filters," IRE Transactions, vol. MTT-4, April 1956, pp.86-93.

Appendix A

Computer programs

A.1 [i] Program for obtaining computed characteristic of a Chebyshev lowpass prototype filter

```
      DIMENSION A(800), W(800)
      OPEN (UNIT=5, FILE='OUT', STATUS='NEW')
      N=6
      AM=0.1
      EP=10.0**(AM/10.0)-1.0
      DO 11 I=1,700
      X=I/500. - 0.002
      IF(X.LE.1.0)GO TO 13
      X1=X+SQRT(X*X - 1.0)
      X4=LOG(X1)*N
      X2=COSH(X4)
      X3=1.0 + EP*X2*X2
      A(I)=10.0*LOG10(X3)
      GO TO 11
13    Y1=ACOS(X)
      Y2=COS(N*Y1)
      Y3=EP*Y2*Y2 + 1.0
      Y4=10.0*LOG10(Y3)
      A(I)=Y4
11    CONTINUE
      DO 15 I=1,700
      F=I/500.0 - 0.002
15    WRITE(5,55)F,A(I)
55    FORMAT(5X,'FREQ.=',F6.4,5X,'ATTEN.=',F7.4)
      STOP
      END
```

A.1 [ii] Program for obtaining computed characteristic of a bandpass filter for Chebyshev response

```
      OPEN(UNIT=5,FILE='OUT', STATUS='NEW')
      F0=1.50
      PIE=3.143
      W0=2.*PIE*F0
      BW=0.12
      AMAX=0.1
      RN=6.00
      W2=W0*(1.0 - BW/2.0)
      RK=W2/W0 - 1.00
      EP=10.0**(AMAX/10.0) -1.0
      WRITE(5,22)
22    FORMAT(4X,'FREQ',5X,'ATTEN.(dB)')
      DO 10 I=445,562
      XW=I/500.0 - 0.002
      F=XW*1500
      YW=-(XW-1.0)/RK
      Z=ABS(YW)
      IF(Z.LE.1.0) GO TO 12
      X1=LOG(Z+SQRT(Z*Z - 1.0))
      X2=COSH(RN*X1)
      X3=X2*X2
      A=10.0*LOG10(1.0 + EP*X3)
      GO TO 14
12    A=10.0*LOG10(1.0 + EP*COS(RN*ACOS(Z))**2)
14    WRITE(5,77)F,A
77    FORMAT(3X,F6.1,5X,F10.6)
10    CONTINUE
      STOP
      END
```

A.2 Program for obtaining static capacitance values of an interdigital narrow-band bandpass filter

```
      DIMENSION G(8),RJ(9,9),RN(8,8),RM(8),CS(8),CM(9,9)
      OPEN(UNIT=5,FILE='OUT',STATUS='NEW')
      F0=1.50
      YA=0.02
      WLP1=1.00
      PI=3.14159
      BW=0.12
      THET1=PI/2.0*(1.0 - BW/2.0)
      WRITE(5,5)F0,YA,BW,THET1
    5 FORMAT(3X,'F0='F4.2, 'GC',3X, 'YA=',F4.2,'MHO',3X,'
     +BW=',F4.2,3X,'THET1=',F7.5)
C     PROTOTYPE ELEMENT VALUES FOR 0.1 dB INSERTION-LOSS
C    +AND SIX REACTIVE ELEMENTS.
      G(1)=1.0
      G(2)=1.1650
      G(3)=1.4040
      G(4)=2.0540
      G(5)=1.5180
      G(6)=1.9000
      G(7)=0.8613
      G(8)=1.0/0.7391
C     CALCULATION OF J-PARAMETERS
      RJ(1,2)=1.0/SQRT(G(1)*G(2)*WLP1)
      RJ(7,8)=1.0/SQRT(G(7)*G(8)*WLP1)
      DO 10 K=2,6
   10 RJ(K,K+1)=1.0/(WLP1*SQRT(G(K)*G(K+1)))
      DO 20 K=2,6
   20 RN(K,K+1)=SQRT(RJ(K,K+1)**2+(TAN(THET1)/2.0)**2)
C     FINDOUT THE ADMITTANCE SCALING FACTOR h
C    +FOR EVEN NUMBER OF RESONATORS(N = 6)
      N=6
      K=(N+2)/2
      C4= 376.7*YA*(RN(K-1,K)+RN(K,K+1)-RJ(K,K+1))- RJ(K-1,K))
```

```
      C34=376.7*YA*RJ(K-1,K)
      C45=376.7*YA*RJ(K,K+1)
      H=5.4/HP
      WRITE(5,15)H
   15 FORMAT(3X,'H=',F8.6)
      RM(1)=YA*(RJ(1,2)*SQRT(H)+1.0)
      RM(6)=YA*(RJ(7,8)*SQRT(H)+1.0)
      WRITE(5,25)RM(1),RM(6)
   25 FOMAT(3X,'M1='F5.4,3X,'M6=',F5.4)
C     CALCULATION OF SELF AND MUTUAL CAPACITANCES
      CS(1)=376.7*(2.0*YA - RM(1))
      CS(8)=376.7*(2.0*YA - RM(6))
      CS(2)=376.7*(YA-RM(1)+H*YA*(TAN(THET1)*0.5+RJ(1,2)**2+RN(2,3)-
     +RJ(2,3)))
      CS(7)=376.7*(YA-RM(6)+H*YA*(TAN(THET1)*0.5+RJ(7,8)**2+RN(6,7)-
     +RJ(6,7)))
      CM(1,2)=376.7*(RM(1) - YA)
      CM(7,8)=376.7*(RM(6) - YA)
      DO 30 K=3,6
   30 CS(K)=376.7*H*YA*(RN(K-1,K)+RN(K,K+1)-RJ(K-1,K)-RJ(K,K+1))
      DO 40 J=2,6
   40 CM(J,J+1)=376.7*H*YA*(RJ(J,J+1))
      WRITE(5,35)
   35 FOMAT(5X,'CN(I)',5X,'CN(I,I+1)',4X,'J(I,I+1)/YA',3X,'N(I,I+1)')
      DO 50 I=1,8
   50 WRITE(5,45)CS(I),CM(I,I+1),RJ(I,I+1),RN(I,I+1)
   45 FORMAT(3X,F7.4,5X,F7.4,8X,F7.4,5X,F8.5,5X,F8.5)
      STOP
      END
```

A.3 Program for computing the line width of interdigital filter using static capacitance values

```
      OPEN(UNIT=3,FILE='INPUT',STATUS='OLD')
      OPEN(UNIT=5,FILE='OUT',STATUS='NEW')
C     READ SELF CAPACITANCES FROM PREVIOUS PROGRAM
      READ(3,5)(C(I),I=1,8)
    5 FORMAT(6.4)
C     THICKNESS=T, GROUND PLATES' SPACING=B, R=T/B
      T=0.187
      B=0.625
      R=0.3
      X=0.35*(1.0 - R)
C     SEPARATION BETWEEN RESONATORS NORMALISED WITH B
     +WHICH ARE OBTAINED FROM GETSINGER'S GRAPH
      SB(1,2)=0.231
      SB(2,3)=0.658
      SB(3,4)=0.755
      SB(4,5)=0.769
      SB(5,6)=0.755
      SB(6,7)=0.658
      SB(7,8)=0.231
C     FRINGING CAPACITANCES FROM GETSINGER'S GRAPHS
      CFE(1,2)=0.320
      CFE(2,3)=0.640
      CFE(3,4)=0.680
      CFE(4,5)=0.699
      CFE(5,6)=0.680
      CFE(6,7)=0.640
      CFE(7,8)=0.320
      CFD=0.80
C     CALCULATION OF WIDTHS OF RECTANGULAR BAR
      DO 10 K=2,7
   10 WB(K)=0.5*(1.0 - R)*(0.5*C(K) - CFE(K-1,K) - CFE(K,K+1))
      WB(1)=0.5*(1.0 - R)*(0.5*C(1) - CFD - CFE(1,2))
      WB(8)=0.5*(1.0 - R)*(0.5*C(8) - CFD - CFE(7,8))
```

```
      WRITE(5,15)
15    FORMAT(5X,'W/B RATIOS', 5X,' W(K)   ',5X,' S(K,K+1) ')
C     WIDTH CORRECTION
      DO 20 I=1,8
      IF(WB(I) - X)11,11,12
11    WBC(I)=(WB(I) + 0.07*(1.0 - R))/1.20
      GO TO 20
12    WBC(I)=WB(I)
20    CONTINUE
      DO 30 J=1,8
30    W(J)=WBC(J)*B
C     CALCULATION OF SEPARATION BETWEEN RECTANGULAR BARS
      DO 40 M=1,7
40    S(M,M+1)=SB(M,M+1)*B
      DO 50 K=1,8
50    WRITE(5,35)WB(K),W(K),S(K,K+1)
35    FORMAT(6X,F7.5,6X,F7.5,7X,F5.3)
      STOP
      END
```

Appendix B

Derivation of image admittances and image phase constants of a single section of the two wire equivalent circuit of an interdigital bandpass filter and a single section of a modified lowpass prototype

B.1 Derivation of the image admittance of a single section of the two wire equivalent circuit of the interdigital bandpass filter of figure 5.2(b)

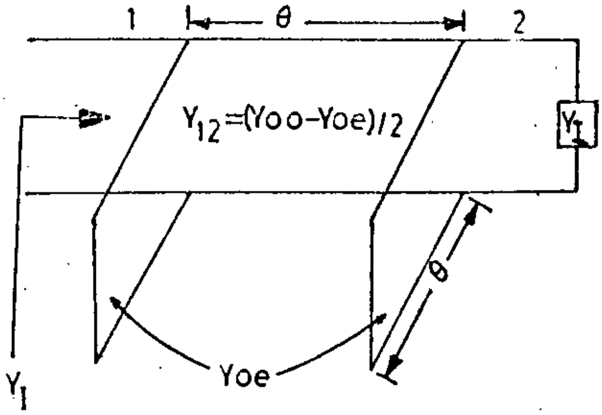

From the above circuit image admittance Y_I is,

$$Y_I = Y_{12}\,\frac{(Y_I - jY_{oe}\cot\theta)\cos\theta + jY_{12}\sin\theta)}{Y_{12}\cos\theta + j(Y_I - jY_{oe}\cot\theta)\sin\theta} - jY_{oe}\cot\theta$$

$$Y_I(Y_{12}\cos\theta + jY_I\sin\theta + Y_{oe}\cos\theta - Y_{12}\cos\theta - Y_{oe}\cos\theta) = -jY_{12}Y_{oe}\cot\theta\cos\theta + jY_{12}^2\sin\theta - jY_{12}Y_{oe}\cot\theta\cos\theta - jY_{oe}^2\cot\theta\cos\theta$$

$$jY_I^2\sin\theta = j(Y_{12}^2\sin\theta - Y_{12}Y_{oe}\cot\theta\cos\theta - Y_{oe}^2\cot\theta\cos\theta - Y_{12}Y_{oe}\cot\theta\cos\theta)$$

$$Y_I^2\sin\theta = Y_{12}^2\sin\theta - 2Y_{12}Y_{oe}\cot\theta\cos\theta - Y_{oe}^2\cot\theta\cos\theta$$

$$Y_I^2\sin\theta = (Y_{oo}-Y_{oe})^2\sin\theta/4 - 2(Y_{oo}-Y_{oe})Y_{oe}\cot\theta\cos\theta/2 - Y_{oe}^2\cot\theta\cos\theta$$

$$Y_I^2\sin\theta = (Y_{oo}-Y_{oe})^2\sin\theta/4 - Y_{oe}Y_{oo}\cos^2\theta/\sin\theta + Y_{oe}^2\cot\theta\cos\theta - Y_{oe}^2\cot\theta\cos\theta$$

$$Y_I^2 = (Y_{oo}-Y_{oe})^2/4 - Y_{oe}Y_{oo}\cos^2\theta/\sin^2\theta$$

$$= [(Y_{oo}-Y_{oe})^2\sin^2\theta - 4Y_{oe}Y_{oo}\cos^2\theta]/(4\sin^2\theta)$$

$$= [(Y_{oo}-Y_{oe})^2 - \{(Y_{oo}-Y_{oe})^2 + 4Y_{oe}Y_{oo}\}\cos^2\theta]/(4\sin^2\theta)$$

Finally,

$$Y_I = [(Y_{oo}-Y_{oe})^2 - (Y_{oo}+Y_{oe})^2\cos^2\theta]^{1/2}/(2\sin\theta)$$

B.2 Derivation of the image phase constant of a section of the two wire equivalent circuit of the interdigital bandpass filter of figure 5.2(b)

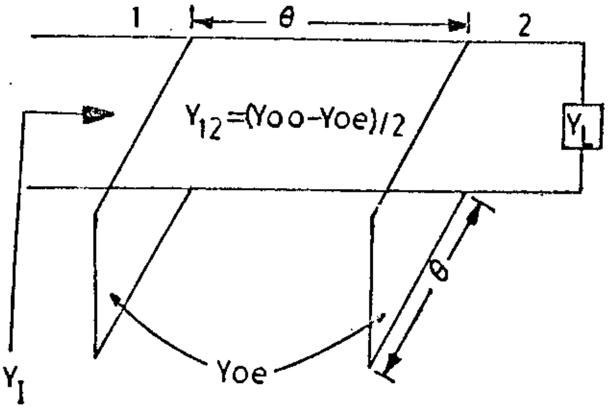

The short circuited admittance Y_{sc} of the above circuit is,

$$Y_{sc} = Y_{12}\,\frac{\{Y_L(\infty) - jY_{oe}\cot\theta\}\cos\theta + jY_{12}\sin\theta}{Y_{12}\cos\theta + j\{Y_L(\infty) - jY_{oe}\cot\theta\}\sin\theta} - jY_{oe}\cot\theta$$

$$= Y_{12}\,\cos\theta/(j\sin\theta) - jY_{oe}\cot\theta$$

$$= -jY_{12}\cot\theta - jY_{oe}\cot\theta$$

$$= -j\,[(Y_{oo} - Y_{oe})/2 + Y_{oe}]\,\cot\theta$$

or, $$Y_{sc} = -j\,(Y_{oo} + Y_{oe})\cot\theta/2 \qquad (1)$$

The open circuited admittance of the abovecircuit

$$Y_{oc} = Y_{12}\,\frac{(-jY_{oe}\cot\theta)\cos\theta + jY_{12}\sin\theta}{Y_{12}\cos\theta + j(-jY_{oe}\cot\theta)\sin\theta} - jY_{oe}\cot\theta$$

$$= -jY_{12}\,\frac{Y_{oe}\cos^2\theta - Y_{12}\sin^2\theta}{\sin\theta\cos\theta(Y_{12} + Y_{oe})} - jY_{oe}\cot\theta$$

$$= -j\,\frac{Y_{12}\{Y_{oe}\cos^2\theta - (Y_{oo} - Y_{oe})\sin^2\theta/2\}}{\sin\theta\cos\theta[(Y_{oo} - Y_{oe})/2 + Y_{oe}\ ]} - jY_{oe}\cot\theta$$

$$= -j\ \left[\frac{(Y_{oo} - Y_{oe})/2\ \{2Y_{oe}\cos^2\theta - (Y_{oo} - Y_{oe}) + (Y_{oo} - Y_{oe})\cos^2\theta}{\sin\theta\cos\theta[(Y_{oo} + Y_{oe})]} + Y_{oe}\cot\theta\right]$$

$$= -j/2\ \frac{(Y_{oo} + Y_{oe})\cos^2\theta\{2Y_{oe} + (Y_{oo} - Y_{oe})\} - (Y_{oe} - Y_{oo})^2\}}{\sin\theta\cos\theta[Y_{oo} + Y_{oe}]}$$

$$\text{or,} \quad Y_{oc} = -j/2 \; \frac{(Y_{oo} + Y_{oe})^2 \cos^2\theta - (Y_{oo} - Y_{oe})^2}{\sin\theta\cos\theta[Y_{oo} + Y_{oe}]} \qquad (2)$$

Now, $\coth\tau = \sqrt{(Y_{sc}/Y_{oc})}$,

where γ = propagation constant

$= \alpha + j\beta$

Therefore,

$$\coth(\alpha + j\beta) = \sqrt{\frac{-j[(Y_{oo}+Y_{oe})\cot\theta/2]x[\sin\theta\cos\theta(Y_{oo} + Y_{oe})]}{(-j/2)[(Y_{oo} + Y_{oe})^2\cos^2\theta - (Y_{oo}-Y_{oe})^2]}}$$

$$= \sqrt{\frac{(Y_{oo} + Y_{oe})^2\cos^2\theta}{(Y_{oo} + Y_{oe})^2\cos^2\theta - (Y_{oo}-Y_{oe})^2}}$$

For lossless line $\alpha=0$

Therefore,

$$\coth(j\beta) = \sqrt{\frac{(Y_{oo} + Y_{oe})^2\cos^2\theta}{(Y_{oo} + Y_{oe})^2\cos^2\theta - (Y_{oo}-Y_{oe})^2}}$$

$$\text{or,} \quad -j\cot\beta = -j\sqrt{\frac{(Y_{oo} + Y_{oe})^2\cos^2\theta}{(Y_{oo}-Y_{oe})^2 - (Y_{oo} + Y_{oe})^2\cos^2\theta}}$$

$$\text{or,} \quad \cos\beta = (Y_{oo} + Y_{oe})\cos\theta/(Y_{oo} - Y_{oe})$$

Therefore,

$$\beta = \cos^{-1}\frac{(Y_{oo} + Y_{oe})\cos\theta}{(Y_{oo} - Y_{oe})}$$

B.3 Derivation of the image admittance of a single section of the modified lowpass prototype of figure 5.3

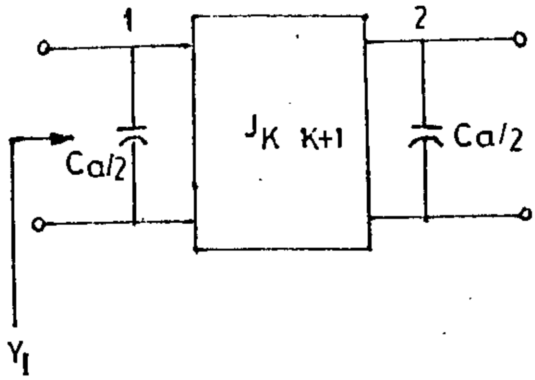

From the above modified prototype section open-circuited admittance Y_{oc} is,

$$Y_{oc} = j\omega C_a/2 + J^2_{k,k+1}/(j\omega C_a/2)$$
$$= [J^2_{k,k+1} - (\omega C_a/2)^2]/(j\omega C_a/2)$$

And, short circuited admittance Y_{sc} is,

$$Y_{sc} = j\omega C_a/2$$

Now, the image admittance Y_I is given by,

$$Y_I = \sqrt{(Y_{sc} x Y_{oc})}$$
$$= \sqrt{\{[\{J^2_{k,k+1} - (\omega C_a/2)^2\}/(j\omega C_a/2)]x(j\omega C_a/2)\}}$$

Therefore,

$$Y_I = J_{k,k+1}\sqrt{\ [1 - \{\omega(C_a/2)/J_{k,k+1}\}^2]}$$

B.4 Derivation of the image phase constant of a single section of the modified lowpass prototype of figure 5.3

When terminal 2 is shorted, short circuited admittance Y_{sc} looking at terminal 1 is,

$$Y_{sc} = j\omega C_a/2$$

And open circuited admittance Y_{oc} when terminal 2 is open circuited can written as,

$$Y_{oc} = j\omega C_a/2 + J^2_{k,k+1}/(j\omega C_a/2)$$

Now, the phase constant γ is,

$$\gamma = \alpha + j\beta = \coth^{-1}\surd(Y_{sc}/Y_{oc})$$

For lossless line $\alpha=0$

Therefore,

$$\coth(j\beta) = \surd[j\omega C_a/2 \times (j\omega C_a/2)/\{J^2_{k,k+1} - (\omega C_a/2)^2\}]$$

or, $$\coth(j\beta) = (j\omega C_a/2)/\surd\{J^2_{k,k+1} - (\omega C_a/2)^2\}$$

or, $$-j\cot\beta = (j\omega C_a/2)/\surd\{J^2_{k,k+1} - (\omega C_a/2)^2\}$$

or, $$\tan(\beta\pm\pi/2) = (\omega C_a/2)/\surd\{J^2_{k,k+1} - (\omega C_a/2)^2\}$$

or, $$\sin(\beta\pm\pi/2) = (\omega C_a/2)/J_{k,k+1}$$

Finally,

$$\beta = \sin^{-1}[(\omega C_a/2)/J_{k,k+1}] \pm \pi/2$$

Appendix C

Designed line parameter values of 13 number of interdigital bandpass filters having same n and ρ but bandwidth ranging from 2% to 45%

Example 1

Design parameters of interdigital bandpass filter having n=6, ρ=0.15, f_0=1.5 GHz, BW=2%

k	C_k/ϵ	$C_{k,k+1}/\epsilon$	$J_{k,k+1}/Y_A$	$N_{k,k+1}$	w_k	$s_{k,k+1}$
0	6.8000	0.7340	0.9265	--------	0.4572	0.2781
1	4.5761	0.0651	0.7819	31.83539	0.2205	0.7219
2	5.1899	0.0491	0.5889	31.83124	0.2308	0.8188
3	5.2075	0.0472	0.5663	31.83083	0.2327	0.8281
4	5.2075	0.0491	0.5888	31.83124	0.2327	0.8188
5	5.1900	0.0651	0.7817	31.83539	0.2308	0.9719
6	4.5762	0.7339	0.9263	---------	0.2380	0.2781
7	6.8001	------	------	---------	0.4747	------

h = 0.011058 M_1 = 0.0219 M_6 = 0.0219 Y_A = 0.02 mho.

Example 2

Design parameters of interdigital bandpass filter having n=6, ρ=0.15, f_0=1.5 GHz, BW=5%

k	C_k/ϵ	$C_{k,k+1}/\epsilon$	$J_{k,k+1}/Y_A$	$N_{k,k+1}$	w_k	$s_{k,k+1}$
0	6.3889	1.1451	0.9265	--------	0.4363	0.2050
1	4.0357	0.1585	0.7819	12.74927	0.1916	0.5812
2	4.8901	0.1194	0.5889	12.73889	0.2063	0.6406
3	4.9315	0.1148	0.5663	12.73787	0.2067	0.6469
4	4.9315	0.1194	0.5888	12.73889	0.2067	0.6406
5	4.8902	0.1585	0.7817	12.74926	0.2063	0.5812
6	4.0359	1.1449	0.9263	---------	0.1916	0.2050
7	6.3891	-------	-------	--------	0.4363	-------

h = 0.026913 M_1 = 0.0230 M_6 = 0.0230 Y_A = 0.02 mho.

Example 3

Design parameters of interdigital bandpass filter having n=6, ρ=0.15, f_0=1.5 GHz, BW=7%

k	C_k/ϵ	$C_{k,k+1}/\epsilon$	$J_{k,k+1}/Y_A$	$N_{k,k+1}$	w_k	$s_{k,k+1}$
0	6.1910	1.3430	0.9265	-------	0.4223	0.1812
1	3.7553	0.2181	0.7819	9.11870	0.1756	0.5156
2	4.7000	0.1642	0.5889	9.10418	0.1969	0.5731
3	4.7556	0.1579	0.5663	9.10275	0.1960	0.5812
4	4.7557	0.1642	0.5888	9.10417	0.1960	0.5731
5	4.7000	0.2180	0.7817	9.11868	0.1969	0.5156
6	3.7555	1.3428	0.9263	-------	0.1756	0.1812
7	6.1912	------	--------	-------	0.4223	------

h = 0.037018 M_1 = 0.0236 M_6 = 0.0236 Y_A = 0.02 mho.

Example 4

Design parameters of interdigital bandpass filter having n=6, ρ=0.15, f_0=1.5 GHz, BW=10%

k	C_k/ϵ	$C_{k,k+1}/\epsilon$	$J_{k,k+1}/Y_A$	$N_{k,k+1}$	w_k	$s_{k,k+1}$
0	5.9497	1.5843	0.9265	-------	0.3988	0.1575
1	3.3953	0.3035	0.7819	6.40093	0.1490	0.4487
2	4.4285	0.2285	0.5889	6.38023	0.1825	0.5089
3	4.5033	0.2198	0.5663	6.37189	0.1841	0.5112
4	4.5033	0.2285	0.5888	6.38022	0.1841	0.5089
5	4.4286	0.3034	0.7817	6.40091	0.1825	0.4487
6	3.3955	1.5840	0.9263	-------	0.1550	0.1575
7	5.9500	------	------	--------	0.4047	------

h = 0.051514 M_1 = 0.02420 M_6 = 0.0242 Y_A = 0.02 mho.

Example 5

Design parameters of interdigital bandpass filter having n=6, β=0.15, f_0=1.5 GHz, BW=12%

k	C_k/ϵ	$C_{k,k+1}/\epsilon$	$J_{k,k+1}/Y_A$	$N_{k,k+1}$	W_k	$S_{k,k+1}$
0	5.8135	1.7205	0.9265	------	0.3908	0.1445
1	3.1832	0.3579	0.7819	5.34685	0.1430	0.4114
2	4.2562	0.2696	0.5889	5.32205	0.1768	0.4719
3	4.3424	0.2592	0.5663	5.31960	0.1733	0.4805
4	4.3424	0.2695	0.5888	5.32205	0.1733	0.4719
5	4.2563	0.3578	0.7817	5.34683	0.1768	0.4114
6	3.1834	1.7203	0.9263	-------	0.1460	0.1438
7	5.8137	------	------	-------	0.3952	-------

h = 0.060758 M_1 = 0.02460 M_6 = 0.0246 Y_A = 0.02 mho.

Example 6

Design parameters of interdigital bandpass filter having n=6, β=0.15, f_0=1.5 GHz, BW=15%

k	C_k/ϵ	$C_{k,k+1}/\epsilon$	$J_{k,k+1}/Y_A$	$N_{k,k+1}$	W_k	$S_{k,k+1}$
0	5.6349	1.8991	0.9265	-------	0.3823	0.1312
1	2.8955	0.4361	0.7819	4.29616	0.1350	0.3719
2	4.0102	0.3284	0.5889	4.26526	0.1630	0.4312
3	4.1115	0.3158	0.5663	4.26220	0.1609	0.4344
4	4.1115	0.3284	0.5888	4.26525	0.1609	0.4312
5	4.0103	0.4360	0.7817	4.29613	0.1630	0.3719
6	2.8957	1.8988	0.9263	-------	0.1350	0.1312
7	5.6352	------	-------	--------	0.3823	------

h = 0.074024 M_1 = 0.0250 M_6 = 0.0250 Y_A = 0.02 mho.

Example 7

Design parameters of interdigital bandpase filter having n=6, β=0.15, f_0=1.5 GHz, BW=17%

k	C_k/ϵ	$C_{k,k+1}/\epsilon$	$J_{k,k+1}/Y_A$	$N_{k,k+1}$	w_k	$s_{k,k+1}$
0	5.5293	2.0047	0.9265	-------	0.3729	0.1250
1	2.7200	0.4859	0.7819	3.80372	0.1250	0.3550
2	3.8541	0.3660	0.5889	3.76878	0.1577	0.4062
3	3.9642	0.3519	0.5663	3.76532	0.1566	0.4175
4	3.9642	0.3659	0.5888	3.76877	0.1566	0.4062
5	3.8542	0.4858	0.7817	3.80368	0.1577	0.3550
6	2.7202	2.0044	0.9263	--------	0.1250	0.1250
7	5.5296	-------	------	--------	0.3729	-------

h = 0.082487 M_1 = 0.0253 M_6 = 0.0253 Y_A = 0.02 mho.

Example 8

Design parameters of interdigital bandpass filter having n=6, β=0.15, f_0=1.5 GHz, BW=20%

k	C_k/ϵ	$C_{k,k+1}/\epsilon$	$J_{k,k+1}/Y_A$	$N_{k,k+1}$	w_k	$s_{k,k+1}$
0	5.3867	2.1473	0.9265	-------	0.3595	0.1187
1	2.4768	0.5575	0.7819	3.25224	0.1180	0.3250
2	3.6311	0.4199	0.5889	3.21130	0.1500	0.3844
3	3.7527	0.4038	0.5663	3.20724	0.1440	0.3919
4	3.7527	0.4198	0.5888	3.21129	0.1440	0.3844
5	3.6312	3.5574	0.7817	3.25219	0.1500	0.3250
6	2.4771	2.1470	0.9263	-------	0.1180	0.1187
7	5.3870	------	------	-------	0.3595	------

h = 0.094636 M_1 = 0.0257 M_6 = 0.0257 Y_A = 0.02 mho.

Example 9

Design parameters of interdigital bandpass filter having n=6, ρ=0.15, f_0=1.5 GHz, BW=22%

k	C_k/ϵ	$C_{k,k+1}/\epsilon$	$J_{k,k+1}/Y_A$	$N_{k,k+1}$	w_k	$s_{k,k+1}$
0	5.3005	2.2335	0.9265	-------	0.3520	0.1141
1	2.3262	0.6032	0.7819	2.96963	0.1030	0.3125
2	3.4895	0.4543	0.5889	2.92474	0.1370	0.3687
3	3.6178	0.4369	0.5663	2.92029	0.1380	0.3750
4	3.6178	0.4542	0.5888	2.92473	0.1380	0.3687
5	3.4897	0.6030	0.7817	2.96958	0.1370	0.3125
6	2.3265	2.2332	0.9263	-------	0.1030	0.1141
7	5.3008	------	------	-------	0.3521	-------

h = 0.102390 M_1 = 0.0259 M_6 = 0.0259 Y_A = 0.02 mho.

Example 10

Design parameters of interdigital bandpass filter having n=6, ρ=0.15, f_0=1.5 GHz, BW=25%

k	C_k/ϵ	$C_{k,k+1}/\epsilon$	$J_{k,k+1}/Y_A$	$N_{k,k+1}$	w_k	$s_{k,k+1}$
0	5.1821	2.3519	0.9265	------	0.3349	0.1062
1	2.1150	0.6688	0.7819	2.63245	0.0870	0.2931
2	3.2873	0.5037	0.5889	2.58170	0.1280	0.3469
3	3.4239	0.4844	0.5663	2.57665	0.1300	0.3531
4	3.4239	0.5036	0.5888	2.58169	0.1300	0.3469
5	3.2874	0.6686	0.7817	2.63239	0.1280	0.2931
6	2.1153	2.3515	0.9263	-------	0.0870	0.1062
7	5.1825	------	-------	-------	0.3350	------

h = 0.113526 M_1 = 0.0262 M_6 = 0.0262 Y_A = 0.02 mho.

Example 11

Design parameters of interdigital bandpass filter having n=6, ρ=0.15, f_0=1.5 GHz, BW=32%

k	C_k/ϵ	$C_{k,k+1}/\epsilon$	$J_{k,k+1}/Y_A$	$N_{k,k+1}$	w_k	$s_{k,k+1}$
0	4.9469	2.5871	0.9265	-------	0.3214	0.0969
1	1.6793	0.8092	0.7819	2.09847	0.0700	0.2594
2	2.8587	0.6094	0.5889	2.03445	0.1090	0.3094
3	3.0089	0.5861	0.5663	2.02804	0.1090	0.3156
4	3.0089	0.6094	0.5888	2.03443	0.1090	0.3094
5	2.8588	0.8090	0.7817	2.09840	0.1090	0.2594
6	1.6795	2.5867	0.9263	-------	0.0700	0.0969
7	4.9473	------	-------	-------	0.3213	-------

h = 0.137370 M_1 = 0.0269 M_6 = 0.0269 Y_A = 0.02 mho.

Example 12

Design parameters of interdigital bandpass filter having n=6, ρ=0.15, f_0=1.5 GHz, BW=40%

k	C_k/ϵ	$C_{k,k+1}/\epsilon$	$J_{k,k+1}/Y_A$	$N_{k,k+1}$	w_k	$s_{k,k+1}$
0	4.7303	2.8037	0.9265	------	0.3002	0.0888
1	1.2578	0.9504	0.7819	1.72609	0.0500	0.2425
2	2.4346	0.7158	0.5889	1.64766	0.0900	0.2819
3	2.5917	0.6884	0.5663	1.63973	0.0860	0.2875
4	2.5917	0.7157	0.5888	1.64764	0.0860	0.2819
5	2.4348	0.9502	0.7817	1.72600	0.0900	0.2425
6	1.2580	2.8033	0.9263	-------	0.0500	0.0888
7	4.7307	------	-------	--------	0.3002	------

h = 0.161337 M_1 = 0.0274 M_6 = 0.0274 Y_A = 0.02 mho.

Example 13

Design parameters of interdigital bandpass filter having n=6, β=0.15, f_0=1.5 GHz, BW=45%

k	C_k/ϵ	$C_{k,k+1}/\epsilon$	$J_{k,k+1}/Y_A$	$N_{k,k+1}$	w_k	$s_{k,k+1}$
0	4.6162	2.9178	0.9265	------	0.2923	0.0844
1	1.0270	1.0294	0.7819	1.56468	0.0330	0.2256
2	2.2007	0.7752	0.5889	1.47771	0.0720	0.2687
3	2.3584	0.7456	0.5663	1.46887	0.0730	0.2800
4	2.3584	0.7752	0.5888	1.47769	0.0730	0.2687
5	2.2009	1.0291	0.8717	1.56458	0.0720	0.2256
6	1.0272	2.9174	0.9263	-------	0.0330	0.0844
7	4.6166	------	------	-------	0.2923	------

h = 0.174742 M_1 = 0.0277 M_6 = 0.0277 Y_A = 0.02 mho.

Appendix D

Measured input and output power values of the experimental filter at different frequencies

Result 1

Measured input and output power values of the experimental filter at different frequencies for figure 9.3

Frequency in MHz	Input power in mw	Output power in mw	Insertion-loss in dB
1360	8.90	0.002	36.50
1380	7.30	0.010	28.63
1400	8.80	0.100	19.40
1410	8.80	0.200	16.40
1420	7.20	0.400	12.60
1430	7.80	7.400	0.23
1440	7.20	3.000	3.80
1450	7.00	1.900	5.66
1460	7.50	3.700	3.10
1470	7.80	7.800	0.00
1480	8.00	3.000	4.26
1490	7.40	2.100	5.50
1500	7.10	3.000	3.75
1510	7.00	1.950	5.55
1520	7.00	1.450	6.84
1530	7.50	2.700	4.40
1540	8.35	7.000	0.77
1550	8.80	2.000	6.47
1560	9.00	1.700	7.24
1570	8.60	3.700	3.66
1580	8.00	6.850	0.67
1590	7.60	3.600	3.25
1600	7.90	6.400	0.91
1610	9.40	9.400	0.00
1620	8.00	5.500	1.86
1630	8.10	3.400	3.77
1640	7.00	2.900	3.83
1650	6.20	4.500	1.39
1660	6.40	2.550	4.00
1670	5.60	0.100	17.50
1690	6.70	0.004	32.24

Result 2

Measured input and output power values of the experimental filter at different frequencies for figure 9.4

Frequency in MHz	Input Power in mw	Output Power in mw	Insertion-loss in dB
1370	9.50	0.002	36.75
1390	8.00	0.008	00.00
1400	9.80	0.030	25.14
1410	9.95	0.100	19.97
1420	8.75	0.200	16.40
1430	8.40	8.400	0.00
1440	7.90	3.000	4.10
1450	7.60	2.750	4.41
1460	7.70	4.850	2.00
1470	8.15	8.150	0.00
1480	7.00	4.600	1.92
1490	7.00	4.500	1.92
1500	7.20	3.400	3.25
1510	7.90	2.500	5.00
1520	7.40	7.400	0.00
1530	7.40	5.700	0.13
1540	8.50	8.500	0.00
1550	9.20	3.200	4.59
1560	9.60	3.400	4.50
1570	9.40	9.100	0.14
1580	8.60	5.000	2.36
1590	8.50	4.600	2.67
1600	8.60	6.600	1.15
1610	9.80	9.800	0.00
1620	9.05	9.050	0.00
1630	8.40	3.800	3.44
1640	7.40	3.300	3.51
1650	6.00	0.800	8.75
1660	5.00	0.110	16.60
1670	4.50	0.024	22.73
1680	4.55	0.023	23.00
1690	6.20	0.001	37.90

Result 3

Measured input and output power values of the experimental filter at different frequencies for figure 9.5

Frequency in MHz	Input Power in mw	Output Power in mw	Insertion-loss in dB
1380	5.70	0.004	31.58
1390	5.90	0.050	20.71
1400	6.00	0.040	21.76
1410	6.00	0.105	17.60
1420	8.20	0.600	11.35
1430	7.40	7.000	0.24
1440	6.50	3.000	3.36
1450	6.40	2.000	5.10
1460	6.30	4.400	1.56
1470	8.60	8.600	0.00
1480	7.10	3.800	2.71
1490	6.10	3.050	3.00
1500	7.20	2.300	4.96
1510	4.20	1.800	3.68
1520	4.10	2.200	2.70
1530	5.40	3.800	1.53
1540	5.80	5.600	0.15
1550	6.50	2.300	4.51
1560	7.00	2.600	4.30
1570	5.50	5.200	0.24
1580	6.35	5.400	0.70
1590	6.30	3.600	2.43
1600	6.00	4.700	1.06
1610	6.90	6.900	0.00
1620	6.60	7.100	0.00
1630	6.30	3.000	3.22
1640	4.40	2.000	3.42
1650	3.80	1.050	5.59
1670	3.00	0.012	24.00
1680	3.20	0.010	25.10
1690	3.70	0.001	35.68

Result 4

Measured input and output power values of the experimental filter at different frequencies for figure 9.6

Frequency in MHz	Input Power in mw	Output Power in mw	Insertion-loss in dB
1370	9.40	0.004	33.70
1380	9.00	0.010	29.54
1390	9.10	0.060	27.54
1400	9.70	0.080	20.84
1410	9.70	0.120	19.10
1420	9.30	2.200	6.26
1430	8.70	8.700	0.00
1440	8.55	4.800	2.51
1450	8.20	4.300	2.80
1460	8.70	6.100	1.54
1470	8.80	8.800	0.00
1480	9.20	6.000	1.86
1490	8.80	5.200	2.28
1500	8.40	5.000	2.25
1510	8.00	4.200	2.80
1520	7.90	4.000	2.95
1530	8.30	7.200	0.56
1540	8.98	8.700	0.09
1550	9.30	4.900	2.80
1560	9.20	4.500	3.10
1570	8.80	8.100	0.36
1580	8.35	7.300	0.58
1590	8.20	5.700	1.58
1600	8.20	6.900	0.75
1610	8.60	8.600	0.00
1620	8.70	9.200	0.00
1630	8.30	5.300	1.95
1640	7.80	4.700	2.20
1650	6.70	3.800	2.46
1660	8.76	1.240	8.51
1670	4.80	0.030	22.04
1680	4.60	0.025	22.65
1690	5.00	0.005	30.00

Result 5

Measured input and output power values of the experimental filter at different frequencies for figure 9.7

Frequency in MHz	Input Power in mw	Output power in mw	Insertion-loss in dB
1360	10.00	0.002	37.00
1370	9.90	0.003	35.20
1380	9.60	0.006	32.04
1390	9.60	0.012	29.03
1400	10.00	0.040	23.98
1410	9.80	0.220	16.50
1420	9.20	1.000	9.60
1430	9.60	9.600	0.00
1440	8.20	4.600	2.50
1450	8.20	4.300	2.80
1460	8.60	6.000	1.50
1470	10.00	10.000	0.00
1480	9.20	6.200	1.71
1490	8.80	4.500	2.90
1500	8.20	4.500	2.60
1510	7.50	4.000	2.70
1520	7.60	4.000	2.70
1530	9.00	9.000	0.00
1540	8.90	8.900	0.00
1550	9.20	4.700	2.90
1560	9.00	4.500	3.00
1570	8.80	7.000	0.90
1580	8.30	8.300	0.00
1590	7.60	5.300	1.56
1600	7.90	6.700	0.72
1610	9.70	9.700	0.00
1620	8.40	5.000	2.25
1640	8.00	4.800	2.20
1650	5.50	3.500	1.96
1660	5.00	0.170	14.70
1670	5.00	0.040	20.97
1680	5.60	0.030	22.71
1690	6.00	0.002	34.77

Result 6

Measured input and output power values of the experimental filter at different frequencies for figure 9.8

Frequency in MHz	Input Power in mw	Output Power in mw	Insertion-loss in dB
1380	8.20	0.002	36.13
1390	7.95	0.010	29.00
1400	8.80	0.035	24.67
1410	9.00	0.150	17.78
1420	9.20	1.900	6.85
1430	8.70	6.900	1.00
1440	8.30	7.200	0.62
1450	7.50	4.400	2.32
1460	8.40	5.000	2.25
1470	9.90	9.900	0.00
1480	8.40	5.500	1.84
1490	8.80	4.800	3.00
1500	8.60	8.600	0.00
1510	8.10	6.000	1.30
1520	8.00	4.600	2.40
1530	7.40	4.000	2.67
1540	8.10	10.000	0.00
1550	8.90	7.000	1.04
1560	8.40	4.400	2.81
1570	8.80	5.900	1.74
1580	7.80	6.900	0.53
1590	8.80	8.000	0.40
1600	8.70	7.800	0.47
1610	8.80	7.600	0.64
1620	9.40	6.600	1.54
1630	9.00	8.000	0.50
1640	8.80	8.600	0.10
1650	8.50	1.800	6.70
1660	8.60	0.440	12.91
1670	8.90	0.050	22.50
1680	8.80	0.0108	29.44
1690	9.00	0.0001	-36.53

Result 7

Measured input and output power values of the experimental filter at different frequencies for figure 9.9

Frequency in MHz	Input Power in mw	Output Power in mw	Insertion-loss in dB
1360	8.60	0.004	36.30
1370	8.20	0.020	26.12
1380	7.90	0.110	18.56
1390	8.00	0.240	15.23
1400	9.00	0.710	11.03
1410	8.80	3.700	3.76
1420	9.60	9.600	0.00
1430	7.20	4.400	2.10
1440	7.40	3.550	3.20
1450	6.30	7.000	0.00
1460	7.50	6.600	0.50
1470	7.80	3.800	3.10
1480	7.80	6.700	0.66
1490	7.80	7.600	0.10
1500	7.00	3.800	3.10
1510	6.50	3.200	3.10
1520	6.60	5.580	0.73
1530	8.00	8.000	0.00
1540	7.65	5.000	1.76
1550	8.20	8.200	0.00
1560	7.80	6.100	1.10
1570	7.00	3.800	2.65
1580	6.40	5.800	0.43
1590	6.40	5.800	0.43
1600	6.20	2.400	4.10
1610	6.50	1.600	6.10
1620	6.50	0.430	11.75
1630	6.50	0.280	13.66
1640	5.60	0.020	24.50
1660	4.00	0.002	33.00